The Thesis committee for Scott Bowes Hamill
certifies that this is the approved version of the following thesis:

Operational Criteria for Battlefield Vehicles

APPROVED BY

SUPERVISING COMMITTEE:

Del Tesar, Supervisor

Ashish Deshpande

Operational Criteria for Battlefield Vehicles

by

Scott Bowes Hamill, B.S.M.E.

THESIS

Presented to the Faculty of the Graduate School of

The University of Texas at Austin

in Partial Fulfillment

of the Requirements

for the Degree of

MASTER OF SCIENCE IN ENGINEERING

THE UNIVERSITY OF TEXAS AT AUSTIN

August 2014

Dedicated to Anna.

Acknowledgments

I would like to thank all of the people who assisted me in the creation of this document and who influenced my thinking along the way.

First I would like to thank Dr. Del Tesar for his guidance and support through this process. His input and expertise on the subject matter have been invaluable.

I would also like to thank Dr. Ashish Deshpande for graciously agreeing to critique this document. His input and patience were greatly appreciated.

The support and understanding of one's colleagues is a critical part of any project, and for that I would like to thank Tim Woodard, Andrew Boddiford, Dhiral Chheda, Chris Hammel, and Gurtej Saini.

Lastly, I would like to thank Mrs. Betty Wilson for her hard work, patience, and unending commitment to the Robotics Research Group.

Operational Criteria for Battlefield Vehicles

Scott Bowes Hamill, M.S.E
The University of Texas at Austin, 2014

Supervisor: Del Tesar

Modern military ground vehicles are no longer able to respond effectively to the rapidly changing mission requirements of modern military conflicts. Military vehicle architectures, which utilize passive suspension components and traditional drivetrain/steering systems, do not provide the operational flexibility to meet the demands of the operator.

Advances in intelligent actuation technology allow for the development of a new vehicle architecture - the Intelligent Corner Vehicle (ICV). The ICV utilizes intelligent actuator technology to actively control the four degrees of freedom of each wheel of the vehicle - drive, camber, steering, and suspension. The utilization of intelligent actuation requires the characterization of the motions and behavior of the tire and the vehicle chassis in order to effectively apply the tire to the road surface - the development of vehicle performance criteria.

A brief review of the state of wheeled military systems is presented. Many modern military vehicles were designed to improve protection at the

expense of mobility - a process that has had negative effects on vehicle capability. An overview of the pneumatic tire used for wheeled vehicles is presented, highlighting the nonlinearities of tire behavior. The complexity of tire force generation drives the need for the application of intelligent actuation. Traditional actuation of wheel motion is presented along with a variety of current efforts to apply intelligent actuation to individual degrees of freedom of the tire. These efforts can be shown to improve vehicle performance, but intelligent actuation must be applied to all aspects of tire motion, requiring the use of the ICV architecture and the generation of performance criteria by which the complex motion of the vehicle may be evaluated. The Robotics Research Group has a history of developing and evaluating performance criteria for complex dynamic systems. and review of performance criteria developed for serial chain robotics is presented. These criteria address task independent actuator motion in addition to actuator ranges and limits, and their application to the ICV is discussed. A brief overview of several important concepts of classical vehicle dynamics are presented. The application of criteria derived from these concepts to the ICV architecture is discussed.

This report presents the complexities of tire behavior and vehicle motion, the need for alternative architectures (the ICV), and a variety of performance criteria required to evaluate vehicle motion in real time. Criteria that are presented are summarized along with their definition and physical meaning. Future work for the development of the ICV involves the generation of a vehicle model for evaluating the application and range values of the presented

criteria.

Table of Contents

List of Tables

List of Figures

Chapter 1

Introduction

1.1 Background

1.1.1 Military Vehicles

Military vehicles are traditionally developed to address sets of operational requirements derived from the expectations of future conflict. A large number of military vehicles currently, such as the High Mobility Multipurpose Wheeled Vehicle (HMMWV), M1 Abrams Tank, and the M2 Bradley Fighting Vehicle, were developed during the Cold War era for conventional vehicle roles (logistics/armor/mechanized infantry) with the expectation that future conflicts would involve large scale warfare between established nations, similar to what had been experienced in Vietnam, Korea, and World War II. In effect, the process of generating requirements was an extrapolation of past observations and experiences.

While the vehicles developed during the Cold War era were initially successful after their deployment, as witnessed during U.S. operations during the First Gulf War, the rise of large scale asymmetric warfare during the conflicts in Iraq and Afghanistan during the 2000's demonstrated that this extrapolation process was no longer appropriate. The rapidly changing mission requirements and unknown threats indicated that conventional vehicle

roles were no longer relevant and that improved ground vehicle capability was needed. The rapid nature of the response of the U.S. military to this issue resulted in the development of a new class of vehicle, the MRAP, based on off-the-shelf military and commercial vehicle technology. The result was an increase in levels of threat protection at the cost of severely reduced vehicle performance and capability. Overall, this process ended with the stagnation of the development of the technology base for military ground vehicles at a considerable cost in time and resources.

1.1.2 Vehicle Architectures

Most ground vehicles utilize similar architectures - internal combustion engines provide torque through transmissions and drive shafts directly connected to the driven wheels. The remaining individual motions of each wheel - camber, suspension, and steering, are controlled by passive elements (springs, dampers, and linkages). As such, the selection of parameters for the passive elements is a process of optimization that requires the designer or engineer to establish a constrained design compromise based on the anticipated operating conditions of the vehicle. If the operating conditions vary significantly, as is the case with military vehicles, the compromises made in the design phase often severely limit the ability of the vehicle to adequately respond to the demands of the operator.

1.2 Problem Overview

The ground vehicle is a tool for the operator that provides mobility for the operator, other occupants, and a variety of cargo and chassis mounted equipment. As such, the ideal ground vehicle is perfectly suited to the task of rapidly responding to the commands of the operator. Rapidly responding to the operator requires a vehicle platform with significant flexibility in design and operation. Tesar, in [82], proposes the development of a vehicle platform that utilizes intelligent actuation to optimally apply the vehicle running gear to the road.

1.2.1 The Intelligent Actuator

The Robotics Research Group (RRG) has conducted research for many years on geartrain and actuator design. The intelligent actuator concept utilizes a variety of actuator sensors and embedded performance maps to provide the operator with real-time information and capability, but also with a structured decision making process that allows the actuator to rapidly and accurately respond to the operator's demands. The intelligent actuator will provide two key capabilities to ground vehicle platforms - standardization and open architecture.

Standardization will allow for the development of minimum actuator sets - a series of actuator designs intended to address all of the actuation needs of a particular design space. The designer or engineer may select one or more actuators from a given set and apply the actuator directly to the

intended application. This process eliminates the need for one-off designs.

Open architecture will allow the direct involvement of any capable party in the development and implementation of intelligent actuation. This will reduce or eliminate legacy technology with proprietary components, allowing for the rapid refreshment and improvement of not only actuator technology, but the overarching control software.

1.2.2 The Intelligent Corner Vehicle

Applying intelligent actuators to each of the four possible degrees of freedom of a wheel (resulting in an intelligent corner) maximizes the ability of the wheel to apply the tire to the road surface (the ultimate goal of the vehicle). The Intelligent Corner Vehicle (ICV) utilizes any number of paired intelligent corners on a military vehicle chassis to create a fully open architecture in a highly responsive and dexterous vehicle system. The benefits of open architecture and standardization provided by the intelligent actuators results in a system that may be assembled on demand from minimum sets of components and the resulting vehicle is suited to actively apply the tire to the road surface as dictated by the operator.

However, any optimization process requires criteria by which any system output (in this case) vehicle motion, may be evaluated. Sets of vehicle performance criteria will allow the operator and vehicle control software to appropriately judge the motion and force application of the intelligent actuators.

1.3 Research Objectives

The goal of this research is to begin the process of developing performance criteria framework for the ICV concept. The RRG has a history of developing and working with performance criteria in highly nonlinear systems, in this case for serial chain robotic systems. This report evaluates the application of previously developed criteria to ground vehicles and presents performance criteria derived from an expanded view of classical vehicle dynamics.

1.4 Report Structure

1.4.1 Chapter 1: Introduction

This chapter provides an introduction to the work and describes the current issues with modern military ground vehicle development. The Intelligent Corner Vehicle concept is introduced, the benefits of the vehicle architecture described, and the requirement for performance criteria presented.

1.4.2 Chapter 2: Background

This chapter briefly discusses the state of current military ground vehicles as well as the current development process. The rapidly changing nature of vehicle requirements and the trends in military vehicle capability are described.

1.4.3 Chapter 3: Tires

This chapter discusses the behavior of pneumatic tires. The concepts of tire slip and force generation are detailed, and the problems with quantifying tire behavior in combined loading conditions on various surfaces are presented. The impact of tire nonlinearities on the ICV architecture are summarized.

1.4.4 Chapter 4: Vehicle Architectures

This chapter presents and discusses traditional vehicle architectures, current trends in active wheel motion actuation, and various non-traditional vehicle platforms. The ICV concept is presented in detail, the the subsequent implications for increased vehicle capability are noted.

1.4.5 Chapter 5: Serial Chain Robotics Criteria as a Framework for Vehicle Criteria Development

This chapter discusses the development of performance criteria for serial chain robotic systems, and the applicability of these criteria to the ICV. The most applicable sets of criteria, those describing actuator limits and chassis energy distribution, are presented along with the meaning of each with respect to the ICV concept which, as a vehicle assembled of N corners, forms a fully parallel system.

1.4.6 Chapter 6: Concepts of Vehicle Dynamics as Applied to the Intelligent Corner Vehicle Architecture

This chapter introduces several models and concepts commonly used in the study of classical vehicle dynamics. The performance criteria that may be derived from these models is presented, in addition to the meaning of each with respect to the ICV concept. This transition to actuator drives/suspensions is a major undertaking deserving a full attention of the needed science.

1.4.7 Chapter 7: Conclusion and Future Work

This chapter concludes the report by summarizing the development of performance criteria for the ICV and by discussing the need for detailed models of the planar motion of the ICV and for the ICV suspension. Validating performance criteria will require simulating realistic vehicle behavior in an effort to observe not only the values of the individual criteria through the vehicle motion, but the relative changes in value among them, so that the physical meaning of each criteria may be further refined in an effort to more accurately characterize vehicle motion. All of this leads to increased safety, efficiency, responsiveness, the reduction of single point failures, and improved operator command due to real time visual criteria display and internal conflict (in milli-sec.) resolution among the $4N$ degrees of freedom.

All of the key concepts from the literature, associated results, conclusions, and recommendations of this report are enumerated and presented at the end of this chapter. The list of 41 key literature concepts describe the de-

velopment of modern military platforms, the complexities of the tire, state of traditional wheel actuation, and detail the groundwork for understanding vehicle dynamics and the application of performance criteria to complex systems. The listing of 32 results indicate the ineffectiveness of military platforms, the potential for performance map characterization of the tire, and the restrictive nature of traditional wheel actuation. The list of 39 conclusions describe the requirement of the ICV architecture to improve military vehicle platforms, need for tire performance maps, and the effectiveness of criteria descriptions of complex motion. Finally, the 19 recommendations for future work detail the need for comprehensive modeling in an effort to evaluate the effectiveness of the ICV architecture and presented criteria.

Chapter 2

The Current State of the Battlefield Vehicle

2.1 Mobility as Requirement

Mobility is the cornerstone of any mechanized military organization. Mobility is key in all areas of military operation (air, sea, land), however, the focus of this chapter is on ground mobility and the subsequent impact on ground troop capability. While a complete study of the historical importance of military vehicle performance is, unfortunately, outside the scope of this document, it is necessary to emphasize the importance of military ground vehicle capability and the impact of vehicle requirements on technology development.

2.2 A Brief History of U.S. Military Ground Vehicles

The widespread use of mechanized ground vehicles began during the First World War. Trucks began to replace pack animals as the main means of materiel transport and the first tanks were developed as a means to support infantry engaged in trench warfare [54]. Vehicle technology (both commercial and military) developed rapidly in the early part of the 20th century and by the Second World War, mechanized units were well integrated into military doctrine and strategy [16]. The inclusion and utilization of mechanized

units continued to increase during the Cold War period along a relatively linear development path: armored combat vehicles operated at the front lines, soft-skinned (non-armored) tactical vehicles provided support and logistics capability. This methodology, however, is no longer appropriate for recent U.S. military conflicts as a result of the new emphasis on expeditionary operations which have no clear line of combat.

2.2.1 Cold War Vehicle Development

The analysis of modern day military ground vehicle requirements and capabilities begins with the study of three vehicles developed during the post-Vietnam, Cold War era arms race: the High Mobility Multi-Purpose Wheeled Vehicle (HMMWV), M1 Abrams main battle tank, and the M2 Bradley Fighting Vehicle.[1] The HMMWV is shown in Figure 2.1, the M1 Abrams in Figure 2.2, and the M2 Bradley in Figure 2.3. It should be noted that the HMMWV represents a family of vehicles utilizing a common core chassis and that the vehicle in Figure 2.1 is one of the more common variants.

The development of these three vehicles was intended to provide updated troop transport/logistics (HMMWV), maximum ground vehicle protection and firepower (M1), and mechanized infantry support (Bradley) capability. These vehicles were developed to address the military doctrine and then current tactics derived largely from analysis of large scale warfare between two

[1]The M1 and M2 vehicles are both tracked systems while the HMMWV is a wheeled vehicle. While both tracks and wheels are utilized in military vehicle architectures, this report will focus on wheeled vehicles.

Figure 2.1: High Mobility Multi-Purpose Wheeled Vehicle (HMMWV) [32]

Figure 2.2: Abrams Tank (M1A1 Variant), Camp Fallujah, Iraq, 2007

Figure 2.3: M2 Bradley Fighting Vehicle (M2A2 Variant), Forward Operating Base MacKenzie, Iraq, 2004

developed, national combatants (e.g. the U.S.S.R and the U.S.) [46]. Understanding the development of these vehicles is critical for three reasons. The first reason is that these vehicles provided the bulk of the U.S. offensive capability during the Gulf War and performed their intended roles effectively for the duration of the conflict. The second reason is that these vehicles reprised their roles as the bulk of the U.S. armored/mechanized vehicle forces during the beginning of the Iraq War, during which the rise of asymmetric warfare drastically changed the requirements for military vehicles.[2] Finally, these vehicles are still currently in use and therefore provide insight into the continually changing nature of ground vehicle utilization and capability.

[2]Asymmetric warfare refers to conflicts where the belligerents involved may be of significantly disproportionate capability and the use of unconventional tactics is common.

2.2.2 Ground Vehicles During the Gulf War

The Gulf War was the first significant, multinational conflict involving large scale military operations since the revitalization of the U.S. military in the post-Vietnam era and the development of integrated, full spectrum capability military doctrine [17]. However, drawing conclusions about ground vehicle capability in this case is difficult due to the brief nature of the ground campaign. Ground operations in Iraq lasted approximately 100 hours and were preceded by an extensive, five week air strike campaign. The M1 Abrams, M2 Bradley, and HMMWV vehicles performed well [67]. However, their interaction with enemy forces was, broadly speaking, limited. The M1 and M2 vehicles, spearheading the coalition ground forces, proved to be vastly superior to Iraqi armored vehicles, allowing coalition troops to sustain rapid ground troop movement, achieve objectives quickly, and avoid extended ground operations [11]. This conflict did, however, highlight two issues related to ground vehicle performance.

The first issue was the problem of vehicle fuel consumption (fuel efficiency). The heavily armored, 70 ton Abrams tank utilizes a gas-turbine engine as a main power plant instead of the more traditional diesel piston engine. As a result, the M1 has excellent acceleration and maximum ground speed characteristics but suffers from poor fuel efficiency. Each M1 consumed five hundred gallons of fuel every eight to ten hours during the First Gulf War ground campaign [11]. The extensive fuel consumption of U.S. ground forces caused delays in the advancement of U.S. troops, but other fuel efficiency issues

were not well documented due to the brevity of ground operations.

The second issue was the lack of sufficient high speed, off-road capability among a variety of ground vehicles. Command and control (C2) vehicles, in addition to logistics vehicles, had difficulty keeping pace with the M1 tank during the rapid advancement of U.S. forces [66].[3] Again, the short duration of the ground conflict kept this performance disparity from significantly affecting the conduct of U.S. operations.

2.3 The Iraq War and Subsequent Changes to Vehicle Requirements

While large scale ground operations during the Iraq War in 2003 were also brief, the subsequent occupation of Iraq resulted in a rapid shift in the nature of the engagement. The rise of insurgency, asymmetric warfare, and the involvement of non-state actors caused the Improvised Explosive Device (IED) to become the predominant threat to ground vehicles and troops. This shift resulted in the need for increased threat protection not only for the armored vehicles (M1, M2) but for the soft-skinned HMMWV as well.

Improved HMMWV variants and armor kits were developed in an effort to provide additional protection against threats [85][58]. An image of a HMMWV variant with upgraded armor is shown in Figure 2.4.

Other tactical wheeled vehicles, such as the Family of Medium Tactical

[3]Command and control vehicles, in this case, refer to the M88A1, M577, and M113.

Figure 2.4: Up Armored HMMWV Variant, Afghanistan, 2007 [69]

Vehicles (FMTV), received similar upgrades during the conflict. The original, soft-skinned vehicle, shown in Figure 2.5, was upgraded to allow the application of additional armor panels. The upgraded base cargo FMTV vehicle is shown in the unarmored state in Figure 2.6, and the armored state in Figure 2.7. These upgrades, while effective to some extent at mitigating IED and small arms threats, had a very negative impact on vehicle mobility and efficiency [47].

2.3.1 Development of the MRAP

Procurement of HMMWV armor kits and upgraded chassis variants was a slow process and the resulting vehicles were not sufficiently effective at

Figure 2.5: FMTV Light Vehicle, Unarmored [6]

mitigating IED threats [59]. In response, the Department of Defense (DoD) sought to procure armored wheeled vehicles in an effort to protect units and patrols. The resulting program was named Mine Resistant Ambush Protected (MRAP) and vehicles were procured from contractors and deployed rapidly. MRAP vehicles, utilizing V-shaped, armored plating and lifted chassis, proved resilient to many IED threats [25]. However, the increased level of protection resulted in several drawbacks. MRAP vehicles were slow, overly heavy for the local road infrastructure, and fuel inefficient. One of the MRAP Variants, manufactured by Force Protection, Inc., is shown in Figure 2.8.

The MRAP program was meant to be a rapid solution built as quickly as possible, which limited the available technology to commercial off the shelf (COTS) solutions. The rapid deployment of the MRAPs was largely a process

Figure 2.6: FMTV Light Vehicle, A-Kit (Base Armor) Configuration [29]

of adapting existing commercial and military truck chassis to accommodate heavily armored cabs and crew compartments, resulting in the continuation of the same vehicle architectures present in military vehicle fleets. As a result, the tech base for ground vehicles was not moved forward despite significant financial investment by the DoD. While this rapid procurement did provide troops with increased protection against various threats, the focus on immediate technology had the effect of divesting the U.S. Department of Defense (DoD) from the overall ground vehicle strategy and doctrine [3][4]. The success of the MRAP program (where protection was the main concern) resulted in continued use of MRAP vehicles during the conflicts in Iraq and Afghanistan.

Figure 2.7: FMTV Light Vehicle, B-Kit (Appliqué Armor Panels Installed) Configuration [29]

2.3.2 Extending the MRAP Architecture

Towards the end of the conflict in Iraq, the U.S. DoD requested proposals (RFP) for a lighter variant of the MRAP capable of traversing the mountainous terrain of Afghanistan [68]. The intent with this RFP was to address one of the most significant weaknesses of the MRAP program, vehicle mobility and performance. The resulting vehicle, the MRAP All Terrain Vehicle (M-ATV), shown in Figure 2.9, was procured in 2010.

However, while the M-ATV platform addressed a few of the concerns of the original MRAP program such as size and weight, the resulting architecture did not represent a significant departure from previous MRAP designs. A visual comparison between the HMMWV and M-ATV is shown in Figure 2.10.

Figure 2.8: Cougar MRAP Variant

Figure 2.9: MRAP All Terrain Vehicle (M-ATV) [9]

Figure 2.10: HMMWV, M-ATV Comparison [9]

The Army is currently working on the development of replacements for the HMMWV and MRAP (including M-ATV) vehicles. The HMMWV no longer addresses the needs and requirements of the military, and the MRAP program represents a niche application and was not intended to be a sustained program [3]. The intended replacements, the Joint Light Tactical Vehicle (JLTV) and the Ground Combat Vehicle (GCV), are a long term development effort to address the concerns of protection and performance for future ground vehicles. The JLTV and GCV, however, are still in development and as such, no significant conclusions may be drawn at this time.

2.4 Future Combat Systems

In the early 2000's, the Army began an initiative to completely modernize the Army in an effort to increase mobility, modularity, and deployability of Army units [30]. This initiative, Future Combat Systems (FCS), called for the development of a family of manned ground vehicles and a group of unmanned ground and aerial vehicles in conjunction with an overarching coordinating network. The FCS program was begun largely in response to the deployment difficulties faced by the Army in the Gulf War (1991) and the conflict in the Balkans (1999). The focus of the FCS program was to improve Army capability at the brigade level, specifically the Brigade Combat Team (BCT), the smallest unit intended for independent operation.

Future Combat Systems was ultimately unsuccessful for a variety of reasons and the Army was left with few results and no procurable vehicles. In 2012, RAND Corporation, at the request of the Army, published a report on the FCS program detailing the lessons learned from FCS and the subsequent program cancellation [72]. The document, "Lessons from the Army's Future Combat Systems Program," provides a history of the program and lists a series of lessons learned from the FCS program.

According to the report, the FCS program was unsuccessful due to shifting development schedules, incorporation of immature technologies, and changing system requirements, all compounded by ambitious program goals. While the conclusions and recommendations listed in the document cover a range of topics, such as program management and contracts, several of the

lessons learned are directly applicable to the development of future ground vehicle technology. The most important concepts discussed in the document (as they pertain to ground vehicle development) are that vehicles will no longer be developed in isolation, utilizing immature technologies may negatively impact the development schedule, and an optimized force or technology has strengths and weaknesses. In effect, future vehicle systems must be developed and updated with regards to total fleet capability, and *programs should avoid significant reliance on unproven technology and concepts* while maintaining awareness of the resulting capabilities and capability gaps inherently created during the development process. Although this is a valid conclusion, this approach will stifle necessary development and give little guidance to research and development programs in the Army, their supporting contractors, and academic researchers.

2.5 Current Military Vehicle Requirements and Capabilities

A separate RAND study, predating the FCS report by a year, responded to a request from the U.S. Congress to assess ground vehicle development for the Army [48]. This report, titled "The U.S. Combat and Tactical Wheeled Vehicle Fleets," focuses on the overall issue of Army vehicle requirements generation, development, and procurement in addition to problems with the current vehicle fleet. This report makes several of observations and recommendations across several areas of interest, such as requirements generation and acquisition

policy. The comments (observations and recommendations) provide significant insight in to the vehicle development and acquisition process, but this present report, for the sake of conciseness, will restrict discussion to a few of the key main points.

Overall, the RAND report emphasizes that predicting future ground vehicle operating conditions is difficult, that current vehicle requirements reflect a current understanding of the role of ground vehicles, and that the compromise between vehicle power, protection and payload (the "iron triangle") is permanent. In addition, the report also notes the important trends of increasing power generation requirements and integration of sensors and networking.

The design of any ground vehicle, military or otherwise, is an exercise in balancing a variety of conflicting requirements. Previous generations of military ground vehicles (e.g. M1, M2, and HMMWV development during the Cold War) were developed for specific, traditional roles. As previously discussed, traditional roles for ground vehicles are no longer appropriate and, as the RAND report notes, the gap between tactical and combat vehicles is shrinking rapidly. Operating conditions, mission roles, and requirements may shift quickly in the future and the military vehicle fleet development and acquisition processes will need to be able to rapidly adapt appropriately. Future threats will remain unknown, and the success of future ground vehicle programs will depend on the flexibility and adaptability of future vehicle platforms. Until the adoption of open vehicle architectures, modular vehicle systems, and intelligent actuation so that the military may rapidly adapt to shifts

in vehicle requirements, the "iron triangle" and continued focus on traditional vehicle architectures will continue to hamper military vehicle development.

2.6 Future Vehicle Development

The current strategy of the Army for updating its ground vehicle fleet is to continue development of the JLTV, GCV, and Armored Multi-Purpose Vehicle (AMPV) while updating and maintaining the M1 Abrams and Stryker platforms [5].[4] As of January 23, 2014, the GCV Program is suspended [55].

Though the current strategy of the Army emphasizes the need for an increasingly expeditionary force, none of the current vehicle development programs incorporate the required technology development to address this need. The protection requirement for ground vehicles that arose during the Iraq War has dominated subsequent requirements, and current platforms are unable to respond to the Army's need for fleet mobility. Developing the combat and tactical ground vehicles of the future will require a significant effort to develop new vehicle technology capable of providing rapid development and acquisition while maintaining the ability to be updated (refreshed) in order to respond to volatile operating conditions and requirements.

In the report *Modernization of Open Architecture Battlefield Vehicles* [82], Tesar discusses a variety of topics pertinent to the development of the next generation battlefield vehicles, the most important of which are standard-

[4]The AMPV is intended to replace the M113, a multipurpose, mechanized infantry vehicle.

ization, open architecture (as previously discussed), and intelligent actuation.

Standardization of vehicle components (including electronics and chassis attachment) and the adoption of quick change interfaces will provide significant flexibility to the vehicle operator in maintenance, repair, and refreshment. Standardization will allow the development of minimum sets of vehicle components providing a basis for any range of specified vehicle requirements. This includes both actuators and electrical components. Each standard set may then be tested and certified to a higher degree, improving performance, reducing costs, and providing engineers and technicians with reliable, readily obtained components.

Open architecture is critical for future vehicle development as it will remove barriers for competition and technology development. A significant degree of current vehicle technology is based on one-off, proprietary designs developed by single contractors. One-off, closed architecture designs are time intensive, expensive, and restrict future developments and improvements by competitors. Reducing vehicle costs and improving vehicle performance requires the reduction or removal of these barriers and design restrictions.

Intelligent actuation is the key to future vehicle development. As previously mentioned, most modern battlefield vehicles are one-off proprietary designs that rely on well established, but ultimately ineffective, design conventions and architectures that rely on passive technology (e.g. beam axles, dampers, etc.). The application of intelligent actuation (actuators) to vehicle design will not only allow for increased freedom in design choices (as will be

discussed in Chapter 4), but will allow the vehicle and the operator to appropriately apply generated power to the road surface. Increasing this capability of power application will provide the vehicle and the operator with the flexibility to optimize the behavior of the vehicle for the given mission requirements. In other words, the operator will be able to specify maximum traction, efficiency, etc., and the intelligent actuation capability will allow the vehicle to be much more responsive.

Standardized intelligent actuation combined with open architecture will allow military vehicle developers to rapidly assemble (on demand), a variety of ground vehicles based on common components that are capable of responding quickly to the demands of the operator for a wide range of operating conditions, thereby maximizing vehicle mobility and capability. It should be noted that the concepts of standardization, open architecture, and intelligent actuation to apply to all articulated vehicle components, such as turrets and weapons systems.

2.7 The Need for Performance Criteria

The application of intelligent actuation to ground vehicles will provide a large number of system inputs and, as a result, will require a structured decision making process. This process requires the characterization of vehicle motion. Responding to the commands of the human operator or human decision maker (HDM) requires the development of performance criteria by which the operation of the vehicle may be evaluated. Performance criteria for

ground vehicles, the subject of this report, illustrate the behavior of the vehicle and may be combined into performance maps and, subsequently, decision surfaces that may then be utilized by the vehicle operator to maximize vehicle performance as desired.

2.8 Chapter Summary

This chapter discusses the development and current state of U.S. military ground vehicles. Current vehicle platforms, many of which were developed during the Cold War, were structured to address traditional battlefield roles defined by past conflicts and the expectation of large scale, multi-national conflicts in the future. The resulting platforms do not adequately address the current, rapidly changing requirements for military ground vehicles in the conflicts in Iraq and Afghanistan. Asymmetric warfare and the involvement of non-state actors has resulted in the convergence of tactical and combat vehicle roles and complicated the process of developing new vehicle fleets to address changing requirements.

The few vehicle platforms that have been recently developed and fielded to address current battlefield issues, such as the MRAP and M-ATV, sacrifice mobility and payload to maximize protection. The continuation of this methodology and emphasis on rapid procurement has resulted in ineffective ground vehicle fleets and a stagnation in ground vehicle development. Despite significant financial investment, the technology base for tactical vehicles has not moved forward as vehicle platforms continue to rely on legacy architec-

tures.

Updating and improving the U.S. ground vehicle fleet requires the application of intelligent actuator technology in order to both provide the vehicle operator with sufficient choices to address the wide ranging mission goals of current vehicles, and to allow for the rapid development, assembly, and maintenance of vehicle systems, ultimately yielding an intelligent, capable vehicle platform that may be easily improved, refreshed, and updated. However, this application of intelligent actuator technology will require the characterization of vehicle motion - the development of vehicle performance criteria. These criteria will form the foundation for the effective application of intelligent actuation.

The chapters of this report will address the following key points:

1. Tire behavior is highly complex and the effective application of the tire to the road surface requires a complete characterization of tire force generation in real time modeling descriptions.

2. Characterizing tire behavior requires the generation of tire performance maps which must be embedded in the system for rapid access.

3. Current vehicle architectures and operating systems are not effective in fully utilizing the capabilities of the tire.

4. Passive suspension/wheel actuation components are not responsive to operator commands and are not able to address a spectrum of emerging

vehicle performance requirements.

5. Effectively utilizing the tire and responding to human command requires the use of intelligent actuation. It is suggested here that this involves, in the general case, a 4 degree of freedom corner (drive wheel, active suspension, steering, and camber).

6. Vehicle performance criteria are the foundation for the structured decision making process required for effective vehicle operation (which may involve hundreds of criteria, performance maps, and operational envelopes as decision surfaces).

7. Responding to human command requires characterizing vehicle motion and the generation of performance criteria which can be represented as performance maps for rapid visualization and comprehension by the operator.

Chapter 3

An Introduction to the Tire

The tire is the most important component of a wheeled ground vehicle. The tires support the vehicle, cushion the suspension and chassis from road disturbances, and apply tractive forces to the road surface. In addition, tires are significant source of driver feedback in vehicles with conventional architectures. As a result, a discussion of basic tire dynamics is required before any meaningful discussion about vehicle operation or dynamics may occur.

The focus of this chapter (and report in general) is on the behavior of pneumatic tires. Tracks and tracked vehicles are not discussed due to the restrictions on vehicle behavior imposed by tracked systems as well as the increased prevalence of wheeled vehicles (as opposed to tracked) in expeditionary military operations.

3.1 Tire Basics - On Road Behavior

The following section addresses tire behavior on conventionally prepared, non-deformable surfaces (asphalt, concrete, etc.). This is the most common operating scenario for passenger vehicles.

3.1.1 A Brief Note on Tire Construction

Modern pneumatic tires are comprised of layers of cords (plies) encased in a toroidally shaped, flexible rubber carcass that is filled with compressed air. The cords are anchored around high strength steel wire (beads). The beads provide a load path to the rim of the wheel.

Modern tires typically come in one of two varieties: the bias ply tire and the radial ply tire. The main difference between the two is the orientation of the cords (plies) in the carcass. Bias ply tires utilize alternating cord layers oriented diagonally to the beads (on the bias). Radial ply tires utilize cord layers that extend radially from bead to bead in conjunction with several separate layers in the tread, called belts. The distinction is shown in Figure 3.1. Radial tires require additional layers in the tread region (belts) for stable operation. While these descriptions are simplified representations, a basic distinction is necessary because tire construction affects all aspects of tire behavior, from cornering properties to ground pressure distribution [87].

3.1.2 Tire Forces - The Basics

Discussions of tire dynamics focus primarily on force generation in two directions (lateral and longitudinal) and the effect of other tire properties and behavior on these two forces. The lateral and longitudinal directions are emphasized because ground vehicle chassis motion is often assumed to be planar (two dimensional) in the plane defined by the ground surface. This assumption is not always appropriate as chassis roll, pitch, and heave greatly affect the

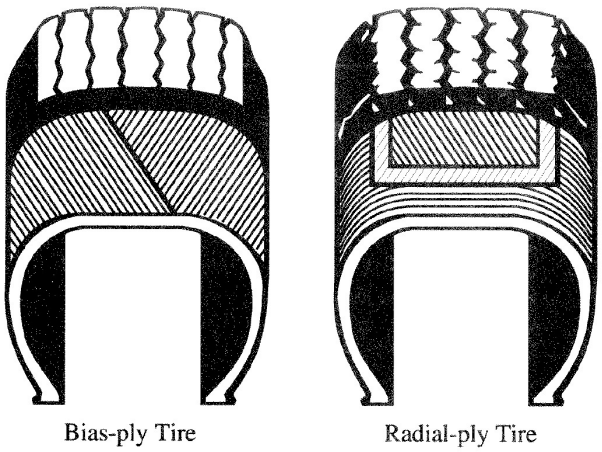

Figure 3.1: Bias and Radial Tire Construction [33]. *Originally provided by Goodyear Tire & Rubber Co.*

planar dynamics, but the planar restriction simplifies the initial discussion of tire behavior and subsequent chassis dynamics. For the following discussion, the standard Society of Automotive Engineers (SAE) tire axis definition will be used (shown in Figure 3.2).

3.1.2.1 The Concept of Tire Slip

The tire carcass is compliant and experiences deformation when subject to a load. As a result, the rolling motion of a loaded tire is not equivalent to that of a free-rolling tire. The driven, or loaded, tire experiences an apparent relative motion to the ground in comparison to the free rolling tire. This relative motion generally occurs without gross sliding and is referred to as slip. Slip in the longitudinal direction, appropriately referred to as *longitudinal slip*

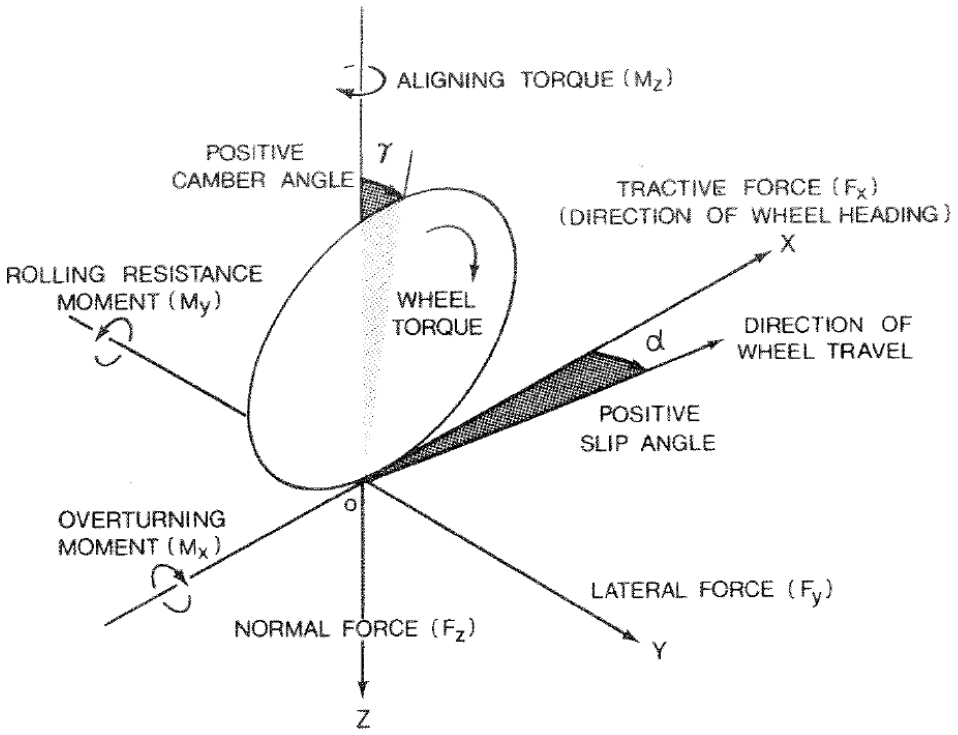

Figure 3.2: SAE Tire Axis Definition [87], originally reproduced from [2]

or *slip ratio*, i, is defined by SAE as [2]:

$$i = (\frac{r\omega}{V} - 1) * 100\% = (\frac{r_e}{r} - 1) * 100\% \tag{3.1}$$

i - slip ratio

r - radius of free rolling tire

r_e - effective rolling radius of the tire

ω - wheel angular velocity

V - linear speed of the center of the tire

Alternatively, J.Y. Wong provides a slightly different definition of slip

[87]:

$$i = (1 - \frac{V}{r\omega}) * 100\% = (1 - \frac{r_e}{r}) * 100\% \tag{3.2}$$

The equations have the same component definitions, but represent slightly different interpretations of slip. For example, if the tire wheel center velocity is zero and the wheel is spinning, the tire is experiencing 100% slip by the Wong definition and infinite slip by the SAE definition. While the definition is arbitrary to an extent, a distinction is required as both definitions are used in this chapter in reference to various figures and equations.

Slip in the lateral direction is defined in a different manner. A tire experiencing a steering input or any lateral loading will tend to move along a path that is not in the wheel plane (X-Z plane of the wheel). Relative motion in the lateral direction is described using the angle between the path of motion and the wheel plane and is referred to as the *slip angle*, α, as shown in 3.2.

As a result of the tire load/deformation relationship, tire forces are described as functions of longitudinal slip, i and slip angle, α. The relationship between lateral load and slip angle is similar (but not identical to) the relationship between longitudinal force and longitudinal slip. In both cases, however, the initial relationship for low slip values is observed to be linear. Force generation in the linear region is primarily due to carcass stiffness - the tire carcass is acting like an ideal spring. In this case, the tire tread in the contact patch, the area of the tire carcass in contact with the road surface, experiences no relative motion with respect to the road surface. However, as the tire forces increase, the tire/force relationship transitions from linear to

nonlinear and sliding begins to occur in the contact patch. Sliding begins with tread elements in the rear of the contact patch (the most heavily loaded portion) and propagates forward as tire forces increase. *Peak force generation generally occurs when some portion, but not all, of the contact patch is sliding* [57]. If slip continues to increase, the lateral or longitudinal force begins to decline until the contact patch is sliding completely and force generation is a function of the sliding friction coefficient, μ_s. In this case the tire is experiencing gross sliding and the result is an unstable operating condition. The ability of the driver to maintain control of the vehicle is compromised in this situation. The increasingly reduced capability of the tire to resist a driving torque increases the rate at which the slip ratio or slip angle is growing. In other words, unstable behavior is exhibited if the peak load capability of the tire is exceeded. The transition zones and locations of peak force value are functions of tire construction, inflation pressure, load, etc.

3.1.2.2 Longitudinal Force vs. Slip Ratio

The slip/force relationship is best understood graphically. A representative longitudinal force (F_{xs})/slip relationship is shown in Figure 3.3.

Note: this figure utilizes the SAE definition of slip and the tire is experiencing a driving torque. SAE defines the onset of tire spin (gross sliding) as occurring at a positive slip value of 1. Regardless of the definition of slip used, maximizing longitudinal tractive effort is an optimization problem that requires maintaining some value of slip. As an example, modern passenger car

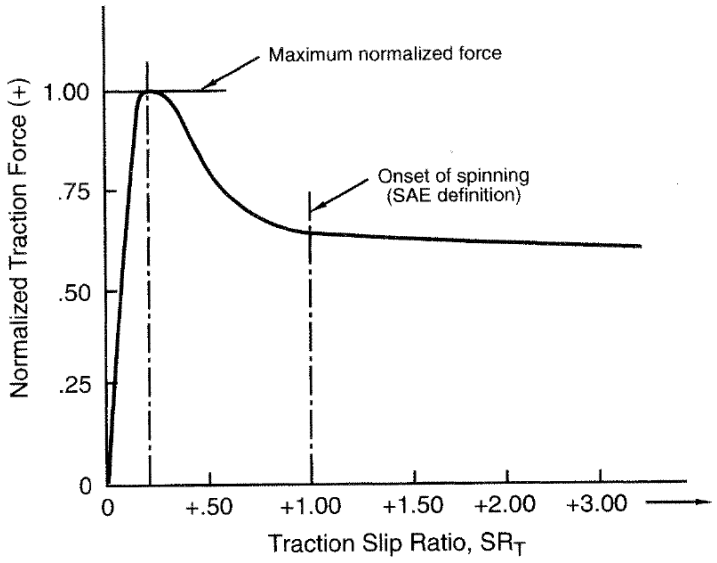

Figure 3.3: Longitudinal Force vs. Slip Ratio [57]

tires achieve maximum tractive effort at slip values approximately between 15% and 20% [87]. Racing (high performance) tires achieve maximum longitudinal tractive effort at much lower slip values because the tire carcass tends to be more stiff, allowing the tire to build forces more rapidly.

The longitudinal force/slip relationship for a tire experiencing a braking torque is shown in Figure 3.4.

This figure utilizes the SAE definition of slip. In the case of braking, some authors utilize a modified definition of slip. Wong, for example, uses a slightly altered definition of slip, or skid:

$$i_s = (\frac{V}{r\omega} - 1) * 100\% = (\frac{r}{r_e} - 1) * 100\% \tag{3.3}$$

i_s - skid-slip

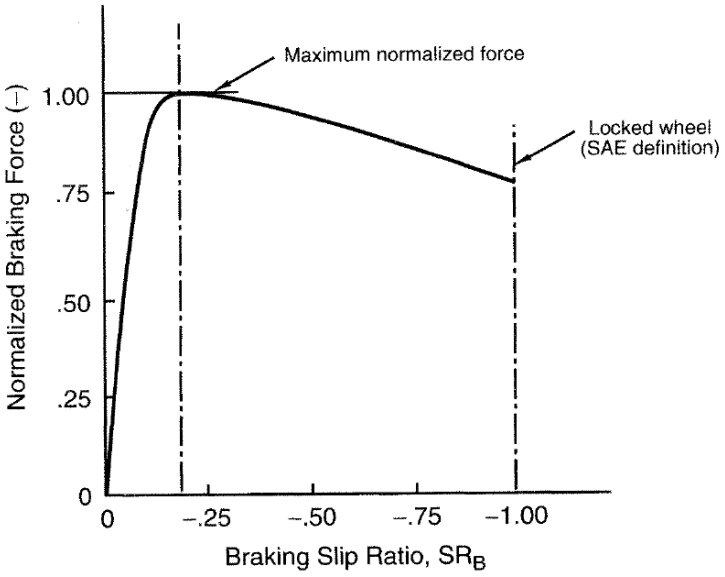

Figure 3.4: Braking Force vs. Slip Ratio [57]

A locked wheel (sliding with no angular velocity) results in a Wong slip value of 100% and a corresponding SAE slip value of -100%. Again, the maximum effort under both conditions occurs at some value of slip where part of the contact patch is sliding with respect to the ground.

The linear portion of the longitudinal force/slip ratio relationship may be characterized as the slope of the force/slip line at the origin:

$$F_x = C_i * i \tag{3.4}$$

for a drive torque and

$$F_x = C_s * i_s \tag{3.5}$$

for a braking torque. In the expressions above, C_i and C_s represent the longitudinal stiffnesses of the tire for a braking and driving torque, respectively.

The stiffnesses are defined as:

$$C_i = \left.\frac{\partial F_x}{\partial i}\right|_{i=0} \tag{3.6}$$

$$C_s = \left.\frac{\partial F_x}{\partial i_s}\right|_{i_s=0} \tag{3.7}$$

F_x - longitudinal force due to slip

i - slip ratio, driving torque

i_s - slip ratio, braking torque (skid-slip)

The longitudinal stiffness values are useful for understanding both tire behavior at low slip angle values and the impact of tire parameters and operating conditions on tire force generation. The impact of various tire parameters is often characterized by how the tire stiffness values are affected.

3.1.2.3 Lateral Force vs. Slip Angle

There exists a relationship between slip angle and cornering force ($F_{y\alpha}$) that is very similar to the relationship between longitudinal slip and tractive effort. This is shown below in Figure 3.5.

Similarly to longitudinal force, lateral force initially increases with slip angle linearly, enters a transition region, reaches a peak value, and then begins to decline as slip angle continues to increase. Understanding this relationship is critical for maximizing vehicle (tire) performance in cornering. The cornering stiffness of the tire may be characterized in the same way as the longitudinal

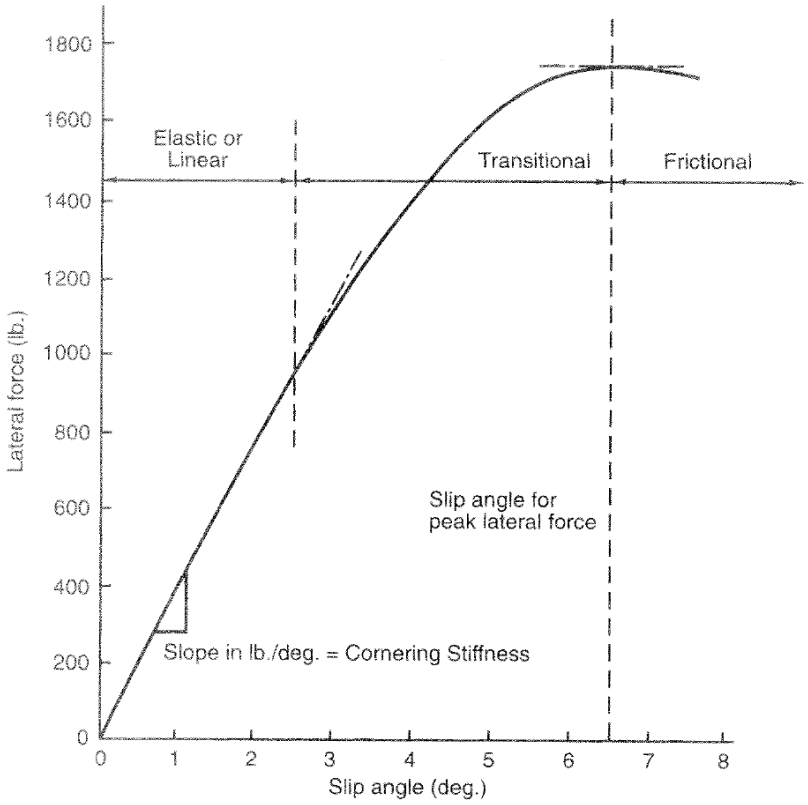

Figure 3.5: Lateral Force vs. Slip Angle [57]

stiffness:

$$F_{y\alpha} = C_\alpha * \alpha \tag{3.8}$$

where C_α is:

$$C_\alpha = \left.\frac{\partial F_{y\alpha}}{\partial \alpha}\right|_{\alpha=0} \tag{3.9}$$

$F_{y\alpha}$ - lateral force due to slip angle

The above expressions are only valid for the linear range of behavior.

3.1.2.4 Tire Load Sensitivity

The lateral force generation characteristics of a pneumatic tire are a function of the normal load on the tire. However, this relationship is nonlinear. As normal load increases, the lateral force (as a function of slip angle) increases but at a diminishing rate [57] as shown in Figure 3.6. As a result the lateral force coefficient, F_y/F_z, decreases as normal load increases.

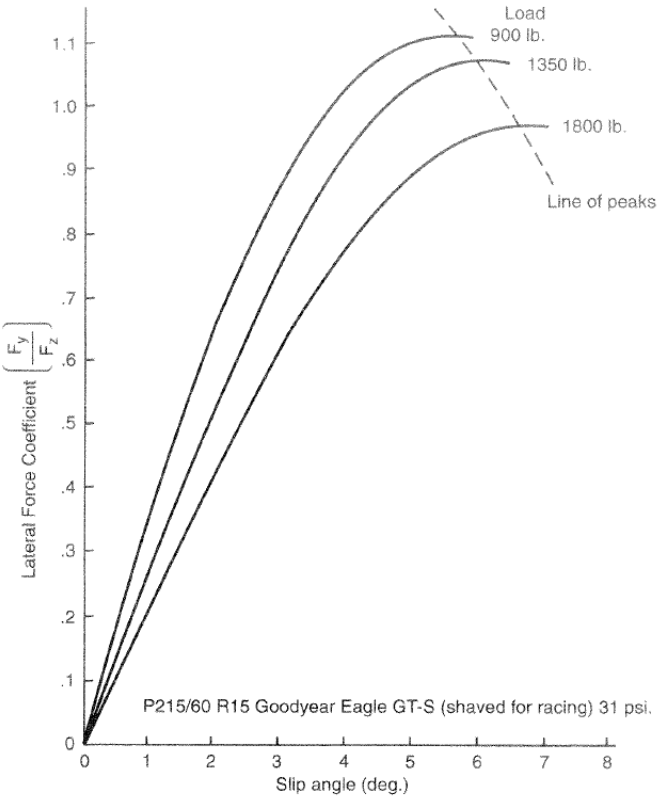

Figure 3.6: Lateral Force Coefficient vs. Slip Angle [57]

This aspect of tire behavior affects the characteristics of vehicle motion during transient motions. Weight transfer between two identical tires on an

axle (as a result of a chassis acceleration) will result in a decrease in cornering capability of the unloaded tire and an increase in capability of the loaded tire, but the overall cornering ability of the axle is reduced. In other words, the gain in cornering capability of the loaded tire is always less than the loss in cornering capability of the unloaded tire due to the nonlinear relationship. As a result, weight transfer is undesirable if maximum performance is required.

3.1.2.5 Tire Camber and the Effects on Lateral Force

The previous discussion of tire forces assumes that the plane of the wheel (X-Z) is perpendicular to the road surface. However, this is not always (if ever) the case. The inclination of the tire plane with respect to the ground plane is the tire camber, γ, defined as positive when the tire is tilted away from the vehicle chassis as shown in Figure 3.7. Generally speaking, a tilted, free-rolling wheel exhibits a lateral motion component in the direction of the angle of inclination. A rolling wheel that is constrained laterally develops a lateral force component in response to the inclination. The contact patch, curved for a static, loaded tire, is "forced" to straighten out as the tire rolls due to the lateral motion constraints of the suspension. This force, referred to as camber thrust, adds to the lateral force developed by a tire [87].

Some camber is desirable for several reasons. From a cornering perspective, camber in the direction of the turn increases the cornering capability of the vehicle. However, the complete implications of camber in cornering scenarios would require a discussion of suspension kinematics. For the purposes

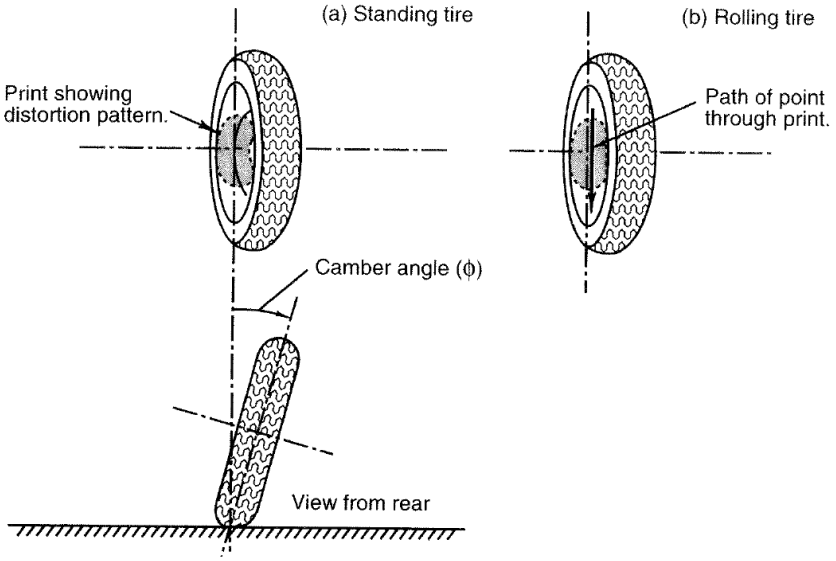

Figure 3.7: Contact Patch Distortion Due to Camber [57]

of the discussion in this chapter, it is important to recognize that some camber is desirable but excessive camber has negative effects on tire performance. Camber distorts the contact patch of the tire, resulting in potentially excessive heat build-up due to the greater and increasingly non-uniform carcass distortion [87]. Excessive heat generation reduces tire capability and lifespan.

The camber/camber thrust relationship is also nonlinear but the initial change in thrust with respect to camber may be defined as:

$$C_\gamma = \left.\frac{\partial F_{y\gamma}}{\partial \gamma}\right|_{\gamma=0} \tag{3.10}$$

C_γ - camber stiffness of the tire

$F_{y\gamma}$ - camber thrust

Camber stiffness is typically significantly less than the cornering stiffness under similar conditions [57]. Tire type, geometry, and operating condition affect camber stiffness to a great degree as shown in Figure 3.8.

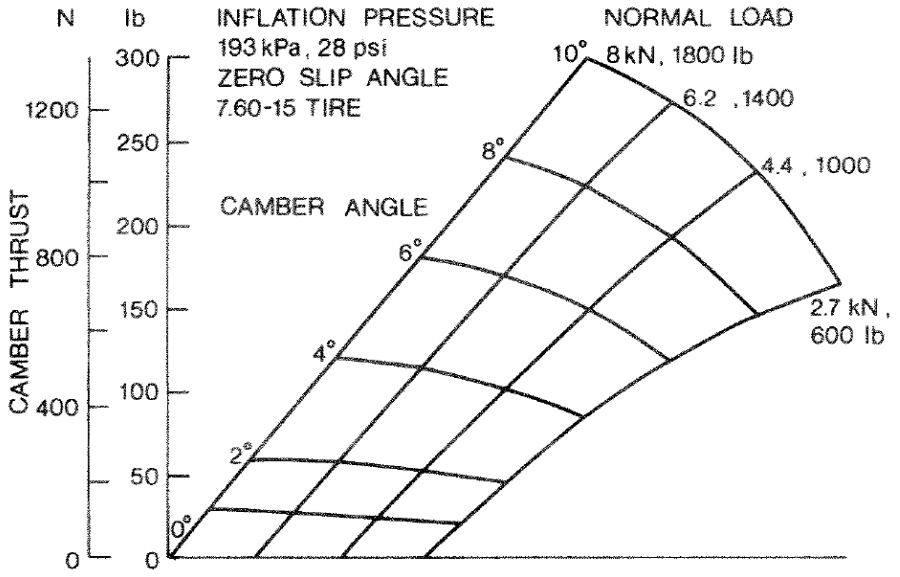

Figure 3.8: Variation of Camber Thrust with Camber Angle and Normal Load for a Car Tire [87], Originally From [65]

As camber force increases with camber angle, eventually the curve drops off. This drop off may occur at a camber angle greater than 5° for wide, passenger car tires (radial) while the camber force drop off may occur at angles greater than 50° for motorcycle tires (bias-ply) [57].

In addition to adding to the lateral force capability of a tire, camber also affects the load sensitivity of the tire. Increased camber causes the sensitivity curves (lateral force vs. load) to "rotate", affecting the peak performance capabilities of the tire.

3.1.3 Rolling Resistance

Rolling resistance is a moment, M_y, about the Y axis that opposes a driving torque. Hysteresis losses, caused by the deflection of the tire tread, are the primary cause of rolling resistance. Most losses are concentrated in the belt/tread region [87].

Tire deflection and distortion result in an uneven distribution of pressure in the contact patch. The center of pressure moves forward as a tire rolls and a moment is produced that opposes forward motion. The resulting horizontal force is the rolling resistance. The ratio of rolling resistance to normal tire load is the coefficient of rolling resistance.

Rolling resistance is affected by tire construction as well as vehicle operating conditions as shown in Figure 3.9.

Bias ply tires exhibit higher rolling resistance values due to the flexing/rubbing of the diamond shaped rubber elements in between the cords. Radial tires do not exhibit this same behavior and, as a result, dissipates as little as 60% of the power dissipated by a bias ply tire under similar conditions [87].

Rolling resistance values are sensitive to speed, inflation pressure, and road surface as shown in Figure 3.10.

Higher speeds result in more deformation of the tire (rolling resistance increases) and higher pressures result in less deformation (rolling resistance decreases). Smooth, prepared surfaces result in smaller tire losses while rough,

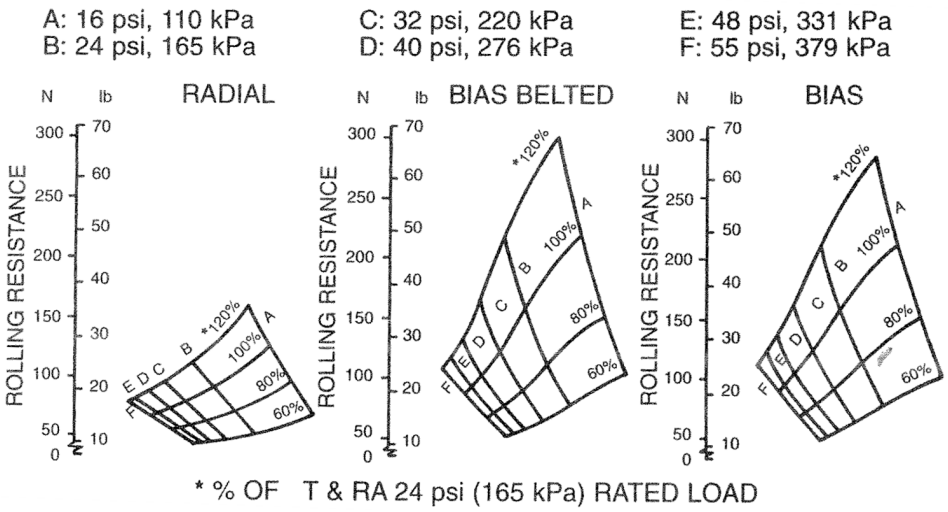

Figure 3.9: Variation of Rolling Resistance of Radial-Ply, Bias-Belted, Bias-Ply Tires With Inflation Pressures and Load [87], Originally Reproduced from [21]

deformable, or wet surfaces result in greater tire loses. All of these relationships are nonlinear and difficult to quantify. Understanding rolling resistance is critical for addressing vehicle losses and motion efficiencies.

3.1.4 Aligning Torque

The distribution of stresses in the tire contact patch is not uniform, and as a result, the point of application for lateral force and the center of the contact patch are not equivalent. This difference, referred to as pneumatic trail, results in a moment about the steering axis, M_z. Generally, the application of lateral force happens behind (aft) of the center of the contact patch and the resulting moment resists steering effort, i.e., the result is a self-aligning torque about the steering axis. Once again, this behavior is non-linear.

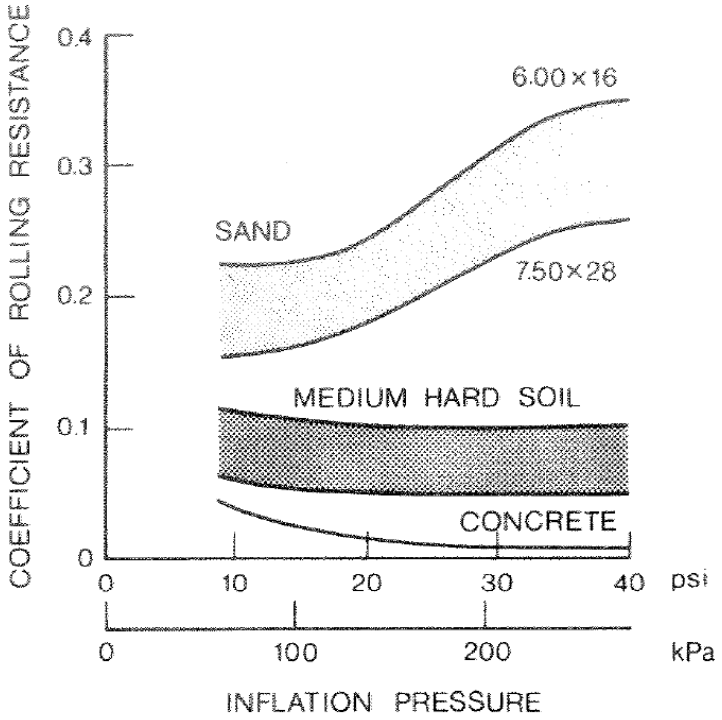

Figure 3.10: Variation of the Coefficient of Rolling Resistance with Tire Inflation Pressure on Various Surfaces [87], Originally Reproduced from [79]

Self aligning torque generally increases with slip angle, peaks, and then declines in a manner similar to the lateral force/slip angle relationship. In addition, self aligning torque increases with increasing driving wheel torque. Generally speaking, self aligning torque is affected by any tire parameter or operating condition that affects the size of the contact patch as alterations to the shape of the contact patch affect the pneumatic trail (self aligning torque moment arm).

At high slip angles and the transition out of the linear region of lateral

force generation, self aligning torque decreases as sliding begins in the rear of the contact patch. At lateral force breakaway (peak of the lateral force curve) the self aligning torque reduces to zero or may even change sign, causing steering instability. This reduction in aligning torque provides a significant source of feedback to the driver of a conventionally steered, performance ground vehicle.

There exist other types of trail that result in self aligning torque. Caster, or the inclination of the steering axis (positive if inclined rearward), results in a point of intersection of the steering axis and the ground plane that is forward of the center of the contact patch and tire force application, as shown in Figure 3.11. The offset of the point of steering axis intersection and the center of the contact patch is referred to as mechanical trail.

The total trail is then a summation of pneumatic and mechanical trail. Though pneumatic trail typically dominates this summation, pneumatic and mechanical trail are generally designed to be in a balance. Mechanical trail provides a positive self aligning torque at peak cornering values, avoiding conditions of steering instability.

3.1.5 Combined Operating Conditions

A tire rarely operates under a purely lateral or purely longitudinal force condition. Tires almost always operate under conditions of combined loading, complicating the issue of understanding and predicting tire performance. Milliken and Milliken [57] present an analysis and discussion of a set of combined

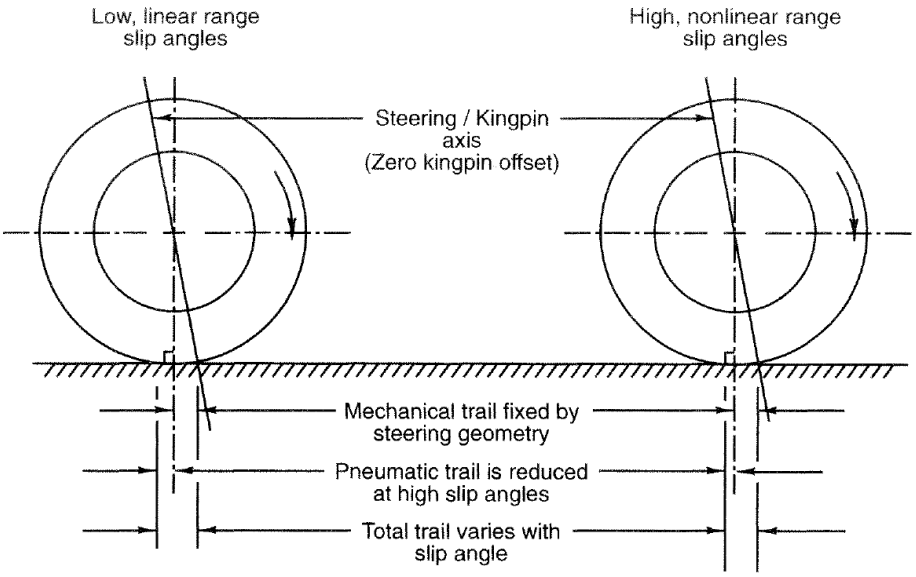

Figure 3.11: Mechanical and Pneumatic Trail [57]

loading data taken by H. Sakai [76]. The data utilize a definition of slip that differs slightly from the Wong and SAE definitions. The Sakai definition for slip in traction is:

$$s_t = [\frac{V \cos \alpha}{\Omega R_e}] - 1 \tag{3.11}$$

And the equation for slip in braking is:

$$s_b = 1 - [\frac{\Omega R_e}{V \cos \alpha}] \tag{3.12}$$

where Ω represents the angular velocity of the tire. Using this definition of slip, Sakai presents several plots of combined loading conditions. Figure 3.12 is a plot of the effect of slip angle on traction/braking forces and slip ratio. Figure 3.13 is a plot of the lateral force against the slip ratio and slip angle.

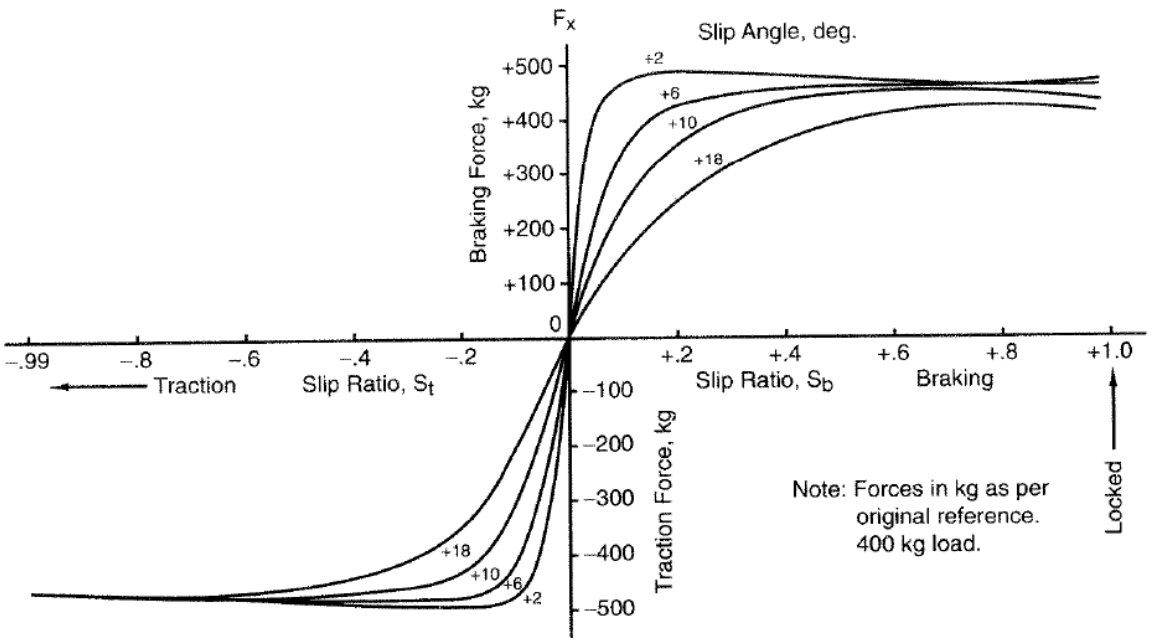

Figure 3.12: Longitudinal Force vs. Slip Ratio and Slip Angle [57], Data Originally from [76]

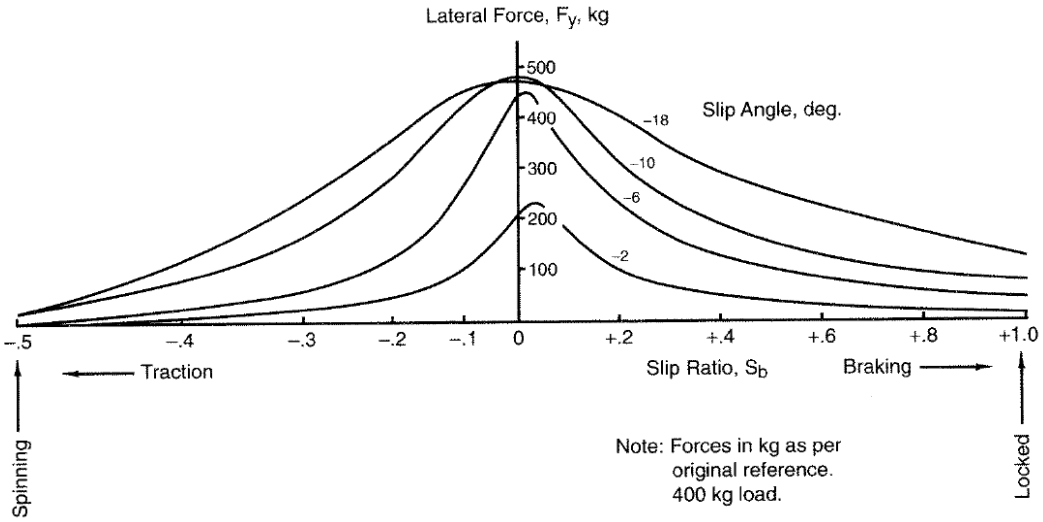

Figure 3.13: Lateral Force vs. Slip Ratio and Slip Angle [57], Data Originally from [76]

These plots show the complexities of tire performance under combined operation (lateral and longitudinal slip). For example, the data shown in Figure 3.12 indicate that peak braking forces occur at higher slip ratios as slip angle is increased. In other words, increased steering angle requires a corresponding increase in slip ratio in order to maximize traction. Figure 3.13, showing the lateral force/slip angle/slip ratio relationship, indicates that the rate at which lateral force increases with slip angle decreases as slip ratio increases. This relationship is more clearly indicated in the following figure, a different plot of the same data shown in Figure 3.14.

The data indicate that cornering (lateral) stiffness decreases as slip ratio increases. Similar to Figure 3.14, Figure 3.15 is a different representation of Figure 3.12 and shows the impact of slip angle on braking capability more

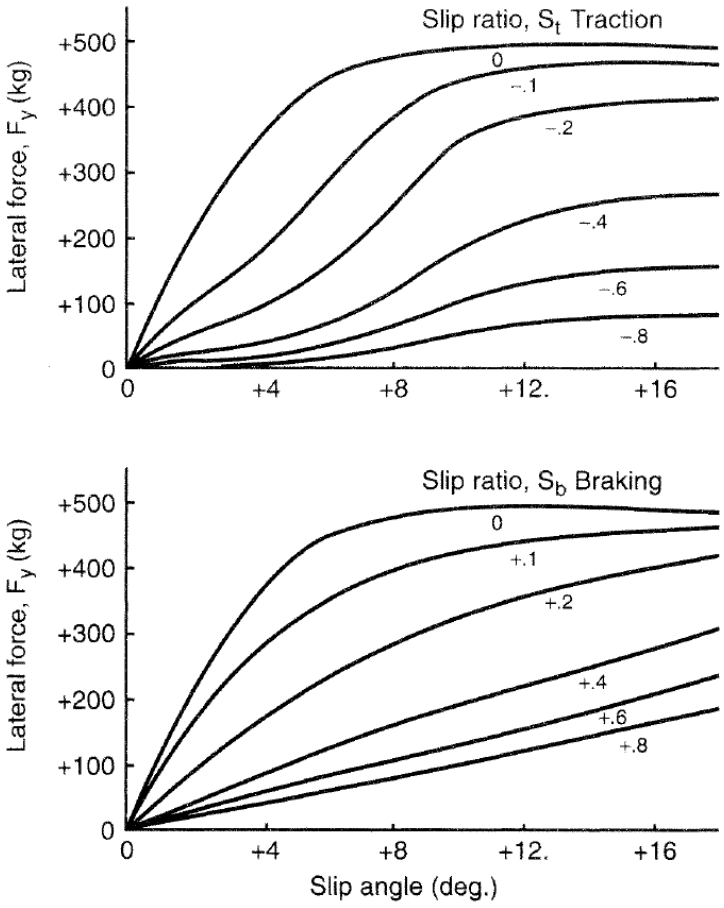

Figure 3.14: Effect of Slip Angle and Slip Ratio on Lateral Force [57], Data Originally from [76]

clearly.

Braking and tractive capabilities are negatively impacted by increasing slip angle. The data from these plots can be combined to form a complete graphical representation of the tire - the friction ellipse.

3.1.5.1 Friction Ellipse

The friction ellipse is a single representation of the lateral and longitudinal force capabilities (limits) of the tire. Each friction ellipse is valid only for a given set of operating conditions (tire pressure, normal load, surface type, etc.). The friction ellipse is sensitive to all of the conditions and factors that affect any aspect of tire force generation (speed, load, pressure, temperature, etc.). An example, taken from Sakai data as discussed previously, is shown in Figure 3.16.

The horizontal axis represents lateral force and the vertical axis represents longitudinal force. The performance of the tire for a given slip condition (slip ratio and slip angle) may be read from the diagram. For this example, point "A" on the diagram indicates that the vehicle is operating at a slip angle of 4° and a slip ratio of -0.36 (Sakai slip convention), approximately. The corresponding force values on the diagram indicate that this operating point results in approximately 800 lb. of lateral (cornering) force and 500 lb. lateral force in braking. In comparison, point "B" represents the maximum lateral force capable for this operating condition - approximately 1100 lb. lateral force with zero corresponding slip ratio (no longitudinal force generation). It should

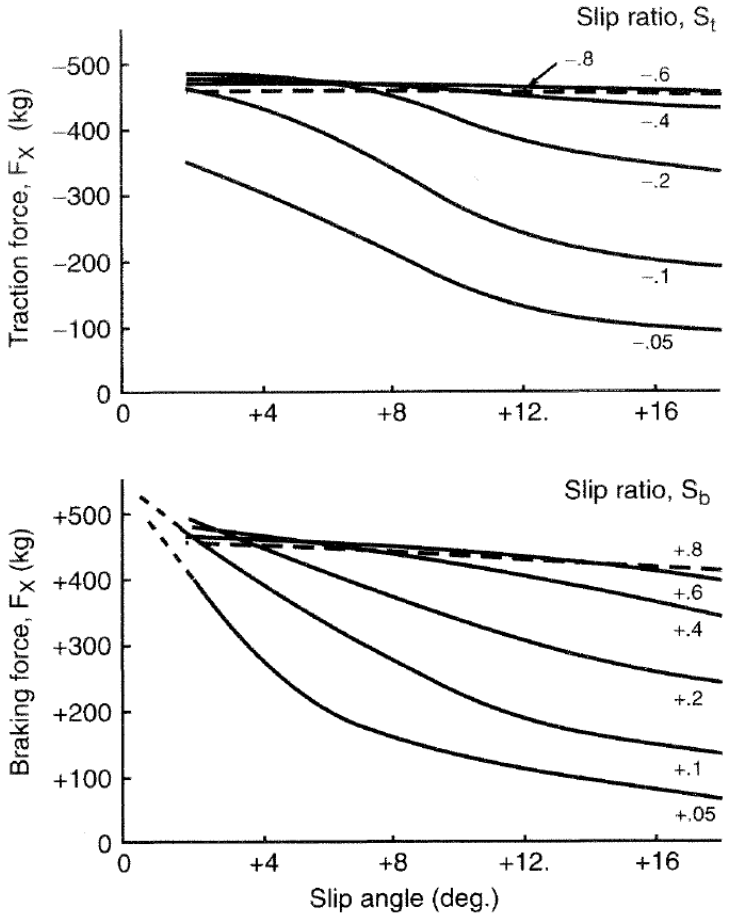

Figure 3.15: Effect of Slip Angle and Slip Ratio on Traction/Braking Force [57], Data Originally from [76]

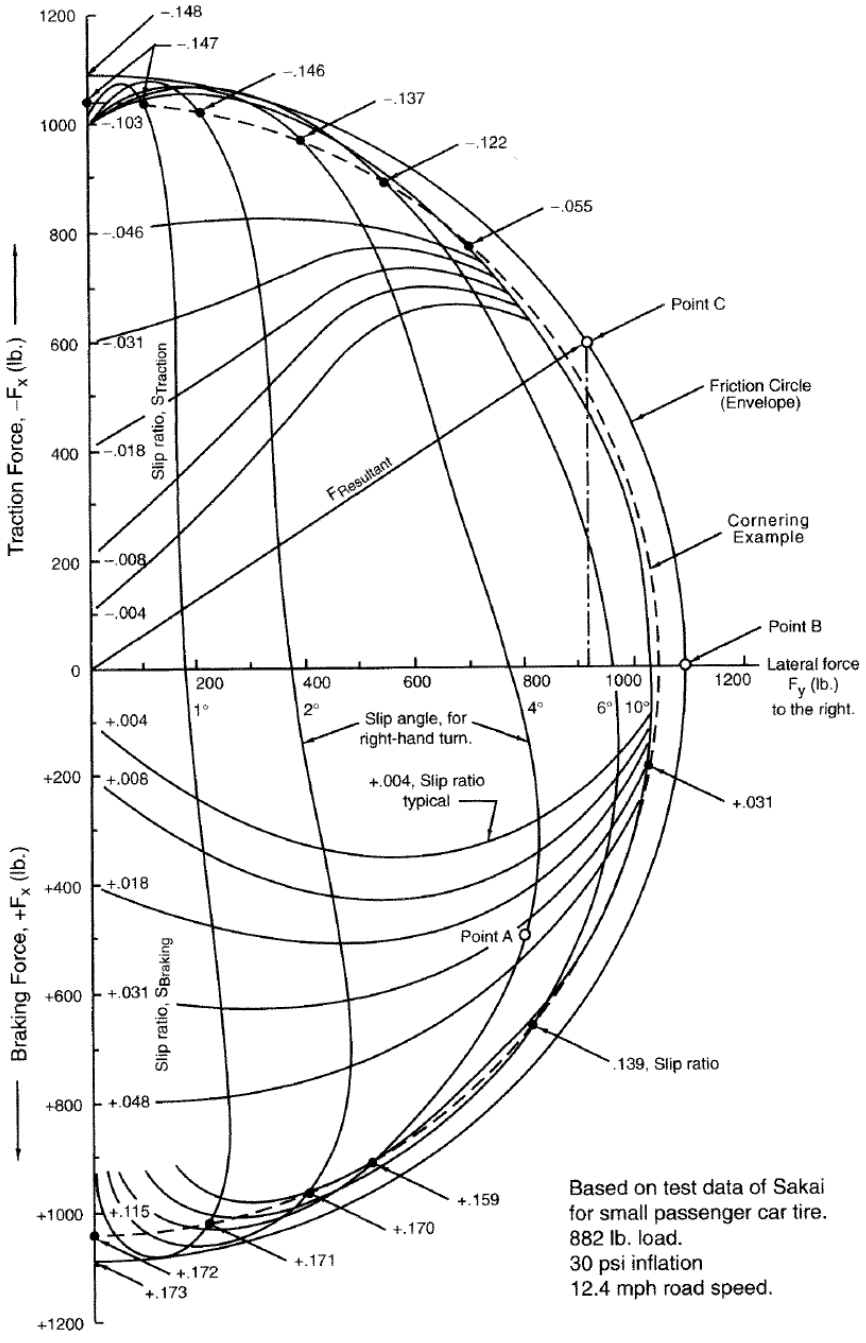

Figure 3.16: Friction Circle Diagram [57], Data Originally from [76]

be noted that the slip angle curves of Figure 3.16 curve back in at the top and bottom of the diagram. This behavior indicates that the tire has exceeded the longitudinal force generation capability.

They key point of the friction circle is that the maximum combined loading condition of a pneumatic tire can be (roughly) approximated by a circle or ellipse. Utilizing the full traction potential of the tire requires operating at a condition close to the edge of the diagram. For example, when considering a racecar driver approaching a corner, rather than maximize straight line braking force approaching the corner, maximum lateral force through the corner, and maximum longitudinal force exiting the corner, the driver should make a gradual transitions from braking to cornering to longitudinal acceleration, thereby operating on the edge of the traction circle and fully utilizing the capabilities of the tires [77]. This behavior is illustrated in Figure 3.17.

The control inputs required of the driver can be read from the friction ellipse for a given cornering operation [57]. However, the ellipse is a complex plot and completely characterizing combined tire forces for all or most tire operating conditions is a complex task because the specific curves of the ellipse are dependent on tire pressure, normal load, speed, etc. Fully characterizing a tire (or set of ellipses) requires recording tire data for a wide range of normal loads, vehicle speeds, tire pressures, etc., which is a complex and expensive task.

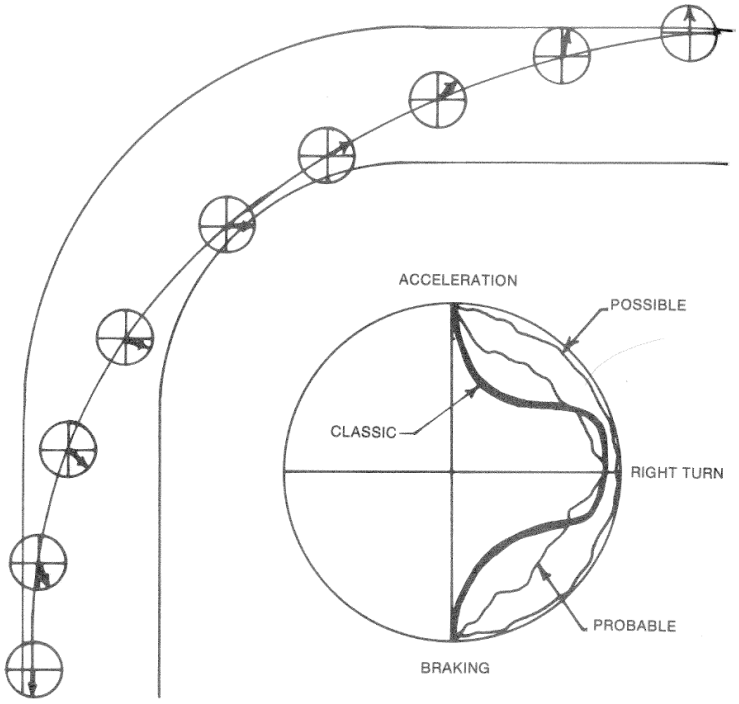

Figure 3.17: The Traction Circle and the Tire Force Vector Around a Corner [77]

3.2 Off-Road Characteristics of Tires: Terramechanics

Tire performance is heavily dependent on the type of terrain on which the tire is operating. In the discussion of tire behavior in the previous section, it was assumed that the terrain was smooth and non-deformable. Unprepared terrain (deformable), however, does not behave the same way under certain loading conditions as prepared terrain. As military vehicles are expected to operate on both prepared (on-road) and unprepared (off-road) surfaces, an understanding of off road tire mechanics is essential in order to construct a

complete representation of ground vehicle operation.

3.2.1 The Influence of Soil Mechanics

The contact patch area and pressure distribution of a pneumatic tire operating on deformable terrain vary with soil attributes (hard/soft, density, cohesion, etc.). The size of the contact area and the corresponding pressure distribution must be known in order to determine stress distributions in the terrain. The performance of the vehicle may then be evaluated or predicted from the attributes of the contact patch, pressure distributions, and soil parameters. Tire tread geometries further complicate the issues of ground pressure and stress distributions. Off-road tires with significant tread protrusions (grousers) cause stress concentrations in the contact patch and result in pressure distributions that vary significantly depending on the softness of the terrain.

Soil dynamics are complex and soil types may differ significantly between geographic regions, or even within the same region. Weather may also affect soil dynamics. As a result, developing widely applicable models for soil behavior under loading from vehicle running gear is difficult. Several techniques, however, have been developed for approximating stress distributions in soil. For example, J.Y. Wong describes several techniques for modeling terrain behavior: modeling the terrain as an elastic medium, modeling as a plastic medium, critical state soil mechanics, finite element analysis, and discrete element analysis [86]. Each process has limitations but does, for specific

soil and operating conditions, provide insight into soil stress states and deformation. While a thorough discussion of modeling methods is outside of the scope of this report, it is important to recognize the complexities in assessing the behavior of deformable terrain.

3.3 Implications for Vehicle Architectures

The overall impact of tire nonlinearities and the complexity of the tire/surface interaction is that a modern ground vehicle utilizing passive vehicle components represents a broad compromise between a variety of design and performance goals. The passive nature of the vehicle components requires all of the vehicle operating and performance characteristics to be decided during the initial design process. For vehicles with a narrow range of expectations or operating requirements, such as a commercial transport vehicle, meeting performance requirements with passive system elements does not require a significant compromise in capability. Transport vehicles operate most often under near steady-state conditions with minimal system disturbances and passive system elements (drivetrain and suspension) are often sufficient for acceptable system performance (unless the vehicle is operating in adverse weather conditions). Designing passive system elements for a vehicle with a broad range of requirements, such as a military ground vehicle, however, is a significant challenge. Military ground vehicles are often expected to operate both on-road and off-road while maintaining an acceptable level of performance. Designing passive suspension elements to apply tire forces on deformable and

non-deformable terrains often results in a system that fails to fully (or even partially) exploit the tire/terrain behavior in either case. The result is a vehicle that does not fully utilize the tire in any condition, a condition that may not impact the performance of a commercial transport but might result in serious liability for a military ground vehicle.

3.3.1 Tire Performance Maps

The application of intelligent actuation to ground vehicles as described in Chapter 2 will allow the vehicle to fully exploit the capability of the tire potential. In other words, intelligent actuation will allow the vehicle system to maximize traction, minimize rolling resistance etc. for the desired operating condition as directed by the human operator, regardless of the level of combined slip or force generation. However, fully utilizing the capability of the pneumatic tire will require the complete characterization of the tire capability. This may be achieved through the development and utilization of performance maps as described by Ashok and Tesar in [10]. In this work, the authors present a method of combining a variety of performance maps to create a visual decision surface that may be used to optimize a system for a desired criterion or set of criteria. An example of this process may be seen in Figure 3.18, which illustrates the combination of a variety of performance maps of a switched reluctance motor to provide a decision surface that may then be evaluated by the operator.

As a result of the highly nonlinear behavior of pneumatic tires as illus-

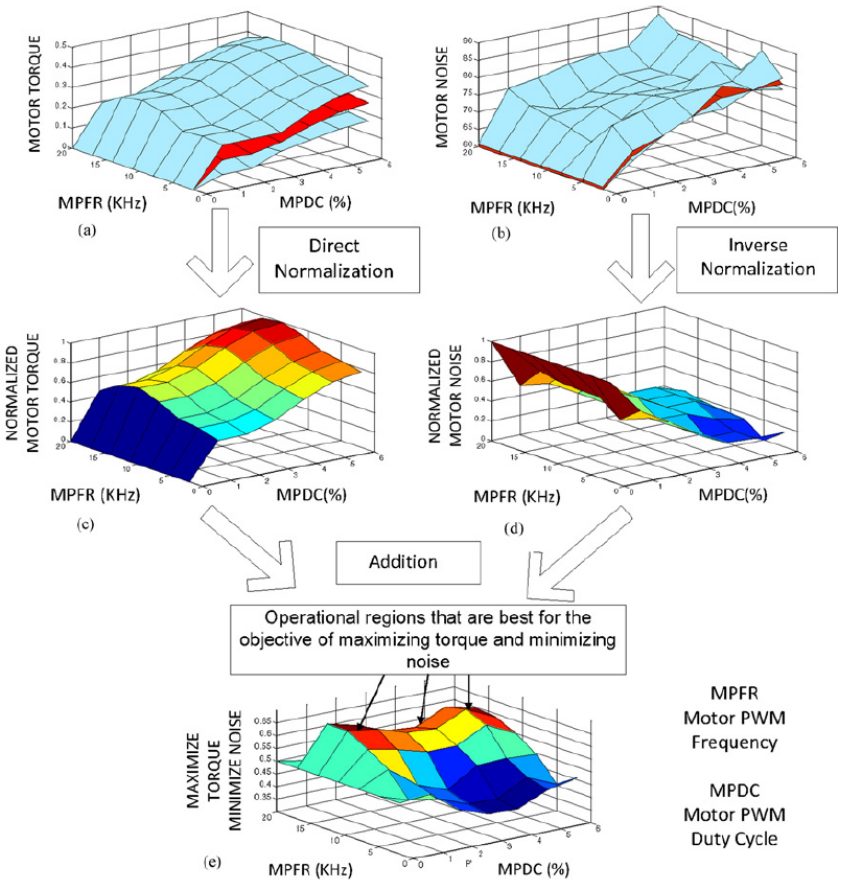

Figure 3.18: Performance Map Combination for a Switched Reluctant Motor [10]

trated in Figures 3.9 and 3.10, the application of performance maps is necessary for optimizing tire behavior. This must be done for both non-deformable (on-road) and deformable (off-road) road surfaces. Performance maps are especially important for characterizing off-road behavior due to the difficulty in quantifying the tire-surface interaction. Providing the optimal slip ratio and slip angle characteristics to the vehicle operator, as will be discussed in Chapter 6, is a critical part of maximizing various criteria. Developing and implementing performance maps for tire behavior will not only allow intelligent actuation technology to apply the tire to the road surface at the performance limit, but will also allow the vehicle system to provide the status and performance margins of the tire (depending on the road surface and loading condition) to the vehicle operator in real time.

3.4 Chapter Summary

This chapter discusses the complexity of pneumatic tires and the need for a complete characterization of tire behavior for a range of operating conditions and road surfaces through the real-time use of embedded performance maps. Table 3.1 presents the key findings, conclusions, and recommendations of the chapter.

Table 3.1: Chapter 3 Key Findings, Conclusions, and Recommendations

Result	**Conclusion**	**Recommendation**
The **pneumatic tire** is the only interface wheeled vehicles have with the road surface and serves as the only method for the application of tractive effort.	Tire force generation must be understood in order for the vehicle to effectively respond to the commands of the operator.	The behavior of the tire should be completely characterized in order for the total traction potential to be exploited.
Tire force generation is characterized by tire slip - slip angle and slip ratio. This relationship is nonlinear as shown in Figures 3.3 and 3.5, and is a function of tire construction, inflation pressure, load, etc.	The nonlinear nature of tire force generation requires a complete characterization of tire behavior.	Completely characterizing the behavior of the pneumatic tire requires the generation of numerous performance maps (Figure 3.18).
The **relationship** between normal load on the tire and maximum force generation **is also nonlinear** as shown in Figure 3.6).	This nonlinear relationship between normal load and tractive capability results in a net loss in maximum possible traction as weight is transferred between tires during chassis accelerations.	Tire performance maps must be generated for a range of normal loads in order to fully capture the maximum performance capabilities of each tire.
Lateral tire forces are a function of tire camber. Camber may be optimized for a given cornering scenario. This relationship is also nonlinear (Figure 3.8).	Optimizing camber for a given cornering condition requires active camber actuation.	Active camber should be included as part of the Intelligent Corner Concept (Chapter 4).

Table 3.1: Key Findings, Conclusions, and Recommendations (Continued)

Result	**Conclusion**	**Recommendation**
Tire behavior (force generation and resistances) is a function of tire construction (Figure 3.10).	The results of tire characterization will vary with tire construction (radial, bias, etc.).	Tire performance maps will need to be generated for each type of tire for a wide range of road conditions.
Simultaneous **lateral and longitudinal** force generation affects the force/slip characteristics of the tire as shown in Figures 3.12, 3.13, 3.14, and 3.15.	These effects should be characterized as a tire is frequently operating in a combined loading condition.	Tire performance maps will need to be generated for a range of combined loading conditions.
Combined loading for a pneumatic tire is commonly illustrated by a **friction circle** (ellipse) as shown in Figure 3.16. The loading condition (total force generation) for a given cornering maneuver may be plotted on the friction circle.	The friction circle is an excellent visual representation of the loading condition and traction potential of the tire, but each friction circle is specific to the properties and condition of each tire (pressure, construction, normal load, etc.).	If the friction circle is to be provided to the vehicle operator in order to provide real-time information on vehicle traction capability, tire performance maps should be generated for a sufficient range of types, loads, and operating conditions.

Table 3.1: Key Findings, Conclusions, and Recommendations (Continued)

Result	**Conclusion**	**Recommendation**
The force generation behavior of pneumatic tires is further complicated if the tire is operating over unprepared (deformable terrain). The size and shape of the tire **contact patch will vary** with the **properties of a deformable terrain** (hard/soft, wet/dry, etc.).	As military vehicles are expected to operate regularly on deformable terrains, the behavior of pneumatic tires in off-road conditions must be characterized.	Tire performance maps should be generated for a variety of operating conditions over a wide range of terrain types.
Ashok and Tesar [10] propose a method of combining three-dimensional representations of complex system behavior (performance maps) into a **visual decision making surface**.	The complexities of tire behavior make ground vehicles and ideal subject for the application of this method of system representation and decision making.	Generating performance maps for pneumatic tires will require evaluating a wide range of tire types, inflation pressures, normal loads, combined lateral/longitudinal loading conditions, and terrain types. This is a complicated testing procedure that should be formalized in future work.

Chapter 4

Vehicle Architectures, the Intelligent Corner Vehicle Concept, and the Need for Performance Criteria

4.1 The Modern Wheeled Vehicle

Most modern wheeled vehicles utilize a similar architecture - an internal combustion (IC) engine coupled with a transmission drives some or all of the wheels. Torque is distributed to each axle and wheel though differentials and transfer cases. Each wheel has four degrees of freedom relative to the chassis - three rotational (steering, camber, drive), and one translational (suspension). Suspension and camber orientations are determined by the suspension linkage and the motion of the linkage is controlled by springs and dampers. The suspension springs support the vehicle and dampers create system stability (return it to steady state). Drive and steering are controlled actively by the human operator (driver). The operator provides the control inputs in the form of steering angle and throttle/brake lever position, respectively.

4.1.1 Traditional Actuation of Individual Wheel Motions

The architectures of many military vehicles are similar to those of passenger and commercial road vehicles. Many tactical wheeled vehicles (support,

logistics, transportation) developed before the Iraq War were direct adaptations of commercial vehicles. While direct adaptation is no longer appropriate due to increased payload and protection requirements, the underlying vehicle architectures are still similar. As such, a brief discussion of the typical methods of actuation/control of the four degrees of freedom of the wheel is necessary.

4.1.1.1 Steering

Modern steering systems are typically comprised of a linkage system between the driver input (steering wheel) and the steered wheels of an axle. The steering linkage transforms the rotational input of the steering wheel into a linear translation of the steering link connected to the wheel. The link attachment geometry in turn transforms the linear motion of the link into a rotation of the tire about the steering axis. The linkage rotates the steered tires about the z axis (SAE definition), changing the orientation of the tire with respect to the heading of the vehicle and inducing the generation of slip angles. Note: steering is considered separately from wheel toe angle, which is a (small) static rotation of the wheel about the steering axis, measured at zero steering angle (shown in Figure 4.1). A representative steering system is presented in Figure 4.2.

The wheels of an axle do not remain parallel as they are steered. For vehicles moving at low speeds and low tire slip angles, the inner wheel must assume a greater angle than the outer wheel so that the instant centers of

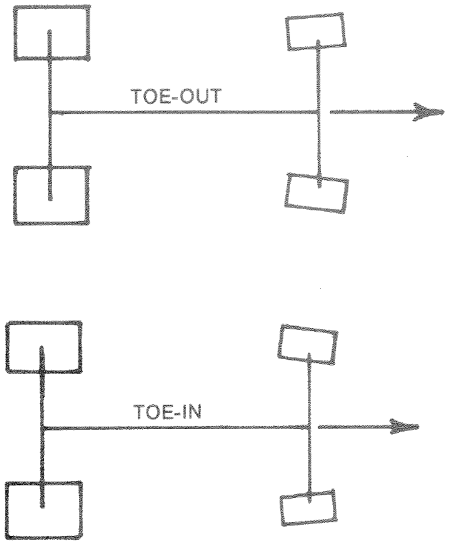

Figure 4.1: Vehicle Toe [77]

motion are equivalent. This steering geometry, Ackermann Steering, is shown in Figure 4.3. This geometry reduces the overall (global) slip and wheel scrub during cornering maneuvers. However, as speeds and lateral forces increase, the influence of tire slip angles and load sensitivity becomes important and standard Ackermann geometry no longer produces an optimal steering arrangement. As previously discussed, the slip angle value that produces the maximum lateral force increases as normal load increases, and as a result, the outside tire (more heavily loaded due to weight transfer) requires more steering angle than the inside tire [57]. This steering geometry (Reverse Ackermann) is typically used on high performance racing vehicles. Passenger and commercial vehicles, which frequently operate at low speeds in parking-lot type maneuvers and don't require maximized performance utilize typical Ackermann Steering

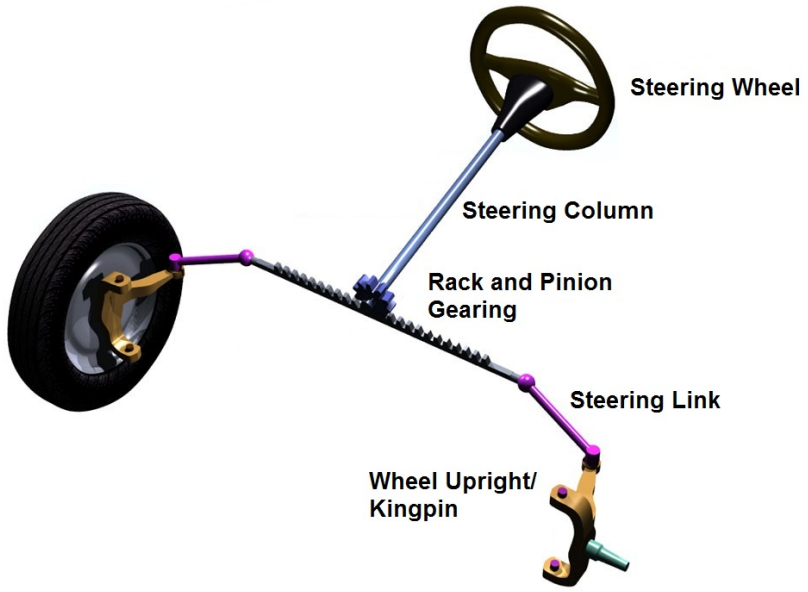

Figure 4.2: Representative Steering Linkage, Modified From [70]

geometries. Overall, the optimal geometry of a steering linkage depends on the expected speeds, loads, and operating conditions of the vehicle.

The steering input (wheel) is connected directly to the wheels and is assisted by a power steering device in most modern vehicles. A representative power steering system is shown in Figure 4.4. The components of this representative system are the 1) vane pump, 2) high-pressure line, 3) cooling circuit, 4) return line, 5) steering gear, 6) steering valve, 7/8) pressure lines to the cylinder, 9) steering column, and 10) steering wheel.

Power steering systems provide positive feedback to the steering input in order to decrease the required steering input force [73]. Active steering systems that regulate steering inputs in order to improve vehicle performance

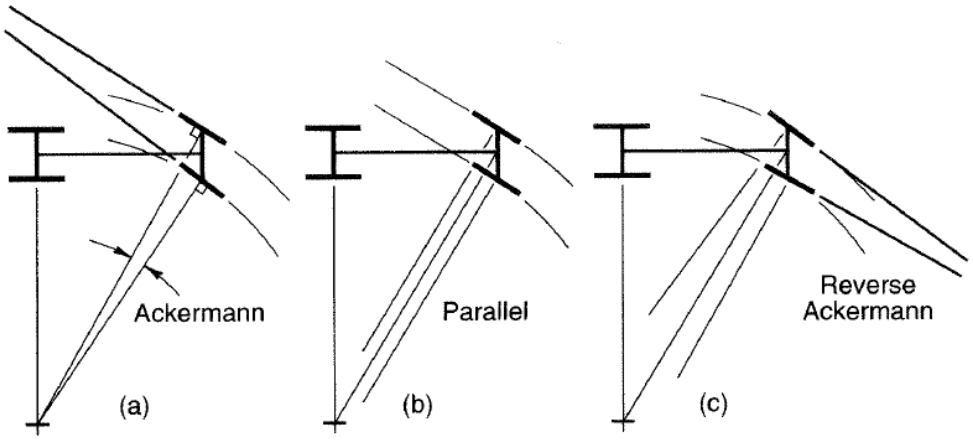

Figure 4.3: Ackermann Steering Geometry [57]

have been studied and implemented on passenger vehicles. In [49], Koehn and Eckrich (BMW Group) present a steering system that utilizes a brushless DC motor to augment the steering linkage gearing, allowing the system to alter the steering input from the driver as shown in Figure 4.5.

The mechanism allows the control system to augment the steering angle input from the driver, thereby providing a variable steering ratio. The system provides a direct steering ratio (small actuator input) at low speeds but reduces the steering ratio at higher speeds in an effort to improve stability and operator control as shown in Figure 4.6. The most convenient steering wheel motions for the operator occur at values less than $\pm 60°$. Operating in this range allows the operator to actively keep both hands continuously on the wheel (no shuffling)

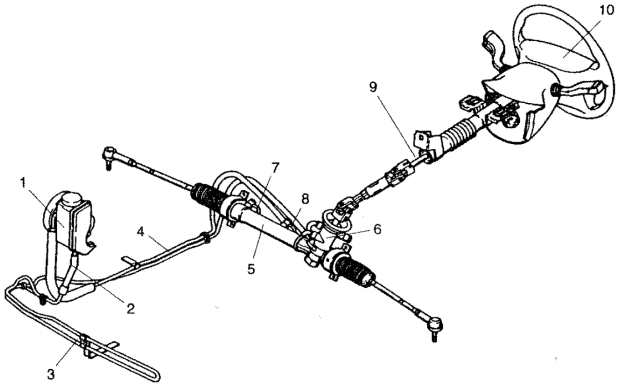

1) Vane Pump
2) High-Pressure Line
3) Cooling Circuit
4) Return Line
5) Steering Gear
6) Steering Valve
7) Pressure Line
8) Pressure Line
9) Steering Column
10) Steering Wheel

Figure 4.4: Representative Power Steering System [73]

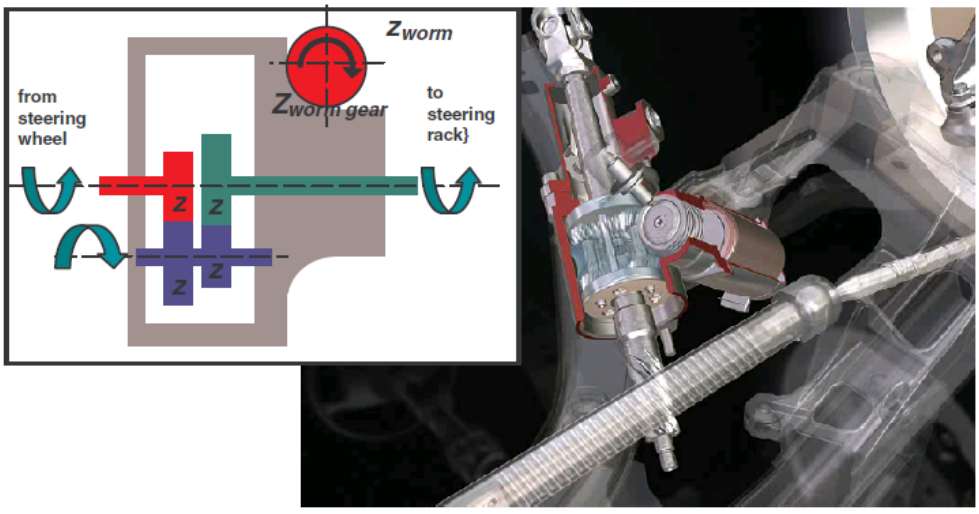

Figure 4.5: Active Steering Mechanical Layout [49]

and, as a result, maximizes the ability of the driver to control the vehicle. The variable steering ratio allows the system to both interpret steering commands in an effort to avoid excessive yaw rates and to provide an optimal steering wheel input range to the operator.

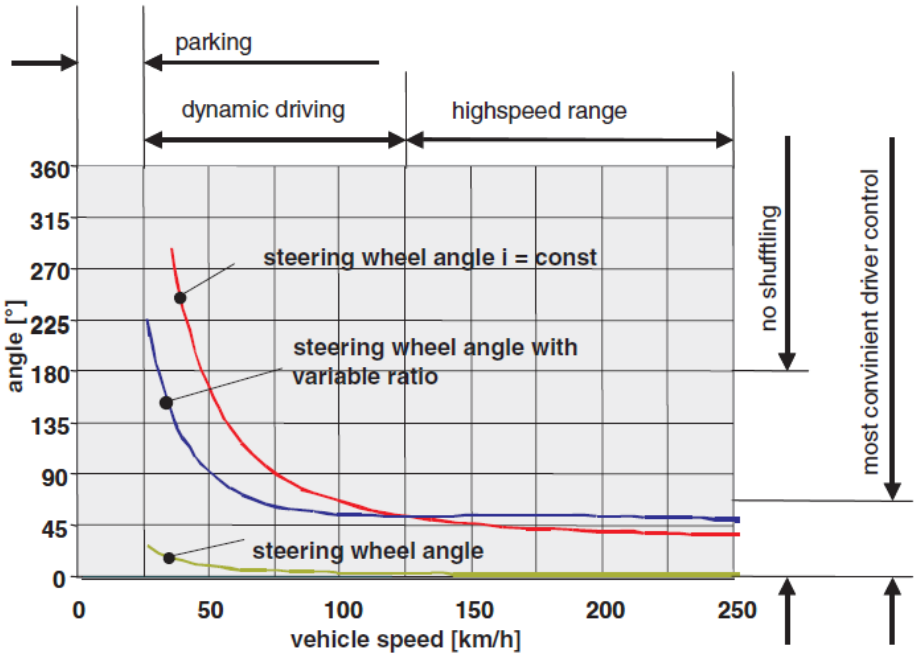

Figure 4.6: Active Steering Ratio Variation [49]

Active steering systems have also been developed for multiple steering axles [45]. In this work, the authors present front and rear steering mechanisms that both utilize DC motors to alter the steering angle input in the front, and to generate appropriate (smaller) steering angles in the rear. Active rear steering may be either in phase (steering the same way) or our out of phase (steering the opposite direction) with the front steering as shown in Figure 4.7.

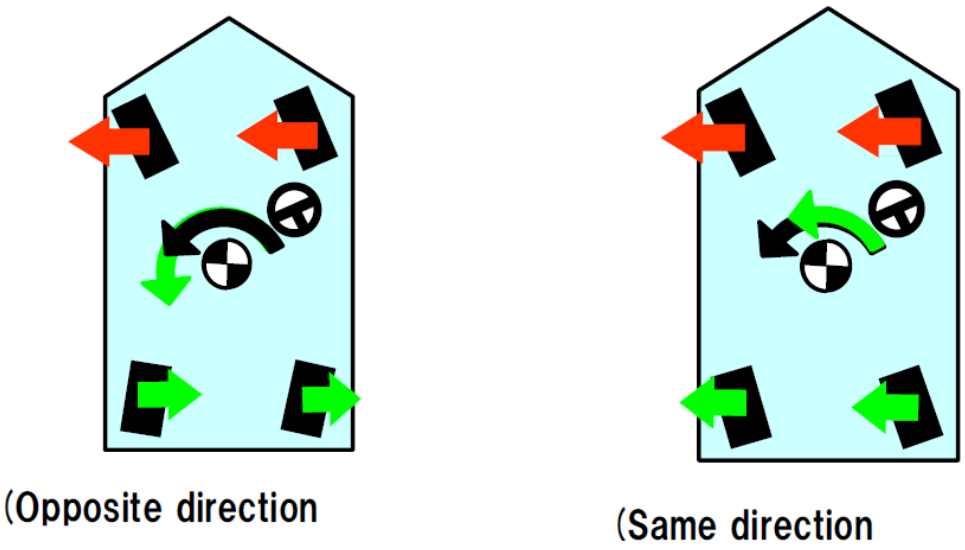

Figure 4.7: Steering Variations for Multiple Steered Axles [45]

The inclusion of the rear wheel steering input allows the control system to address both yaw and lateral motion for a given steering input by the operator. As with the BMW system discussed previously, the front steering ratio and rear steering inputs are both dependent on vehicle speed. A visual representation of the variation of the front steering ratio is shown in Figure 4.8. The gearing ratio varies from a moderate value at low vehicle speeds to "quick" (high gearing ratio) at medium speeds to increase vehicle responsiveness and then to "slow" (low steering ratio) at high speeds to improve vehicle stability. A high gearing ratio results in large changes in wheel angle for small steering wheel inputs, and a low gearing ratio results in low wheel angle changes for large steering wheel inputs. The variation of the desired steering

gear ratio in Figure 4.8 indicates that a moderately high ratio is desirable for low speed, parking lot type maneuvers, a high ratio is desirable for moderate vehicle speeds so that the vehicle responds quickly to the operator ("nimble feeling"), and a low gearing ratio is desirable for high vehicle speeds so that large steering inputs will not result in large wheel motions which may result in vehicle instability ("secure feeling"). Simulations of the resulting system during a lane change maneuver show a reduction in required steering angle input, yaw motion, and lateral acceleration.

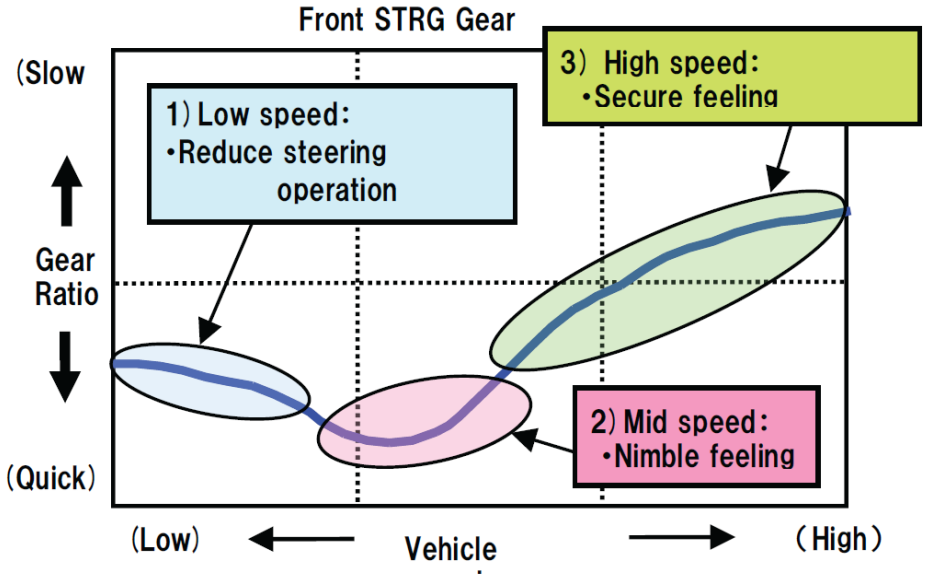

Figure 4.8: Front Steering Gear Ratio [45]

Though these systems can be shown to improve vehicle stability and handling, the traditional steering linkages are retained. As such, while these active steering systems are able to interpret and augment the commands of the

driver (thereby improving vehicle performance), coaxial, steered wheels are still coupled by the linkage and may not be actuated independently. Independently steered wheels are critical for any vehicle that is required to optimize tractive performance while operating over a wide range of operating conditions.

4.1.1.2 Camber

For traditional architectures, camber is dictated by the kinematics of the suspension and is not actuated actively. Some suspension types, such as beam axles (Figure 4.20), result in static camber values while others, such as four bar mechanisms (Figure 4.21), result in camber values that are a function of suspension displacement. As mentioned previously, camber affects cornering capability (lateral force generation) and as such, certain camber values are desirable for certain operating conditions. Passive suspensions attempt to optimize camber values though the suspension displacement, but this process is hindered by a variety of design constraints. As an example, Cuttino, Shepherd, and Sinha present a linkage in [24] that attempts to decouple camber and heave while maintaining appropriate camber for cornering maneuvers. This linkage, the Variable Camber System (VCS) is show in Figure 4.9. In this assembly, the kingpin has three connecting links - one from the chassis (bottom control arm) and two from the suspension linkage on the common "axle." This linkage is unique in that it provides a lateral and vertical input from the opposing wheel.

The vertical input is provided through the roll bar (sway bar) - a chassis

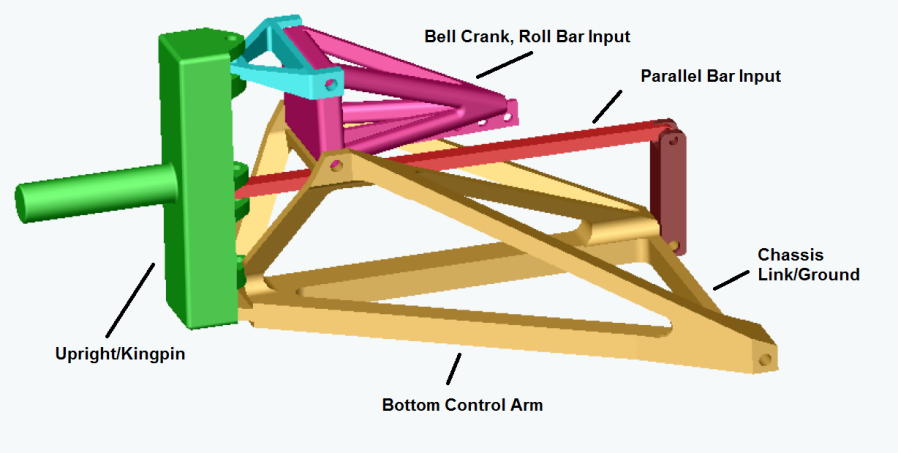

Figure 4.9: VCS Linkage Assembly [24]

mounted torsion bar that opposes asymmetric wheel motion. As one wheel moves vertically, the roll bar applies a vertical force to the opposing wheel, which is applied in this case to the upright via the bell crank. The lateral input is from the parallel bar, which directly connects the rotations of the kingpins on each side of the vehicle. These inputs are more clearly illustrated in Figure 4.10. A comparison of the kinematics of the VCS with a traditional double wishbone suspension (four bar linkage) is shown in Figures 4.11 and 4.12.

The changes in tire camber due to chassis motion are reduced for the VCS linkage. However, while the solution presented offers some improvement over the kinematics of comparable suspension linkages, the presented linkage is complex and may be difficult to implement.

Work has been done on active camber and toe systems with the goal of improving the performance of a high performance sports car [75]. This system

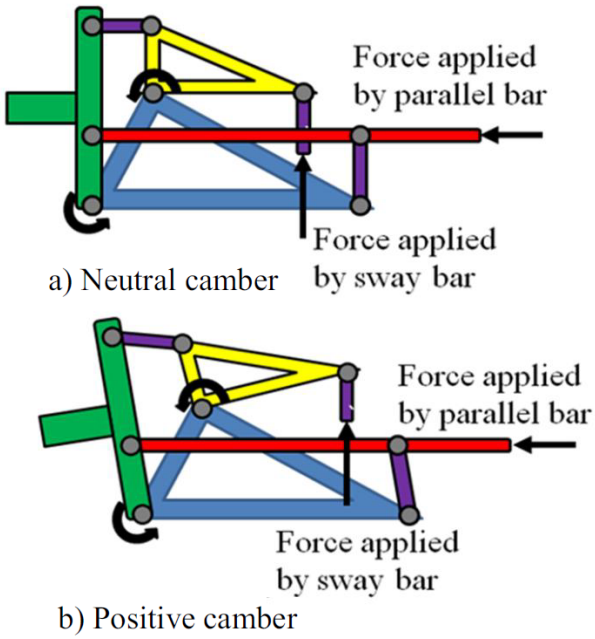

Figure 4.10: Sway Bar and Parallel Bar Inputs for the VCS Linkage [24]

is shown in Figure 4.13.

This system provides a camber variation of $+2/-6^\circ$ and a toe variation of $\pm 2^\circ$. A simulation of the implementation of this system shows improvements in vehicle yaw response due to a sudden steering wheel input (step input). However, the system referenced presents significant packaging challenges (due to the limited available wheel-well area of the sports car chassis) and the cost and complexity limit the application of this technology to less expensive (passenger) vehicles. In addition, the range of motion of the proposed system, while appropriate for relatively stiff, high-performance tires, is not suitable for tires or suspension systems with significant range of motion (e.g. off road tires

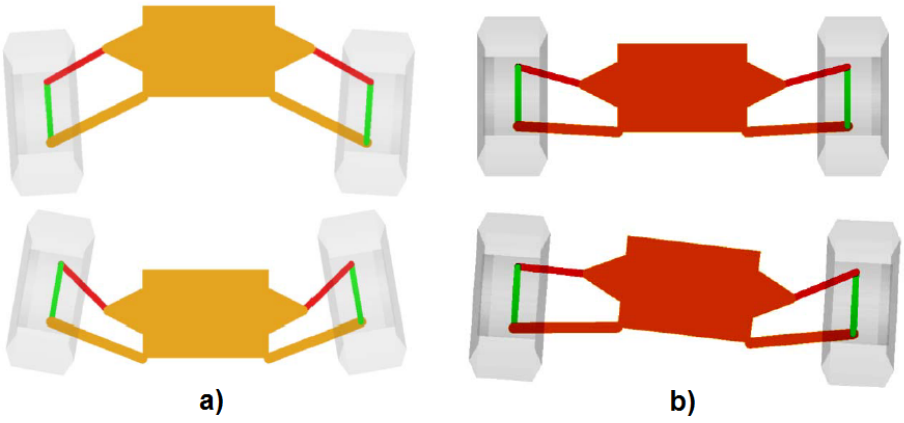

Figure 4.11: Double Wishbone Suspension Experiencing a) Vertical Chassis Motion, b) Chassis Roll (Lateral Acceleration) [24]

that have much lower cornering stiffnesses and the relatively large suspension deflections of military vehicles).

4.1.1.3 Drive

The drive input to each powered wheel is typically supplied by an IC engine coupled with a transmission. The transmission provides gearing choices that enable a set of input/output speed relationships in order to best match the engine dynamics to the vehicle dynamics and operating condition. Figure 4.14 is a visual representation of how the inclusion of a transmission (gearing) affects the ability of the IC engine to apply torque to the road surface.

However, these relationships represent (ideally) linear speed transformations and while there may be several selections, they do not individually react to the commands of the operator. Torque provided by the engine and

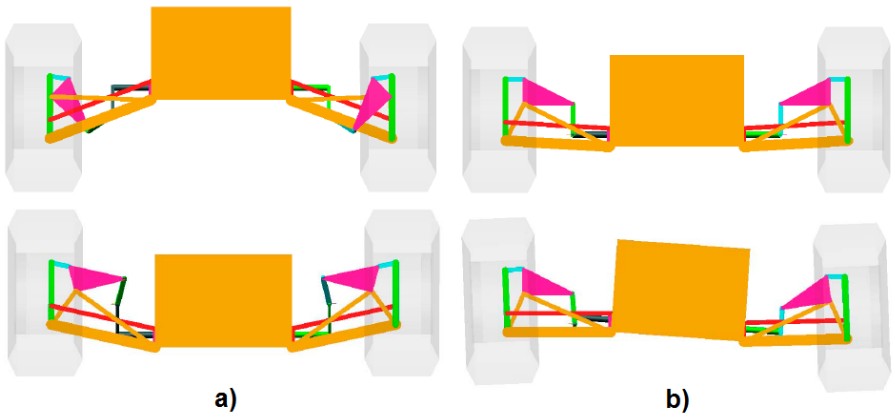

Figure 4.12: VCS Assembly Experiencing a) Vertical Chassis Motion, b) Chassis Roll [24]

transmission is generally applied to drive wheels through some combination of transfer cases and differentials. Transfer cases distribute torque to different drive axles (interaxle distribution) and are utilized in vehicles with multiple drive axles. Transfer cases typically distribute torque at some predetermined percentage (front/rear), depending on the number of drive axles. [1] Differentials regulate torque distribution laterally to symmetric wheel pairs (interwheel distribution).

The use of differentials is intended to equalize the lateral torque distribution while allowing both wheels on one axle to turn at different rates (as is required during a cornering maneuver), thereby avoiding a yaw moment generated by unequal torque distribution. However, because the torque split

[1]The symmetric wheel pairs of ground vehicles are commonly referred to as "axles" regardless of the type of suspension or drive used.

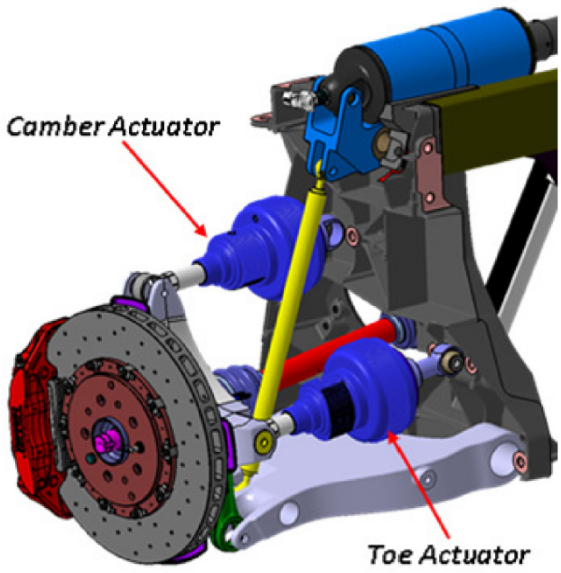

Figure 4.13: Active Kinematics Suspension Assembly [75]

between differentially coupled wheels is equal, the total traction limit of the axle is limited to the lower traction potential of the two wheels. An image of the gearing that allows equal torque distribution (an open differential) is shown in Figure 4.15.

There are several types of differential designs that attempt to impose locking conditions (forcing wheel speeds to be equal) under certain conditions in an effort to avoid loss of traction when a disparity in traction potential occurs [63]. These differentials (limited slip or locking type) reduce penalties from disparate traction conditions but a the torque distribution is no longer equal and a yawing moment is generated. Limited slip differentials with active locking capability have been developed in an effort to improve vehicle handling

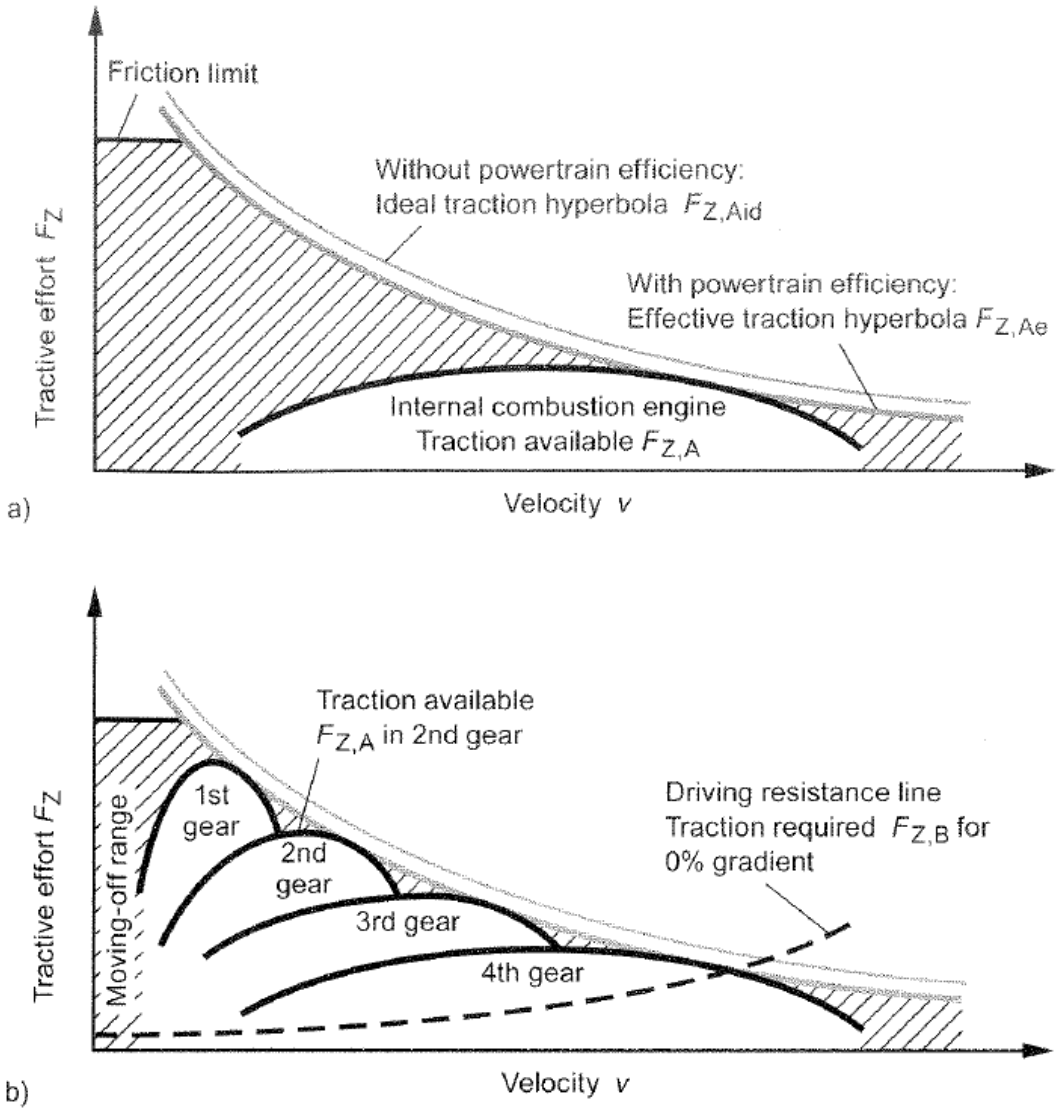

Figure 4.14: Traction Profile, Internal Combustion Engine Without Gearbox (a), and With Gearbox (b) [63]

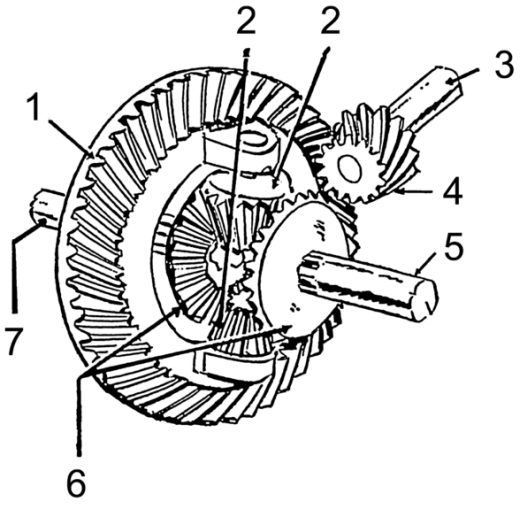

Figure 4.15: Open Differential Gearing [31]

and performance, especially under conditions of non-uniform traction capability [71]. Park, Dutkiewicz, and Cooper in [71] present an active differential system, shown in Figure 4.16 capable of improving vehicle performance by altering the ratio of torque transfer between driven wheels. The difference is readily apparent for a maneuver involving aggressive throttle application and a steering input (causing significant vehicle weight transfer) as shown in Figures 4.17, 4.18 and 4.19. Figure 4.17 shows a comparison between the difference in left/right wheel speeds of the active differential and a passive differential on a split μ surface. Figure 4.18 is an illustration of the longitudinal tire forces of a vehicle with an open differential. In this case, the longitudinal forces experienced by the left and right rear (driven) wheels are the same, but the equal torque split results in wheel spin and reduced overall traction. Figure 4.19 shows the longitudinal forces for the active differential - the differential

distributes more torque to the wheel with more traction, increasing the overall vehicle tractive capability. While the application of active differentials may provide some capability for active torque distribution to powered wheels, the vehicle is still subject to the design restrictions of conventional vehicles (Section 4.1.2) due to the retention of the traditional drivetrain elements.

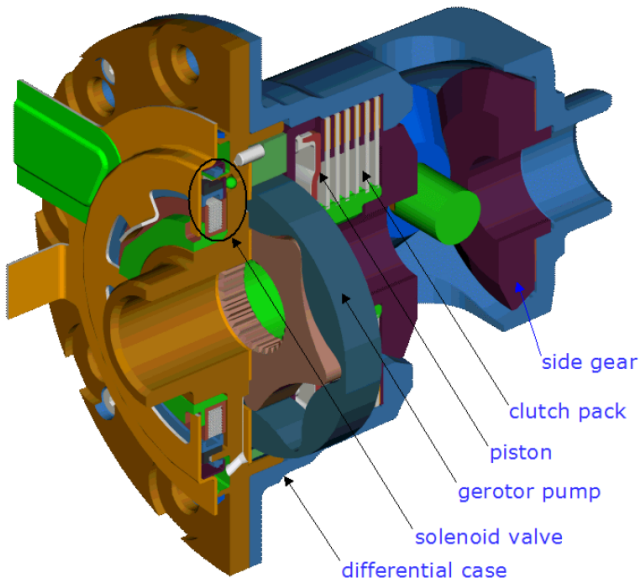

Figure 4.16: Active Limited-Slip Differential, Dana Corporation [71]

This technology is heavier and (most likely) more expensive than traditional differentials. In addition, active differential technology provides the greatest benefit when the vehicle is operating on inhomogeneous terrain that presents a wide range of maximum tractive capability. Most vehicles (commuting passenger vehicles) do not operate on inhomogeneous terrains and do not approach the tractive limits imposed by the road surface As such, most

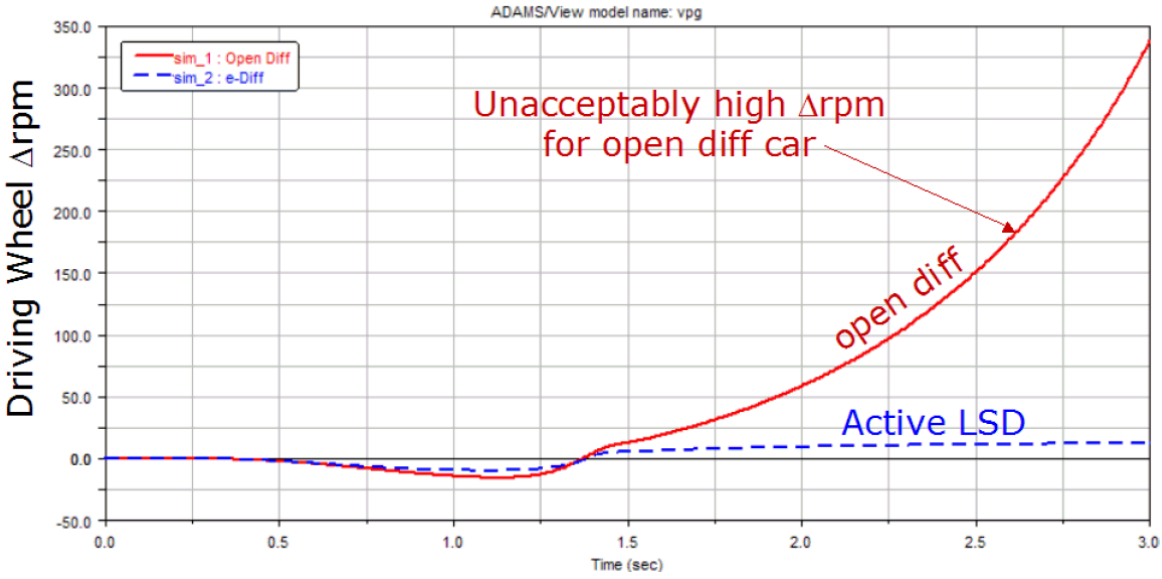

Figure 4.17: Wheel Speed Difference, Open vs. Active Differential [71]

vehicles do not benefit significantly from this type of technology. In contrast, military vehicles frequently operate over a wide range of terrain types and may benefit from active differential technology. However, as previously mentioned in Chapter 2, many modern military ground vehicles utilize traditional, passive drivetrain elements.

4.1.1.4 Suspension

Suspension systems isolate the chassis from road disturbances while keeping the tire in contact with the road surface. Suspensions generally include spring and damping elements in order to support the chassis, settle suspension disturbances, and control roll, pitch, or bounce (heave) of the chassis. The

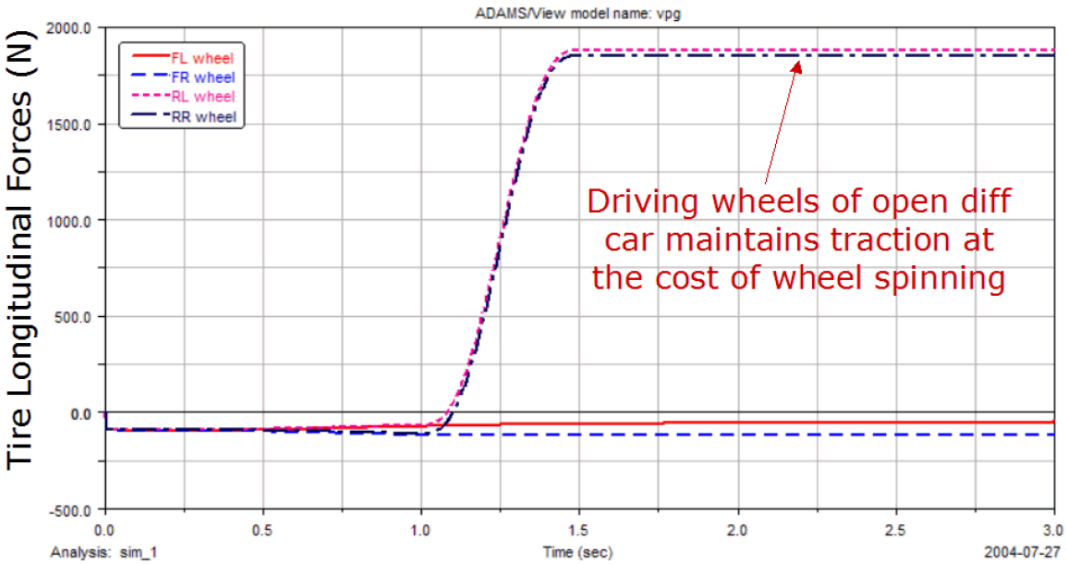

Figure 4.18: Longitudinal Tire Forces, Open Differential [71]

kinematics of the suspension, which may differ between axles on the same vehicle depending on the axle location and/or drivetrain (driven/un-driven), have a significant effect on the behavior of the vehicle. A complete discussion of the impact of suspension kinematics is outside the scope of this report, but it is important to recognize that a large number of different types have been developed and implemented. A few representative suspension types are presented for reference.

Figure 4.20 depicts one of the oldest suspension/drivetrain layouts - a beam axle located by leaf springs. This suspension type is still widely used for trucks and commercial vehicles as the beam provides a robust load path to the wheels, a critical consideration when heavy chassis loads are involved.

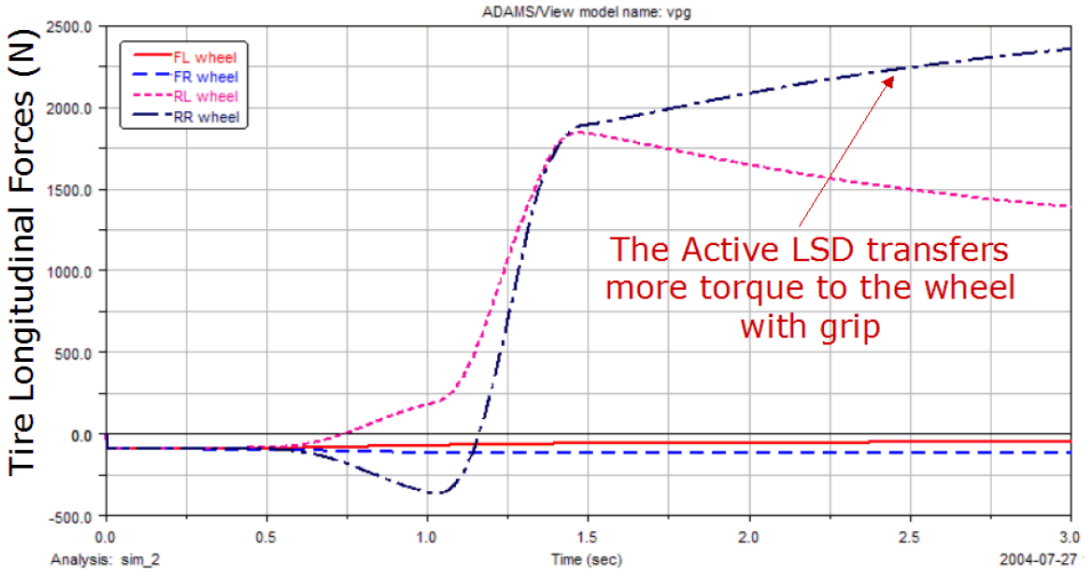

Figure 4.19: Longitudinal Tire Forces, Active Differential [71]

Figure 4.21 shows a double wishbone suspension, used on passenger cars and racing vehicles. The double wishbone design provides the ability to select (by design) the camber of the wheel throughout the travel of the suspension, which affects performance as the chassis undergoes roll, pitch, or bounce. However, the kinematics must also take into account the driven/un-driven nature of the wheel (driveshaft placement), the steering action, and packaging restrictions. This layout is essentially a four bar mechanism where the chassis provides the grounding link and the wishbones (commonly referred to as links or A-arms) are the linkages connected to the grounding link. The kingpin, or upright, is the fourth link in the system and provides the wheel bearing/wheel hub attachment point. The four bar layout and attachments

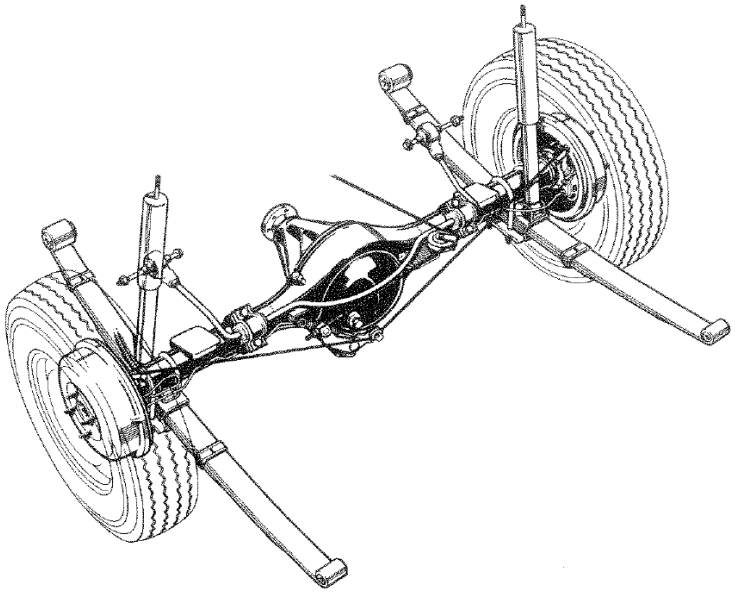

Figure 4.20: Representative Beam Axle and Leaf Spring Suspension[26]

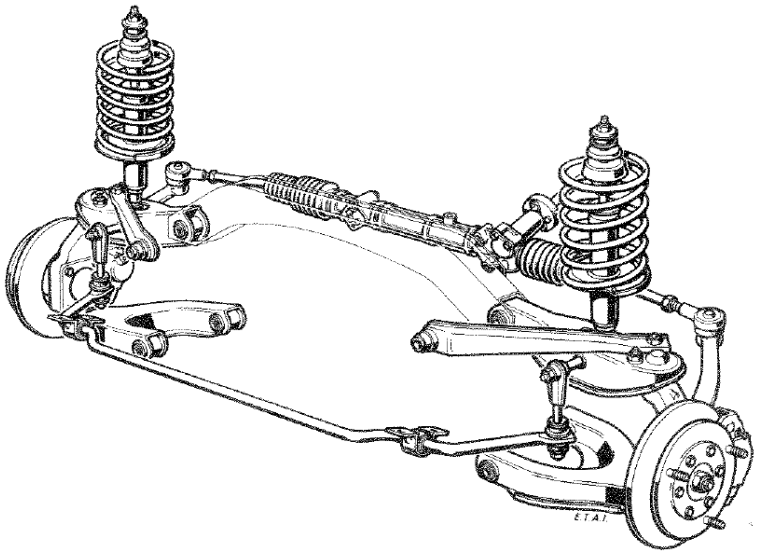

Figure 4.21: Representative Double Wishbone Suspension [26]

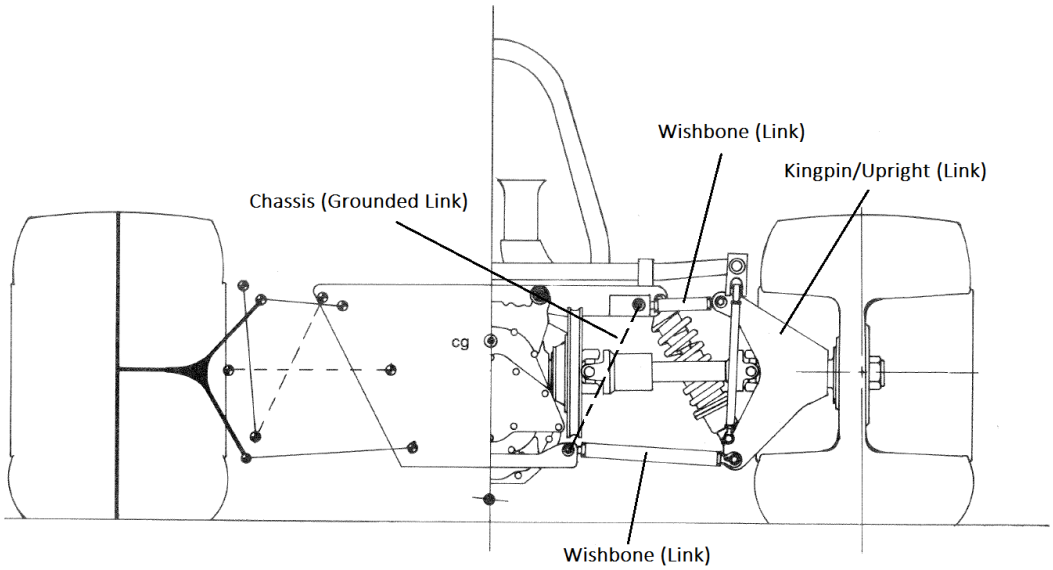

Figure 4.22: Four Bar Suspension Linkage, Racing Vehicle[77]

may be seen in Figure 4.22, which is a representation of a racing suspension.

A modern, "multi-link," suspension is shown in Figure 4.23. Multi-link suspensions are common on modern vehicles as they provide more flexibility in the kinematics and linkage packaging than the four bar design. However, this suspension type is still subject to the same design restrictions as the double wishbone and the benefits of the design come at the cost of system complexity.

It is important to note a key difference between the double wishbone/multi-link designs and the beam axle design - the wishbone/multi-link systems are independent whereas the beam axle is not. In other words, the motion of one wheel on a beam axle directly affects the motion of the other wheel, whereas the motions of the wheels of an independent suspension type are (relatively)

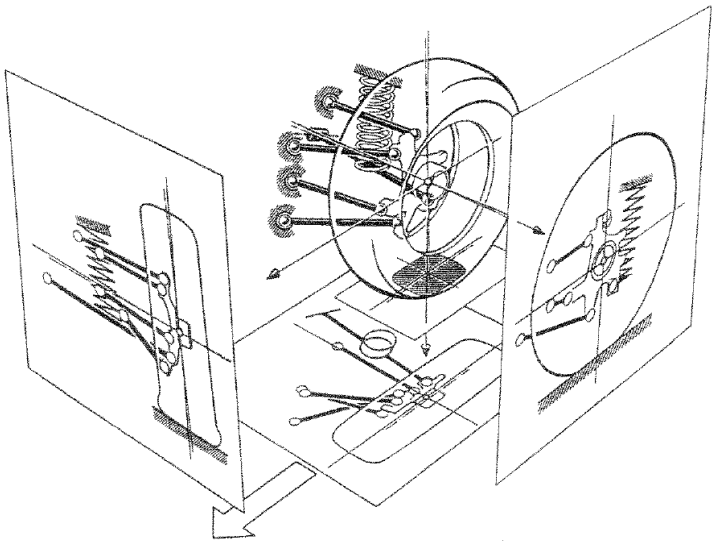

Figure 4.23: Representative Multi-Link Suspension[26]

isolated from one another. Isolating suspension movements provides performance benefits as greater control may be exerted over the individual motions of the wheels. It is also important to note that almost all suspensions, independent or not, employ some variety of anti-roll bar, a torsion spring that provides a force that opposes asymmetric suspension displacement. The addition of the roll bar affects the behavior and performance of the vehicle as it increases the weight transfer of the vehicle by providing a direct coupling between co-axial wheels. As a result, roll bar effects must be taken into account when selecting suspension geometries and parameters.

Suspension springs and dampers on modern vehicles are typically passive but the idea of active and semi-active suspension capability has been

around for many years [13, 19]. Active suspension concepts propose replacing the typical damping element with a force generation element that may be controlled to optimize one or more performance indices. Semi-active suspension concepts typically propose modifiable damping/spring elements that allow for either continuous damping/spring rate adjustment or switching between operating modes. While proposed active and semi-active suspension systems indicate the potential for significant increases in handling and ride characteristics, most systems involve cost and mass increases as well as challenges in component packaging. Several auto manufacturers have developed and implemented semi-active suspension systems, but implementation of these systems is not widespread [1, 34, 56, 78]. References [1] and [78] are implementations of active roll control by BMW and Toyota, respectively, which provide a variable roll resistance in order to reduce chassis roll during cornering maneuvers. Reference [34] describes the development of a magneto-rheological fluid damperby Audi that provides active variation of damping forces. Mercedes has developed a fully active suspension, as described in [56], that utilizes hydraulic servomechanisms in conjunction to traditional spring/damper suspension elements. While the Mercedes system appears to provide substantial ride benefits, widespread implementation is unlikely in the near term to due to the substantial system weight and added cost. In addition, as all of these systems are industry developed, obtaining detailed and meaningful data is difficult.

4.1.2 Design Restrictions Caused by Conventional Architectures

A mechanical connection between the transmission and drive wheels imposes several restrictions on the design of suspension kinematics. Designing a suspension linkage requires considering the placement and movement of the drive shaft (torque delivery), wheel camber as a function of the suspension displacement, movement of the steering linkage (for steered wheels), and placement of the linkage attachment points (packaging restrictions). These elements are often in conflict and, as a result, the design of suspension kinematics generally represent a compromise between the desired system attributes.

The selection of parameters for passive suspension elements (springs and dampers) also a process of compromise. The suspension parameters are expected to provide adequate vehicle performance over a wide range of conditions (speed, road type, terrain type, cargo mass, weight distribution, etc.) while addressing other concerns such as passenger comfort.

The weight and payload requirements of certain types of vehicles often results in the utilization of suspension components that may reduce cost or vehicle complexity at the expense vehicle performance. For example, military transport vehicles such as the FMTV cargo variants shown in Figures 2.6 and 2.7 utilize beam axle suspension types as a method of providing an inexpensive but robust load path from the cargo area to the wheel/tire assembly. Beam axle technology has several drawbacks such as static wheel camber, high CG location, poor roll characteristics, and dependent wheel motions. As a result, once this technology is selected, the designer/engineer is left with few options

for improving vehicle performance.

4.2 Moving Away From Conventional Architectures

The previous discussion focuses on vehicles utilizing an IC (gasoline or diesel fuel) engine as a prime mover but IC engines are not the only available methods of torque generation. Alternatives include different engine types, such as continuous combustion (gas turbine), external combustion (steam engine), and electrical motors. Alternative prime mover concepts are certainly not a novel concept, though improvements in certain technologies such as batteries have recently made alternatives to traditional IC engine drivetrains more attractive [64].

4.2.1 Electric Vehicles

There has been significant recent interest in utilizing electric motors and electrical energy storage elements (among other energy generation/storage types) as opposed to IC engines and hydrocarbon fuels. Many auto manufacturers, as well as start-up companies such as Tesla Motors, have developed or are developing electric platforms in order to address the current issues with hydrocarbon fueled vehicles [22]. Electric vehicles produce no emissions during operation and the torque speed characteristics of electric motors offer some advantages over IC engines [63].

Electric motors generate peak torque at low rotational speeds (albeit at low efficiency) while IC engines produce little to no torque at low speeds. The

torque output of an IC engine increases with speed (up to a certain point) whereas the torque output of an electric motor decreases with speed. The differences in torque/speed characteristics are shown in Figure 4.24. Hybrid vehicles, those utilizing *both* types of prime movers, decouple the operation of each prime mover (depending upon the configuration), thereby providing the operator with choices for each operating regime. These choices provide the ability to optimize the operation of each prime mover for vehicle efficiency, torque output, etc. Hybrid vehicles are discussed in Section 4.2.2.

While electric vehicles offer improved low speed torque, energy conversion efficiency, and reduced noise, electrical energy storage elements (batteries) add significant weight. In addition, the range of comparatively priced/sized electric vehicles is considerably less than that of vehicles using IC prime movers.

It is important to note that the leading electric vehicle platforms (Tesla Model S, Nissan Leaf, Chevrolet Spark EV) use only one electric motor in their respective drivetrains [23, 60, 61]. The base platform of the Tesla Model S is shown in Figure 4.25. It should be noted that the battery pack of the vehicle is mounted low in the chassis, which reduces the CG of the vehicle (generally desirable).

The use of one motor can be thought of as a one-to-one mapping of the power generation functionality from one energy domain (mechanical) to another (electrical) and as such, the traditional drive elements are retained and the chassis and suspension experience many of the same restrictions as

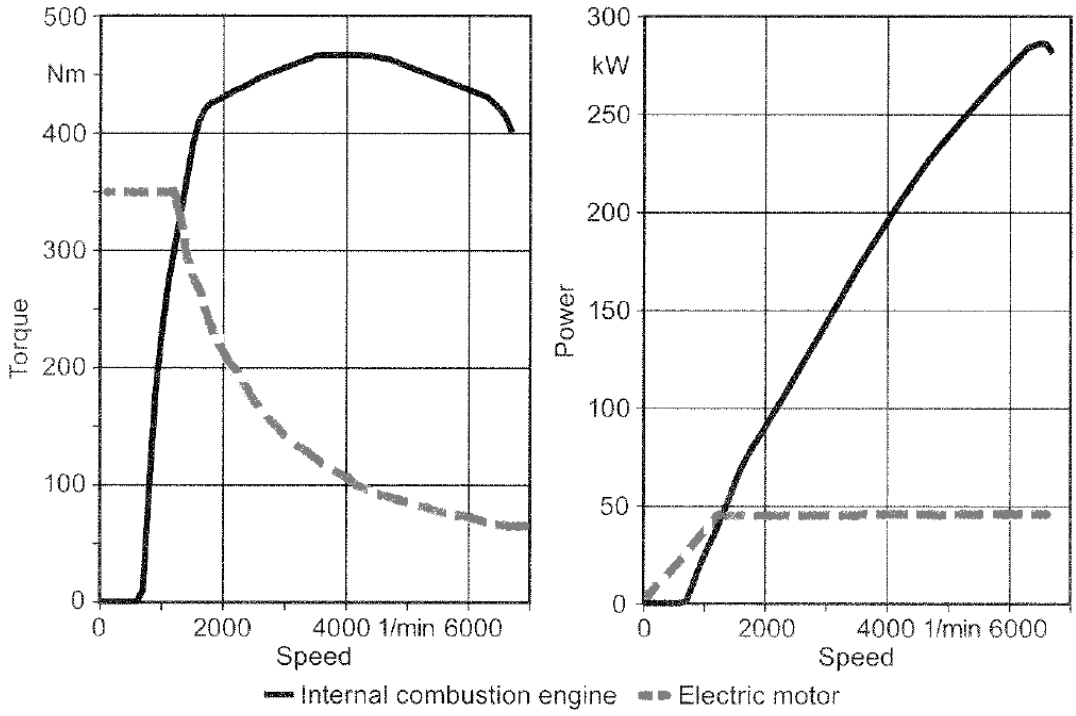

Figure 4.24: Characteristic Torque/Speed Curves for Electric Motors and Internal Combustion Engines [63]

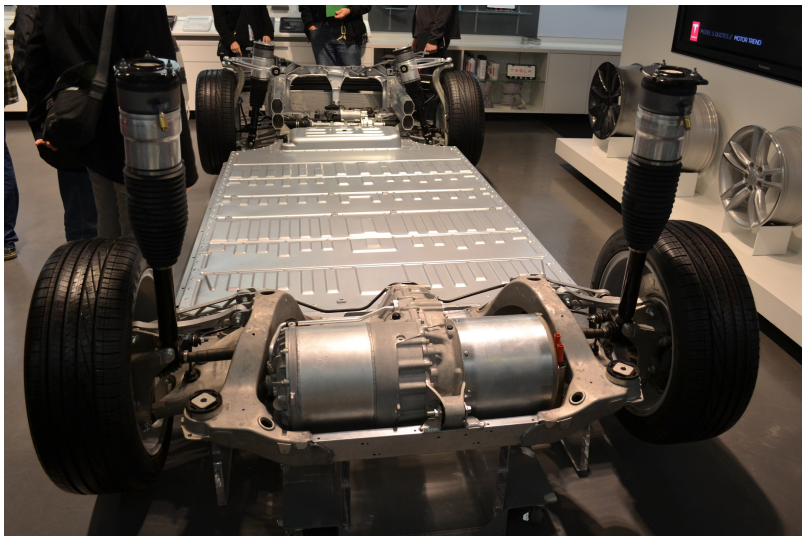

Figure 4.25: Tesla Model S Base (One Drive Motor) [8]

conventional vehicles.

Some electric vehicles, such as the Rimac Concept One, manufactured by Rimac Automobili, utilizes two electric drive motors [12] on the rear axle. The powertrain of this vehicle is shown in Figure 4.26.

This layout has greater influence in vehicle yaw as the two motors (one for each rear wheel) operate independently. This could be very helpful for torque vectoring/yaw control (as discussed in Chapter 6). However, as this vehicle is an industry effort and still in development, useful performance data is not available.

Toyota has explored replacing IC engine drivetrain components with in-wheel electric motors while retaining a traditional double wishbone suspension [62]. This layout allows the drivetrain to capitalize on the benefits of

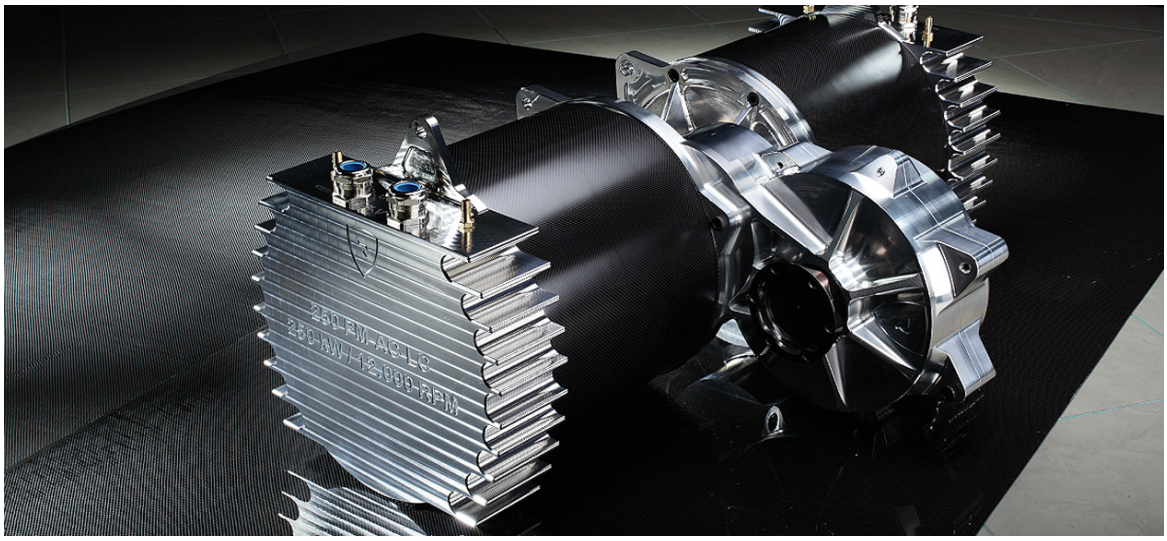

Figure 4.26: Dual Motor Drivetrain, Rimac Concept One (Two Drive Motors) [12]

electric prime movers while avoiding many of the design/performance issues associated with driveshafts and differentials. The independently driven wheels allow for torque vectoring and precise traction control (allowing each wheel remain the in peak/slip force region independently). While test results indicate improvements in vehicle performance, this architecture retains traditional steering, camber, and suspension control elements.

4.2.2 Hybrid Vehicles

Hybrid vehicles architectures add energy storage and management capabilities to the vehicle powertrain. Hybrids utilize (typically electrical) energy generation, storage, and utilization (drive) capabilities in addition to the existing powertrain layout [63]. These vehicles generally fall into one of two main

categories - serial and parallel. The distinction is shown in Figure 4.27.

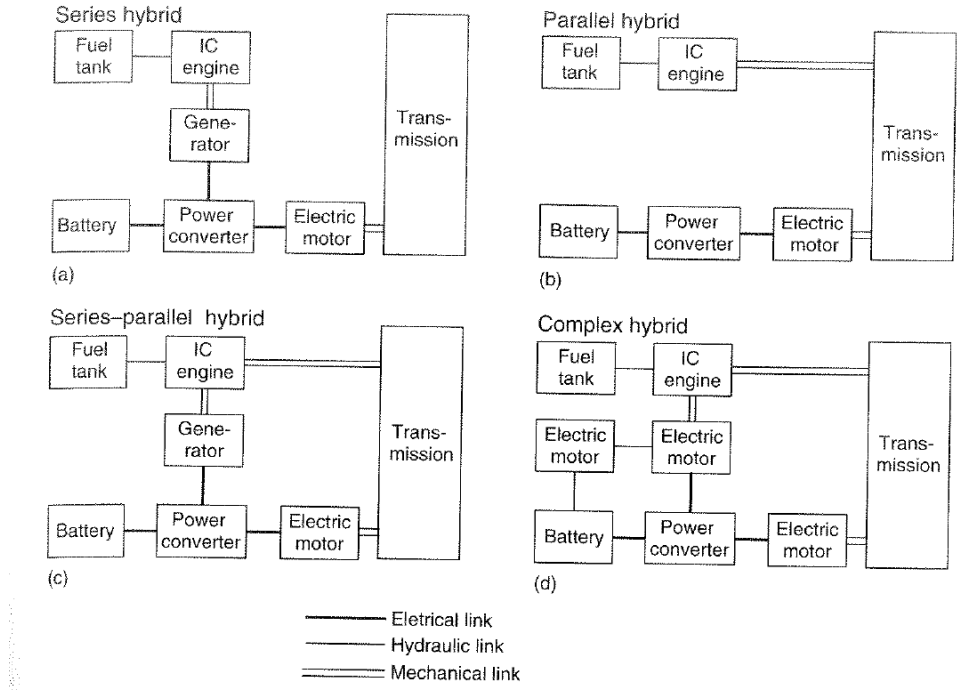

Figure 4.27: Comparison of Hybrid-Electric Drivetrain Layouts [28]

Parallel hybrids include the additional energy storage and utilization elements while retaining the mechanical drivetrain. While the energy management capabilities of the hybrid elements give the system additional control over energy utilization, the restrictions on vehicle design imposed by the traditional drive elements are still present.

Serial hybrids place the additional energy storage and utilization elements in between the IC engine and drive elements, thereby decoupling the two. This decoupling provides more flexibility in power utilization (application of torque). However, most serial hybrid vehicles only utilize a single output

(motor) to provide torque to the drive wheels. As such, despite the decoupling of the IC engine and driven wheels, the traditional drive shaft/differential elements are generally included in the vehicle design and the associated design restrictions are still present.

4.2.3 Rovers and Space Exploration

Rovers and vehicles associated with space exploration present another deviation from standard vehicle architectures. Vehicles intended for operation outside of an atmosphere must utilize a prime mover that does not require some external fuel source (e.g. air for an IC engine) and as such, rovers typically utilize electric drivetrains. However, rovers differ from other electric vehicles in the layout and articulation of the drivetrain due to payload weight and packaging restrictions in addition to differences in operational requirements. Assessing rover architectures is important as these differences affect rover performance and capability in unique ways.

4.2.3.1 NASA Exploration Rovers

There have been three successful, major rover expeditions to mars: Mars Pathfinder, MER Spirit/Opportunity, and MSL Curiosity. The most recent rover design, MSL Curiosity, was undertaken by NASA's Jet Propulsion Laboratory. All three of these rover types utilized a similar architecture - the rover chassis (mission equipment) is suspended by a dual rocker-bogey system in conjunction with in-wheel prime movers [35]. This suspension setup, seen

in Figures 4.28 and 4.29, is beneficial in this case not only because of its low mass and high dexterity (important factors in space travel), but because the dual-bogey geometry provides a passive means to equalize the normal force of the wheels of the suspension (keep all of the wheels in contact with the ground surface).

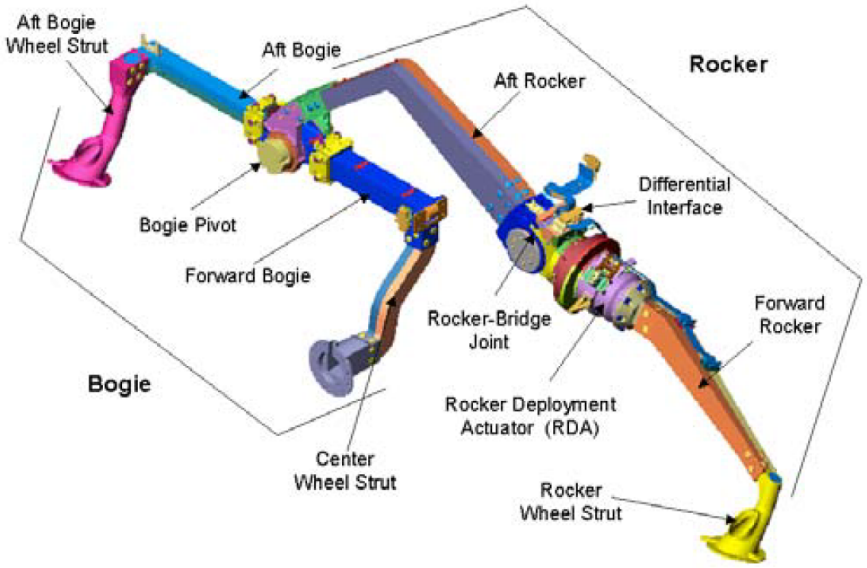

Figure 4.28: MER Rocker-Bogie Assembly [53]

The main mobility concern of rover systems is operating in soft terrains (regoliths) at low speeds [42]. The architecture of the MER systems (also used on the MSL system) utilizes in wheel motors (all wheel propulsion) and rigid wheels with grousers [52]. In wheel motors increase system dexterity and reduce the complexity of the drivetrain. However, exploration rovers are not designed to move at a high rate of speed, and, as a result, the rover architecture

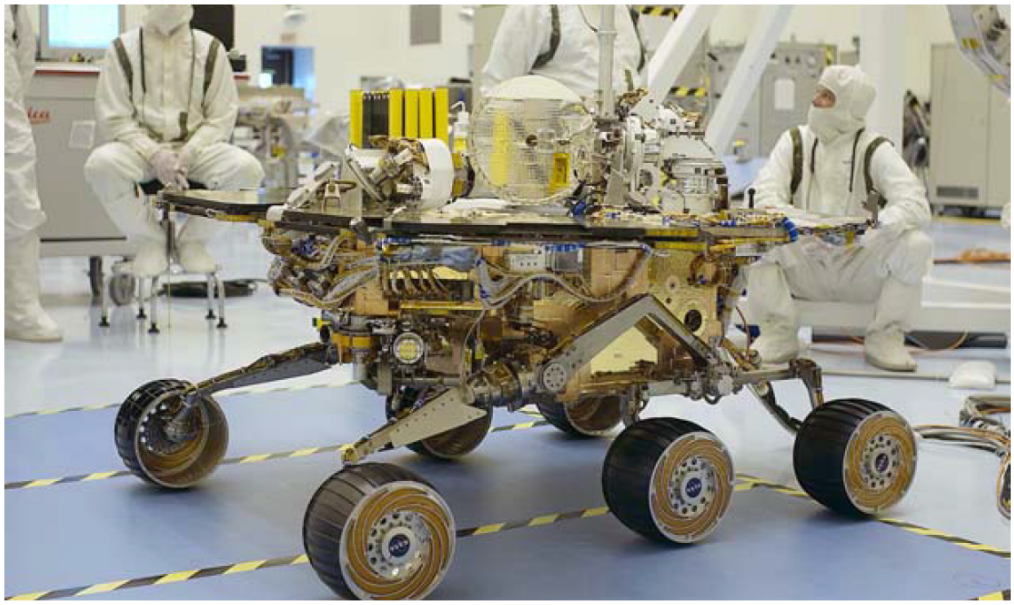

Figure 4.29: MER 'Spirit', JPL Assembly Facility [53]

is often assumed to be quasistatic during operation (little to no inertial effects) [42]. The exclusion of dynamics simplifies the operational requirements and mobility expectations of rover systems.

4.2.3.2 NASA Manned Exploration Ground Vehicles

The Johnson Space Center branch of NASA is currently developing manned mobile platforms for use during manned exploration missions [36]. This development is a response to the need for improved over-ground mobility on the lunar surface during future manned missions. The proposed vehicle, the Chariot, uses a combination active/passive suspension in addition to all wheel full rotation steering (independent), and in-wheel drive motors

on all six wheels. A model of the Chariot is shown in Figure 4.30. The active/passive suspension is a combination of active and passive elements - active elements control suspension ride height while the passive elements (traditional spring/damper) address road disturbances. An image of the Chariot suspension is shown in Figure 4.31.

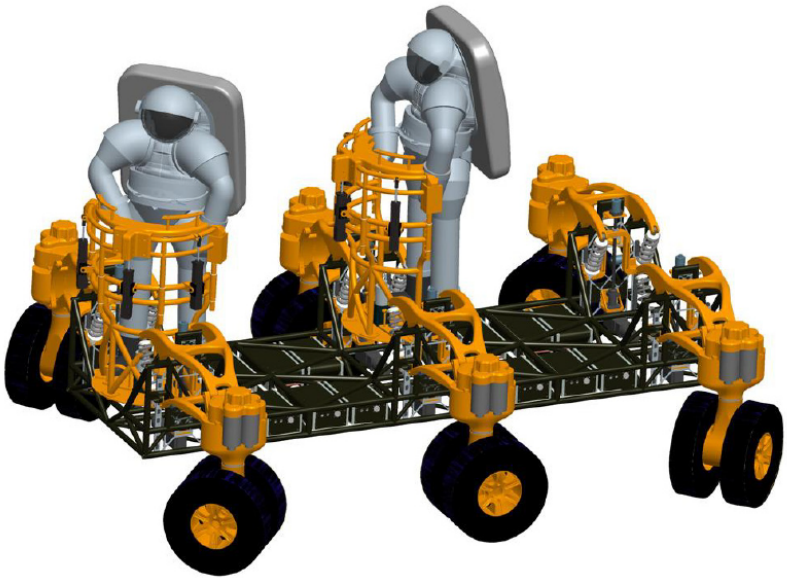

Figure 4.30: Chariot Concept [36]

This architecture gives the Chariot significant mobility - the steering allows the chassis to rotate about any designated point and the active/independent suspension allows the operator to lower the frame to the ground or to climb obstacles. However, the drive elements, which provide two gearing options (high/low), are intended for lunar operation. As such, the drive wheels are capable of significant tractive effort but limit the maximum speed of the plat-

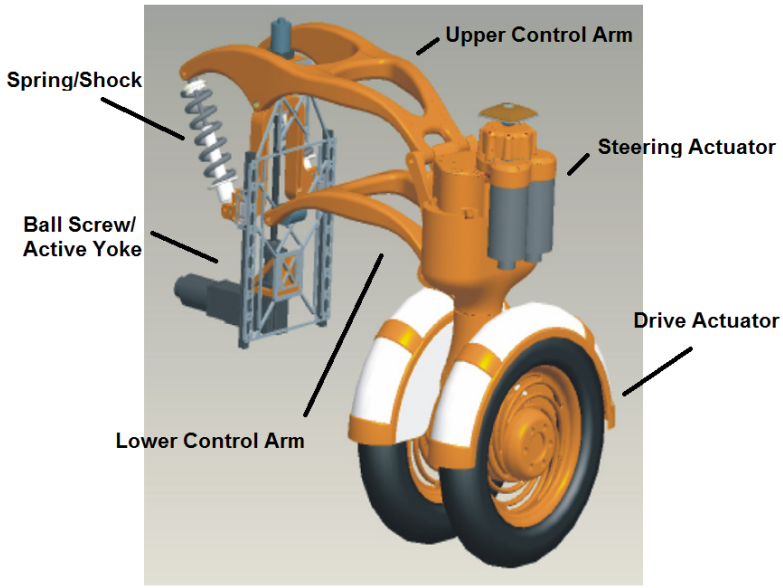

Figure 4.31: Chariot Wheel Module with Suspension [36]

form to 15 mph [36]. An image of the Chariot prototype with a bulldozing attachment is shown in Figure 4.32.

NASA, Johnson Space Center, is also developing an alternate version of the manned Chariot system for potential use in other multi-mission environments. This platform, the Space Exploration Vehicle (SEV) (Figure 4.33), provides a pressurized cabin, docking hatch, and suitports for external activity.[2] The reason for the cabin is to provide an open space living compartment, provisions, and life support.

The SEV platform is an excellent example of a manned ground vehicle system that avoids many of design restrictions of traditional architectures.

[2]Suitports refer to external cabin attachment points for space suit ingress/egress.

Figure 4.32: Chariot Platform with Bulldozing Attachment (Grading Blade)

Figure 4.33: Space Exploration Vehicle (SEV) Prototype [7]

While this system is intended to operate primarily in low-speed, off-road conditions, the SEV promotes dexterity, flexibility, and mobility and the result is a vehicle completely suited to respond to the commands of the operator.

4.3 Intelligent/Active Chassis Elements in Military Vehicles

Military vehicles experience from the same design restrictions and mobility issues as commercial and passenger vehicles. In addition, military vehicles have operational requirements that often specify a wide range of terrain types (both prepared and unprepared), unlike commercial or passenger vehicles that operate mostly on one type of terrain for which the vehicle may be optimized. The application of intelligent actuation to military vehicles is required in order to address the issues of mobility and multi-terrain capability as vehicle costs and weights increases while operational requirements become more complex.

4.3.1 Intelligence as a part of FCS

This concept of the application of machine intelligence and actuation to military vehicles was one of the main concepts of the Future Combat Systems initiative of the early 2000's [43]. Part of the FCS program was to explore the application of a variety of robotic technologies to ground systems in an effort to create intelligent manned and unmanned systems. These technologies include advanced perception for increasing autonomous mobility (terrain data,

etc.), intelligent control architectures for increasing the autonomous capabilities of ground vehicles (depending on the intent of the commander) as well as providing tactical behavior capability (changes in vehicle behavior based on terrain information, enemy/friendly ground force information), and structured human/machine interaction in order to provide soldiers with the ability to manage multiple systems. However, few of these technologies reached maturity with the failure of the FCS program.

4.3.2 Central Tire Inflation System

It is important to note one exception to the otherwise passive suspensions of wheeled military vehicles - the Central Tire Inflation System (CTIS). This system monitors tire pressures and gives the operator the ability to select one of several pressure settings depending on the terrain type and conditions. CTIS allows the operator to lower the tire pressure for operation over soft (unprepared) terrain, for example, lowering the ground pressure of each wheel in an effort to improve mobility [44]. Though simplistic, this ability indicates a recognition by the military of the need for adaptable vehicle elements.

4.3.3 Semi-Active and Active Suspension on Military Vehicles

The mobility benefits of intelligent suspension systems have explored by the U.S. Military for many years. In [39], Hoogterp, Saxon, and Schihl describe the implementation of a semi-active, hydro-pneumatic strut on a 19 ton, tracked vehicle testbed. The goal of this work (published in 1993) was

to demonstrate an improvement in testbed mobility through active damping (changing the damping characteristics of the suspension as a function of vehicle speed, etc.), with the end goal of increasing the cross-country mobility of the M2 Bradley to that of the M1 Abrams. A simple, two dimensional simulation was conducted, evaluating the pitch angle and pitch rate of the vehicle hull for a variety of road surface roughness conditions. The simulation demonstrated a moderate decrease in both pitch angle (19%) and rate (20%). In [38], Hoogterp, Eiler, and Mackie briefly describe the development of active suspension for commercial vehicles and the application this technology to the HMMWV. This work, published in 1996 and conducted by U.S. Army TARDEC (Tank Automotive Research, Development and Engineering Center), focuses on the utilization of hydraulic actuators to control the heave, pitch, and roll of the HMMWV chassis and discusses several controller types, such as bang-bang, LQG based fuzzy logic, and sky-hook chassis control. The authors indicate that simulations of these controllers have potential for increased HMMWV mobility.

Active suspension systems have been implemented on both HMMWV and FMTV vehicles.These systems focus primarily on vehicle ride rate in an effort to reduce chassis motion (heave and roll) and to improve the comfort of the occupants/driver. In, [18], the authors describe the implementation of an active suspension actuator developed by The University of Texas Center for Electromechanics (UT-CEM) on a HMMWV chassis. This system utilizes a feedback linearization process to lower the variation of the chassis position

for a given suspension input. A similar system is adapted for use on a Light Medium Tactical Vehicle (a FMTV variant) in [37]. Again, this system only addresses chassis displacement (chassis absorbed power) as a measure of ride quality and chassis tilt as a measure of vehicle stability. While these systems offer improvements in vehicle performance, this technology is not currently implemented on production military vehicles.

4.3.4 Hybrid Military Platforms

Reducing the fuel consumption of military vehicles is a significant priority to the Army and considerable research has been done in evaluating hybrid powertrains for military vehicles . In [50], Kramer and Parker (of RDECOM-TARDEC and Michigan Technological University, respectively) describe a variety of hybrid vehicle test platforms (serial and parallel) representing a range of vehicle weight classes that have been developed by the military for assessing hybrid powertrain performance.. For the platforms discussed, the HMMWV represents the light vehicle category, the FMTV represents the medium category, and the Heavy Mobility Expanded Tactical Truck (HEMMTT) represents the heavy category. The authors comment that while significant improvements in fuel economy can be demonstrated (especially for light vehicles), the unique challenges of addressing the complex vehicle performance requirements (both on and off road) complicates the issue of addressing hybrid capability. Many military hybrid vehicle studies do not directly address the (ever increasing) requirements for military ground vehicles, such as cooling and speed on grade

requirements. *Vehicles that can not meet requirements standards are not useful to the military, regardless of improvements in fuel economy.* Complicating this issue is the slow nature of military vehicle development cycles and the significant expected life cycles of military vehicle platforms. Alleviating this issue will require the development of open architecture, rapidly refreshable vehicle components in addition to intelligent running gear actuation that will allow vehicles to effectively meet requirement standards.

4.4 The Intelligent Corner Vehicle Concept

Traditional vehicle architectures meet most of the requirements of the majority of operators. These vehicles are intended to operate on prepared surfaces, under controlled conditions, and at a fraction of the traction limits of the tires. However, the design compromises present in these platforms hinder the performance and capability of vehicles that are required to operate over a wide variety of terrains, under uncertain operating conditions, and at or near the traction limits of the tires. this is especially true for military vehicles.

Tesar proposes the development of a new vehicle architecture - the Intelligent Corner Vehicle (ICV) [82]. This concept, shown in Figure 4.34, is intended to provide a ground vehicle platform that provides sufficient operational flexibility to address the diverse set of mobility requirements of military vehicles.

The core concept of the ICV is that of a series hybrid powertrain connected to a series of fully actuated, intelligent corners. An IC engine (most

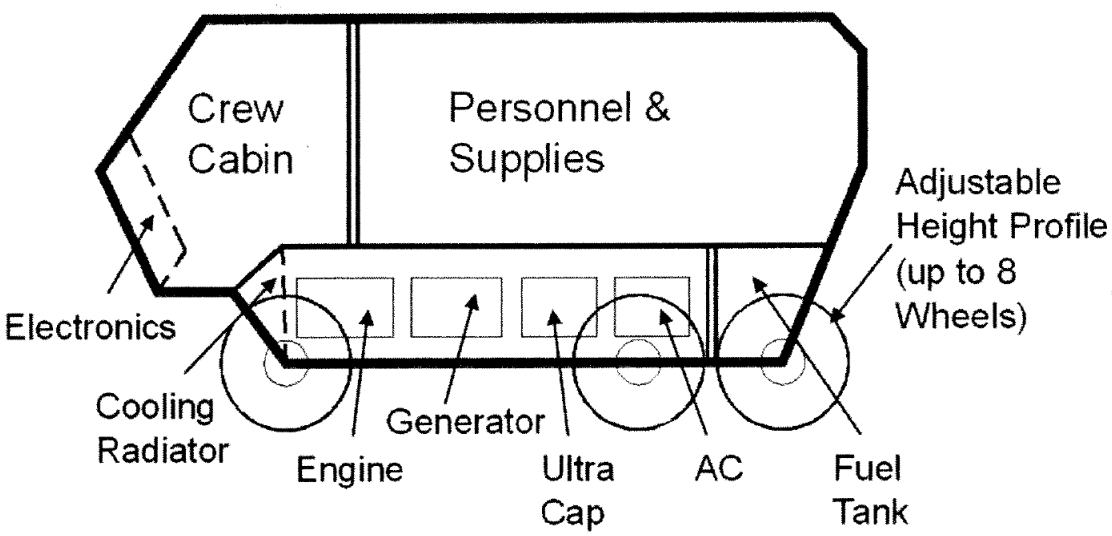

Figure 4.34: Intelligent Corner Vehicle (ICV) Concept [82]

likely a light-duty diesel) coupled with a generator element provides electrical energy that is stored and supplied on demand to wheel actuation elements. Each wheel, or corner, is controlled in the four required degrees of freedom (camber, steering, drive, and suspension) by intelligent, electromechanical actuators embedded with a variety of sensors and embedded computing elements. This architecture allows for complete control of the orientation of every wheel on the vehicle, allowing the system to completely address the requirements of the operator - the human decision maker (HDM).

The ICV platform is intended to be a scalable platform built upon either two, three, or four wheel pairs (four, six, or eight wheels). The actuators from each series (camber, steering, drive, and suspension) are all drawn from

minimum sets of standardized, highly certified actuators, allowing the vehicle designers, technicians, and operators to rapidly draw from these sets to assemble a vehicle suited to the current mission requirements. The representative families of component sets are shown in Figure 4.35.

4.4.1 The Intelligent Corner

As previously mentioned, each wheel (corner) is treated as an individual system and is completely actuated by intelligent actuators. The steering and suspension actuators are mounted inboard, i.e. fixed to the chassis rather than the wheel, as both require a grounding link. The camber and drive actuators, however, are mounted on the kingpin or upright. This arrangement of actuators provides significant flexibility in the design of the chassis and suspension kinematics, which reduces the number of design restrictions. A representative corner is shown in Figure 4.36.

4.4.2 The Intelligent Actuator

The key to the intelligent corner concept is the intelligent actuator. The Robotics Research Group has done significant work in developing intelligent actuation systems. Woodard and Tesar, in a UTexas RRG Report [89], present a design process for the drive actuator for the ICV that may be scaled for a family of vehicles. The drive actuator, the Multi-Speed Drive Wheel (MDW), illustrated in Figure 4.37, utilizes two gearing choices for increased flexibility of operation.

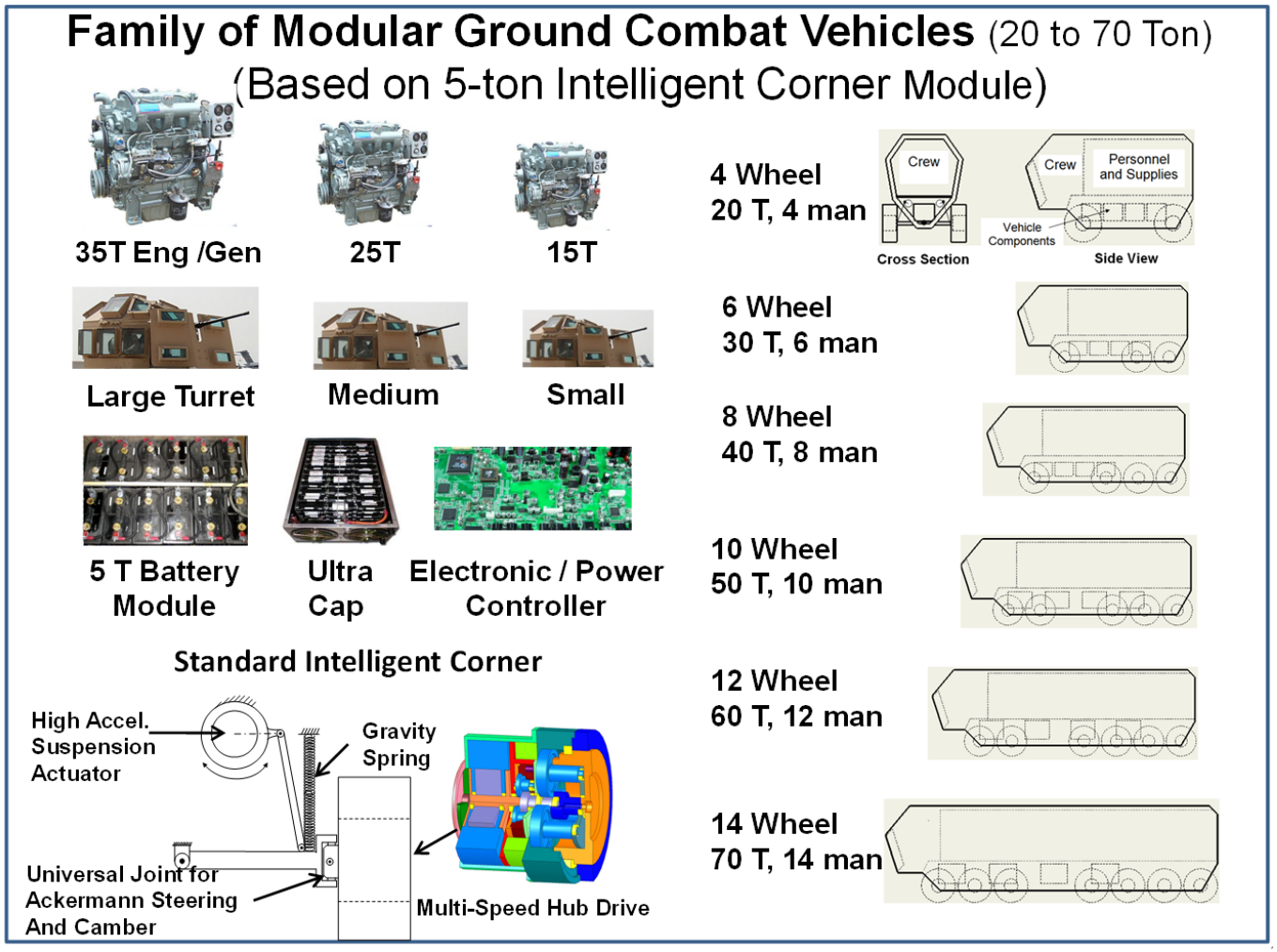

Figure 4.35: Intelligent Corner Vehicle Component Sets [82]

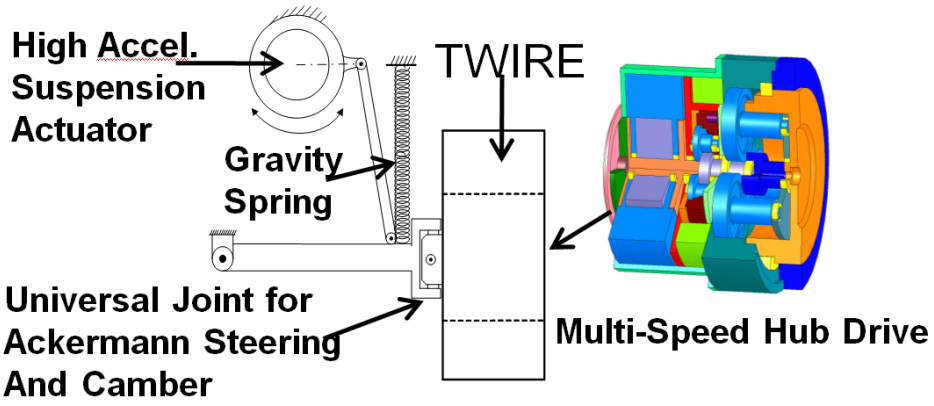

Figure 4.36: Intelligent Corner Vehicle Representative Corner [82]

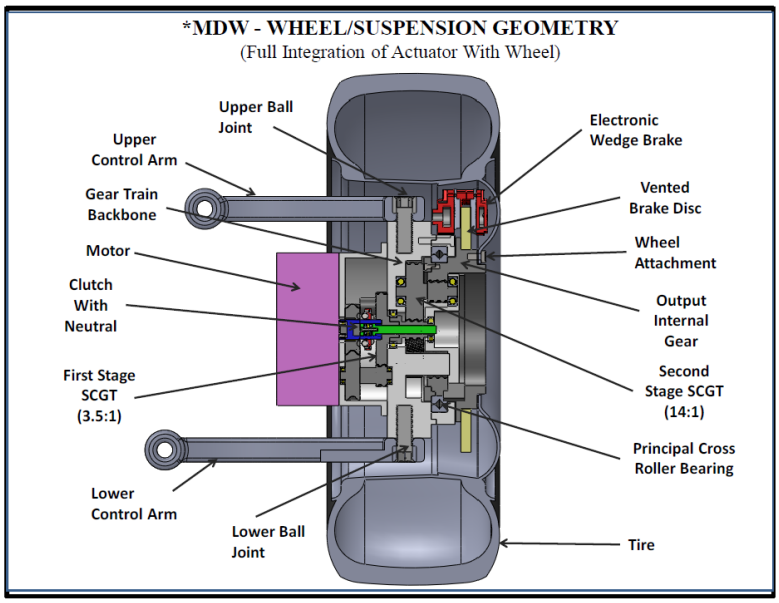

Figure 4.37: Intelligent Corner Vehicle Multi-Speed Drive Wheel [82]

The testing and certification process will produce the performance data for each actuator, compiled into embedded performance maps. This process, illustrated in Figure 4.38, will result in the complete characterization of each actuator. In combination with a variety of embedded sensors, the performance map data will maximize the capability of each actuator within the ICV system. As the operating conditions change, the actuators will be able to fully address the demands of the vehicle operator.

4.5 The Requirement of Performance Criteria

This process of responding to the continually changing commands of the vehicle operator requires a complete characterization of the vehicle system behavior, in addition to the characterization of the individual system actuators. The intelligently actuated vehicle corners provide a large number of system inputs, and the result is a force redundancy when considering planar vehicle motion. This redundancy can be exploited in order to optimize vehicle behavior.

The development of intelligent actuation systems and performance map based decision making allows the implementation of a formal decision making process that will allow the ICV to react in real-time to the needs of the operator. The ICV will be able to address operator commands such as maximizing performance, minimizing vehicle noise, maximizing fuel economy, etc. However, responding to these commands requires the development of vehicle operational criteria - representations of vehicle behavior that will allow the de-

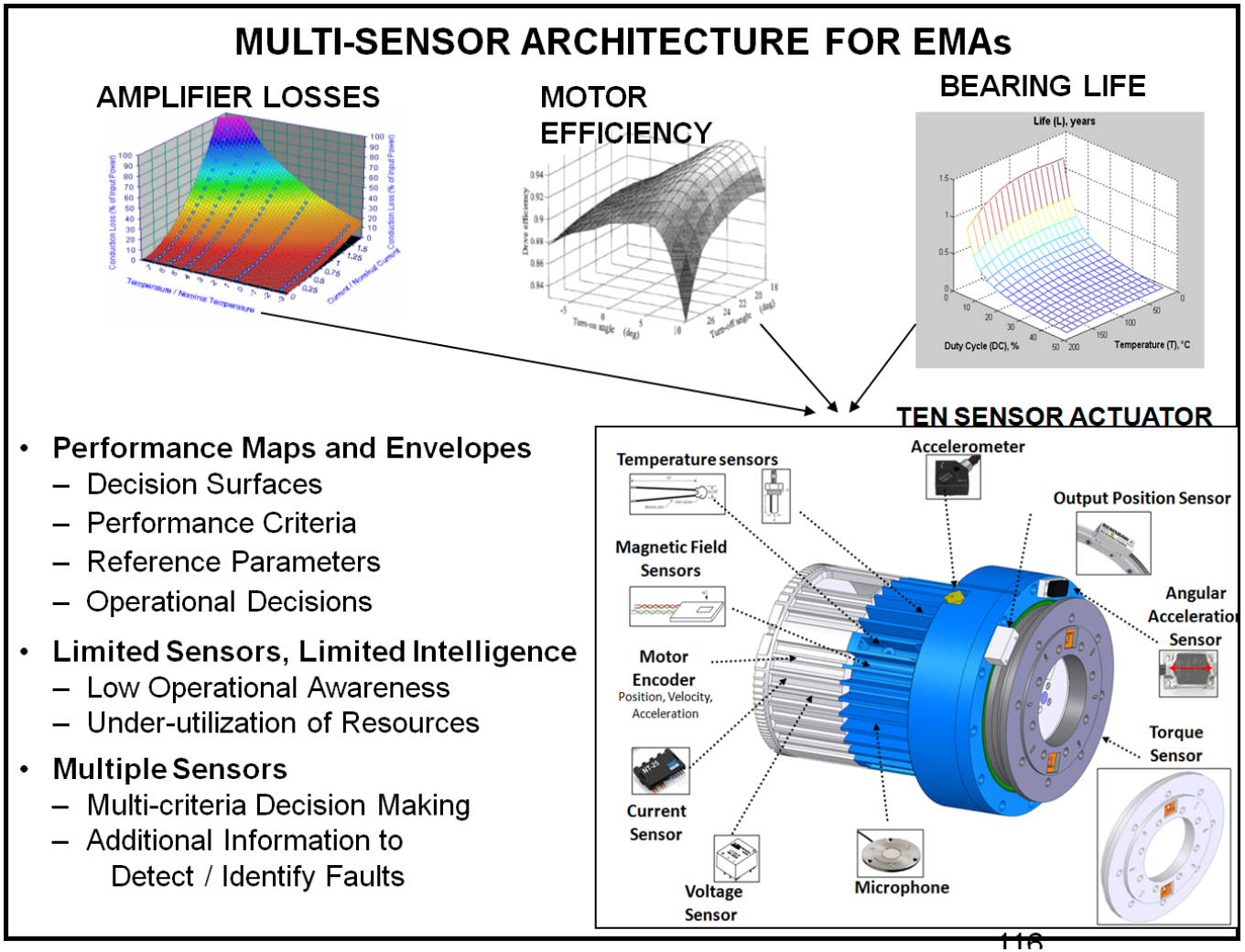

Figure 4.38: Embedded Performance Maps for Intelligent Actuators [81]

cision making process to fully exploit the intelligent actuators to respond to the commands of the operator. The following chapters describe the development of performance criteria for the Intelligent Corner Vehicle.

4.6 Chapter Summary

This chapter discusses modern vehicle architectures, efforts to develop the impact of the application of intelligent actuation to ground vehicle drive-train and suspension components,and the requirement of performance criteria for effectively evaluating vehicle motion. Table 4.1 presents the key findings, conclusions, and recommendations of the chapter.

Table 4.1: Chapter 4 Key Findings, Conclusions, and Recommendations

Result	**Conclusion**	**Recommendation**
Modern steering systems are typically linkage systems, Figure 4.2, and utilize Ackermann steering geometry, Figure 4.3.	Ackermann steering reduces tire slip (globally) but does not provide optimal steering angles for all speeds and tire normal loads.	Maximizing ground vehicle performance requires decoupled, actively controlled steering.
Active power steering systems (Figure 4.5) allow for a variable steering ratio that is a function of speed (Figures 4.6, 4.8) for single or multi-axle steering (Figure 4.7).	Though these systems are capable of improving vehicle stability and handling, the traditional steering linkages and geometry are retained. While the commands of the driver are augmented to improve vehicle performance in this case, the motions of steered wheels remain coupled.	Independently steered wheels are required for optimizing vehicle performance over a range of operating conditions.
Wheel camber is determined by suspension kinematics for traditional wheeled vehicles, and linkage system that attempt to provide optimal camber values can be quite complex (Figure 4.9).	Though the system of Figure 4.9 reduces unwanted variations in camber imposed by vehicle bounce and roll, implementing the linkage is complex and may be difficult to implement.	Maximizing vehicle cornering performance requires actively actuated wheel camber.

Table 4.1: Key Findings, Conclusions, and Recommendations (Continued)

Result	Conclusion	Recommendation
Active camber systems, such as the system shown in Figure 4.13 developed for a sports car, can be shown to improve vehicle cornering performance.	The range of motion of this system, though appropriate for sports cars with relatively stiff tires, is insufficient for vehicles that experience significant suspension displacements or have tires of significantly lower stiffness values.	Optimizing vehicle camber requires active camber actuation with sufficient range of motion as described in the Intelligent Corner concept (Section 4.4).
Traditional vehicles are typically driven by a combination internal combustion engine and transmission in conjunction with transfer cases and differentials (Figure 4.15) for distributing torque.	Though gear selection (Figure 4.14) provides some options to the operator, the direct coupling of the torque generation and torque utilization elements of the drivetrain limit the ability of the system to respond to the commands of the operator.	The torque generation and torque utilization elements of the drivetrain must be decoupled in order for the vehicle to fully respond to the commands of the operator.
Managed differential systems (Figure 4.16) have been developed in an effort to improve the torque distribution between co-axial, driven wheels as shown in Figures 4.17, 4.18 and 4.19.	While managed differential technology does demonstrate improvements in torque distribution for improved vehicle traction (especially in split μ conditions), the traditional drivetrain elements are retained, and as such, the vehicle is still subject to the associated design restrictions (Section 4.1.2).	Avoiding the limitations of differential/traditional drivetrain technology requires decoupling the torque generation and torque utilization elements. Maximizing vehicle performance over a range of operating conditions requires each wheel to be driven independently.

Table 4.1: Key Findings, Conclusions, and Recommendations (Continued)

Result	Conclusion	Recommendation
Traditional vehicle suspensions typically utilize passive elements (springs/dampers). Active suspension systems (both active and semi-active) have been proposed by automakers that indicate the potential for improvements in vehicle performance.	These systems, however, involve increases in cost, vehicle mass, and challenges in packaging. In addition, implementation of these systems is not widespread and performance data is not readily available.	The lack of data for commercial active suspension requires the development of complete vehicle models of both the proposed commercial systems as well as the ICV concept for purposes of comparison of active suspension systems.
The design process for traditional architectures represents a compromise as many of the attributes of the drivetrain and suspension conflict are in conflict and may not adequately address the full range of expected vehicle operating conditions and terrain types.	The operational requirements and design restrictions of certain vehicle types, such as military vehicles, results in the utilization of components that sacrifice performance for reductions in cost and/or complexity.	Intelligent, active actuation of each of the degrees of freedom of a driven wheel and the decoupling of the power generation/utilization elements of a vehicle architecture will allow the design limitations of traditional vehicles to be overcome.

Table 4.1: Key Findings, Conclusions, and Recommendations (Continued)

Result	**Conclusion**	**Recommendation**
Electric vehicles are being developed as an alternative to traditional, internal combustion powered vehicles. These vehicles, such as the Tesla, Nissan Leaf, and Chevrolet Spark EV, utilize an electric motor (in conjunction with a battery pack) as the prime mover.	While electrical motor drivetrains offer some advantages over IC engines (4.24), vehicle range is reduced (compared to IC vehicles), the required electrical energy storage elements increase vehicle weight, and single electric motor (Figure 4.25) layouts require the retention of many traditional drivetrain elements that impose traditional design restrictions.	Electric motor drivetrain components are capable of improving vehicle performance and responsiveness to the operator, but torque should be applied to the wheel directly (as described in the ICV concept, Section 4.4) in order to eliminate the design/performance compromises of traditional architectures.
Hybrid vehicle architectures provide flexibility in power generation and utilization as well as flexibility in drivetrain component layout (Figure 4.27).	However, certain hybrid architectures (parallel systems) retain traditional drivetrain elements, and as such, are subject to the same design/performance restrictions.	The Intelligent Corner Vehicle concept (Section 4.4) should utilize a series hybrid powertrain configuration in order to eliminate traditional design restrictions and to provide maximum flexibility in the Intelligent Corner implementation.

Table 4.1: Key Findings, Conclusions, and Recommendations (Continued)

Result	**Conclusion**	**Recommendation**
Unmanned rovers (NASA - Pathfinder, Spirit, Curiosity) utilize electrical powertrain components in conjunction with in-wheel drive motors (all wheel drive). The motors provide significant flexibility in torque application to the terrain.	This architecture prioritizes low complexity, low weight, and high dexterity over maximum vehicle speed and performance, and, as a result, can not be scaled effectively.	While these vehicle types do not suffer from the design restrictions of traditional architectures, rover drivetrain layouts are insufficient for vehicles with moderate speed, payload, and performance requirements.
NASA has developed a manned ground vehicle system (intended for space exploration) that utilizes **in-wheel drive motors and active suspension** components. This system, the Chariot (Figure 4.30), provides the operators with significant mobility and tractive capability, but limits the maximum speed of the vehicle to 15 mph.	While this vehicle is an excellent example of a wheeled vehicle system that eliminates many of the design/performance restrictions of traditional vehicle architectures, the Chariot is intended only for low speed, off-road operation.	Though the Chariot system provides excellent low speed mobility, dexterity, and several important design features, vehicles designed for space exploration will not be able to address the requirements of military vehicles. The Intelligent Corner concept should share many of the design features of the Chariot while addressing the speed and robustness requirements of military applications.

Table 4.1: Key Findings, Conclusions, and Recommendations (Continued)

Result	**Conclusion**	**Recommendation**
The United States Military has previously attempted to apply active/intelligent chassis elements to ground vehicles (Section 4.3). With the exception of the monitoring and inflation (Central Tire Inflation System, CTIS), none of the evaluated technologies were sufficiently developed or put into production on military vehicles.	The adoption of CTIS indicates a recognition by the military of the need for active chassis elements, but active suspension technology has not been implemented and the FCS program was ultimately unsuccessful due to issues of project management and the complexity of systems integration.	The development of intelligent actuation components for military vehicles must incorporate open architecture and modular components in order to facilitate a transparent and continuous design/development process.
The United States **Military** has explored the development of **hybrid powertrain systems** for a range of military vehicles (Section 4.3). Though significant improvements in vehicle fuel economy were reported, addressing the complex vehicle performance requirements for military platforms was a challenge.	Vehicles that can not meet the full range of requirements standards are not useful to the military, regardless of improvements in fuel economy. This problem is further complicated by the slow nature of military vehicle development cycles.	Developing, evaluating, and improving military vehicle technologies requires the adoption of both open architecture standards and intelligent actuation in order to enable rapidly refreshable vehicle platforms that are able to address military requirements.

Table 4.1: Key Findings, Conclusions, and Recommendations (Continued)

Result	**Conclusion**	**Recommendation**
Tesar [82] proposes the development of the **Intelligent Corner Vehicle** (Figure 4.34) in an effort to provide a vehicle with sufficient operational flexibility to address the wide range of mobility requirements of military vehicles.	The core concept of the ICV, the Intelligent Corner, has the potential to provide significant capability and responsiveness to the operator. However, controlling a vehicle of this complexity (each wheel has four independent inputs) requires the development of criteria by which the motion and state of the vehicle may be evaluated - performance criteria.	Pursuing the development of the ICV concept requires the generation of sets of performance criteria (Section 4.5), that may be then utilized to generate performance maps, so that the operation of the ICV may be evaluated effectively (the subject of further sections of this report).

Chapter 5

Serial Chain Robotics Criteria as a Framework for Vehicle Criteria Development

5.1 Influence of Previous Work

A variety of reports and papers have been published by the Robotics Research Group on the topics of motion planning, serial chain kinematic redundancies, and the need for performance criteria. A review of the development of performance criteria for serial chain mechanisms is beneficial in understanding the application of performance criteria to the Intelligent Corner Vehicle.

5.1.1 Serial Chain Kinematics

The use of performance criteria for evaluating the motion of complex dynamic systems at the RRG began with the analysis of serial chain robotic systems. A serial chain robotic system is comprised of a series of links connected with either rotational (rotary) or translational (prismatic) joints. Figure 5.1 shows a six degree of freedom (DOF) industrial robotic arm manufactured by Motoman. The individual rotary actuators are labeled $R1$ through $R6$.

The tool at the end of the robotic arm, referred to as the end effector (EEF), is generally a location of interest and motion planning for serial robotic

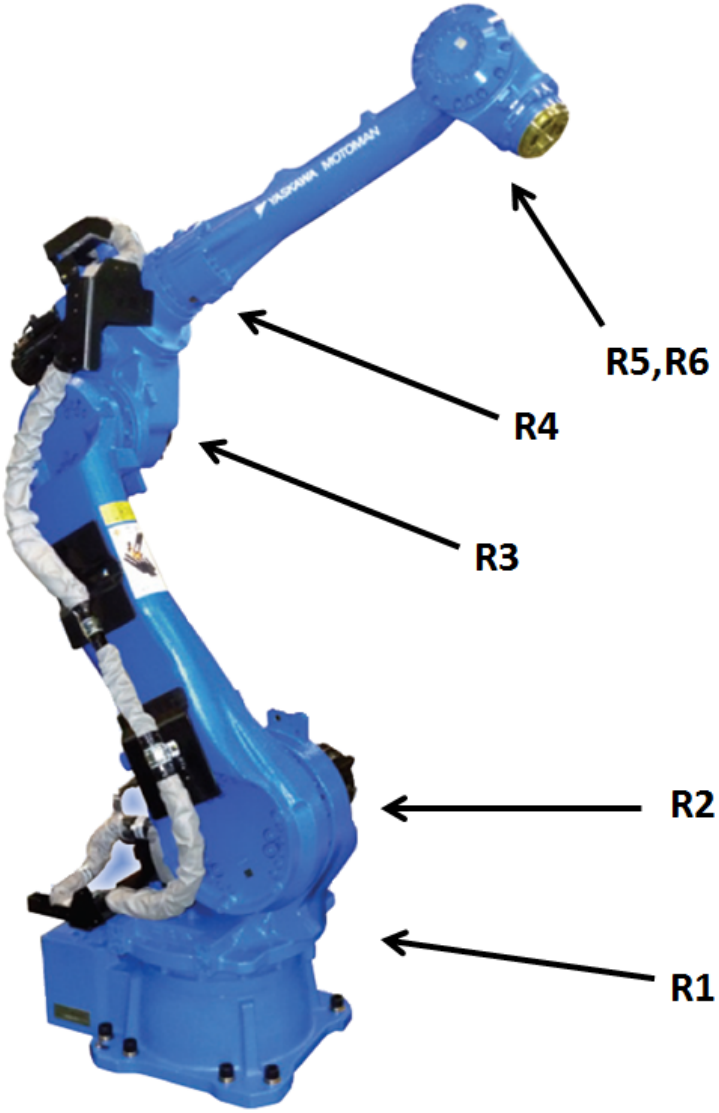

Figure 5.1: Yaskawa Motoman 6 DOF Industrial Robot [74]

systems typically involves defining a desired EEF motion or position. For example, a serial chain robotic system used for package handling operations may follow a specific series of EEF positions (point to point) whereas a system used for welding or painting may be required to follow a precise trajectory as a function of time. A standard industrial robot may have six degrees of freedom as there are six parameters required to specify the location and orientation of an end-effector in three-dimensional space. The process of determining inverse kinematic expressions, or the individual joint angles and velocities required for a desired EEF motion, for a six DOF arm is a mathematically complex process that may yield several possible solutions. These solutions must then be evaluated by the operator or controlling software. The inverse kinematic problem is made significantly more complex if redundancy is present in the serial chain mechanism. In this case, the number of system inputs exceeds the number of system outputs and there may exist an infinite number of possible solutions that must also be evaluated. An example of a redundant system is a snake robot, shown in Figure 5.2. This robot utilizes a series of short links and rotary actuators to create a highly dexterous system capable of snake-like locomotion.

Assessing possible solutions to the inverse kinematics of serial chain mechanisms is a problem of optimization and as such, various criteria are required in order to effectively evaluate the behavior of the mechanism. The Robotics Research Group has systematically developed a large set of performance criteria for serial chain robotic systems. Developing criteria with real

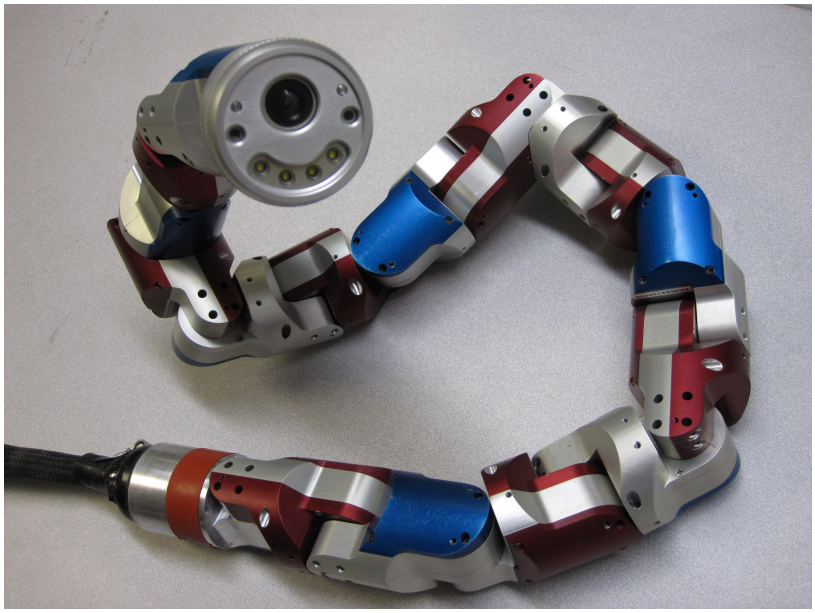

Figure 5.2: Modular Snake Robot [51]

physical meaning is critical in order to provide the operator with an understanding of the motion and capabilities of the system. Cleary and Tesar [20] described a variety of criteria in several categories (geometric, inertial, kinetic energy distribution, system compliance) and indicated the importance of developing criteria that are task independent. The criteria described by Cleary and Tesar are functions of the geometry, state, and physical parameters of the serial chain mechanism rather than derived from the intended end-effector behavior. Task independent criteria are a more versatile representation of system behavior, applicable to any task or system objective. Task independent criteria may also be derived from EEF trajectories. Knowledge of the higher order properties of trajectory characteristics such as curvature and torsion may

be exploited, for example, in order to generate desirable joint behavior for a desired EEF motion [80].

Many of these criteria are derived from Kinematic Influence Coefficients. Kinematic Influence Coefficients, developed by Benedict and Tesar [14] for planar mechanisms and later expanded to spatial mechanisms by Thomas and Tesar [83], provide a general kinematic description of multi-degree of freedom, serial chain systems. The kinematics of a general, n degree of freedom mechanism may be expressed as:

$$\phi = \phi(t) = \{\phi_1(t), \phi_2(t), ..., \phi_n(t)\}^T \tag{5.1}$$

$$\dot{\phi} = \dot{\phi}(t) = \{\dot{\phi_1}(t), \dot{\phi_2}(t), ..., \dot{\phi_n}(t)\}^T \tag{5.2}$$

$$\ddot{\phi} = \ddot{\phi}(t) = \{\ddot{\phi_1}(t), \ddot{\phi_2}(t), ..., \ddot{\phi_n}(t)\}^T \tag{5.3}$$

where ϕ_i refers to the angular position of joint i, $\dot{\phi_i}$ refers to the angular velocity of joint i, and $\ddot{\phi_i}$ refers to the angular acceleration of joint i. Note - prismatic joints are represented with a translation parameter r_i rather than a rotational parameter, ϕ. However, this report restricts itself the use of rotational joints for simplicity. If the EEF for a 6 DOF robot is measured in the traditional six spatial degrees of freedom, the output may be expressed as:

$$u = \{u_1, u_2, u_3, u_4, u_5, u_6\}^T = \{x, y, z, \Psi_x, \Psi_y, \Psi_z\}^T \tag{5.4}$$

where x,y, and z represent translations in a fixed (grounded) reference frame, and Ψ_x, Ψ_y, Ψ_z represent rotations about the respective fixed axes. In

general, the EEF outputs are expressed as functions of each joint position:

$$\begin{aligned} x &= f(\phi_1, \phi_2, ..., \phi_n) \\ y &= f(\phi_1, \phi_2, ..., \phi_n) \\ z &= f(\phi_1, \phi_2, ..., \phi_n) \\ \Psi_x &= f(\phi_1, \phi_2, ..., \phi_n) \\ \Psi_y &= f(\phi_1, \phi_2, ..., \phi_n) \\ \Psi_z &= f(\phi_1, \phi_2, ..., \phi_n) \end{aligned} \tag{5.5}$$

The time derivative of the mechanism output, u, may then be expressed as:

$$\dot{u} = \frac{du}{dt} = \frac{\partial u}{\partial \phi}\frac{d\phi}{dt} \tag{5.6}$$

The matrix of partial derivatives of the system output with respect to the joint positions is the set of first order influence coefficients, also referred to as G functions:

$$\dot{u} = \frac{\partial u}{\partial \phi}\frac{d\phi}{dt} = [G^u_\phi]\frac{d\phi}{dt} = [G^u_\phi]\dot{\phi} \tag{5.7}$$

$$[G^u_\phi] = \begin{bmatrix} \frac{\partial u_1}{\partial \phi} \\ \frac{\partial u_2}{\partial \phi} \\ \vdots \\ \frac{\partial u_n}{\partial \phi} \end{bmatrix} = \begin{bmatrix} \frac{\partial u_1}{\partial \phi_1} & \frac{\partial u_1}{\partial \phi_2} & \cdots & \frac{\partial u_1}{\partial \phi_n} \\ \frac{\partial u_2}{\partial \phi_1} & \frac{\partial u_2}{\partial \phi_2} & & \vdots \\ \vdots & & \ddots & \vdots \\ \frac{\partial u_n}{\partial \phi_1} & \cdots & \cdots & \frac{\partial u_n}{\partial \phi_n} \end{bmatrix} \tag{5.8}$$

If the system output is the set of spacial parameters of Equation (5.4), the first order influence coefficient matrix is:

$$[G^u_\phi] = \begin{bmatrix} \frac{\partial x}{\partial \phi} \\ \frac{\partial y}{\partial \phi} \\ \vdots \\ \frac{\partial \Psi_z}{\partial \phi} \end{bmatrix} = \begin{bmatrix} \frac{\partial x}{\partial \phi_1} & \frac{\partial x}{\partial \phi_2} & \cdots & \frac{\partial x}{\partial \phi_6} \\ \frac{\partial y}{\partial \phi_1} & \frac{\partial y}{\partial \phi_2} & & \vdots \\ \vdots & & \ddots & \vdots \\ \frac{\partial \Psi_z}{\partial \phi_1} & \cdots & \cdots & \frac{\partial \Psi_z}{\partial \phi_6} \end{bmatrix} \tag{5.9}$$

It is important to note the separation of joint (geometric) and time derivatives - the first order influence coefficients are a function of joint position only. Kinematic Influence Coefficients may be formulated around any point of interest on the structure of the robot, but if they are utilized to relate the EEF velocities to the joint velocities, the G matrix is referred to as the Jacobian of the system.

Influence coefficients for EEF accelerations may be derived in a similar manner. The coefficients represented by the second partial derivative of the system output with respect to the joint positions may be grouped together in the same manner as the first order coefficients:

$$\ddot{u} = \frac{d^2u}{dt^2} = \frac{d}{dt}(\frac{\partial u}{\partial \phi}\frac{d\phi}{dt}) \tag{5.10}$$

$$\ddot{u} = (\frac{\partial u}{\partial \phi})\ddot{\phi} + (\frac{\partial^2 u}{\partial \phi^2})\dot{u}^2 \tag{5.11}$$

$$\ddot{u} = [G^u_\phi]\ddot{\phi} + \dot{\phi}^T[H^u_\phi\phi]\dot{\phi} \tag{5.12}$$

The resulting Hessian matrix, H, relates the centripetal and Coriolis effects to the accelerations of the system output.

Hooper and Tesar [40] developed a method by which the inverse kinematics of serial chain mechanisms could be determined through a direct search method utilizing multiple performance criteria. In discussing the importance of these criteria, Hooper presents a list of desirable criteria traits:

- Physically significant - must display mathematical or experimental improvement

- Multiple physical meanings - this increases criteria effectiveness without additional computational expense
- Varies over workspace - allows decision making
- Single valued - allows deterministic solutions
- Continuous - allows integral and differential calculations
- Computationally efficient - important for real-time evaluation
- Mathematically independent - avoids overlapping effects
- Bounded in magnitude - makes normalization possible
- Task independent - one formulation regardless of task being performed

It is important to keep these traits in mind during the discussion of the application of various performance criteria to the Intelligent Corner Vehicle (ICV).

Hooper discusses the criteria groupings previously mentioned (geometric, inertial, kinetic energy, system compliance - proposed by Cleary and Tesar) but, Tisius and Tesar [84] more recently suggested the following groupings as a more task-based approach:

- Constraint-Based Criteria
  - Joint Limit Avoidance
  - Peak Torque Avoidance and EEF Payload Capacity

  - Velocity Limit Avoidance
  - Acceleration Limit Avoidance
  - Obstacle Avoidance
  - Fault Tolerance
  - Singularity Avoidance
- Non Constraint-Based Criteria
  - Dexterity
  - Transmissibility
  - Efficiency
  - Smoothness
  - Stiffness
  - Impact Force Reduction
  - Conservative Motion

Recognizing the difference between constraint-based and non constraint-based criteria is important in addressing ICV performance because, as it will be discussed in the following section, constraint based criteria are more readily applicable to the ICV architecture.

5.1.2 Criteria for Serial Chain Systems

The following is a description of a series of criteria, the physical meanings of each, and their applicability to the Intelligent Corner Vehicle. The

following discussion of criteria is focused on the corner actuators and a chassis fixed reference frame is assumed.

5.1.2.1 Geometric Criteria

It is important to note the prevalence of the G and H matrices (influence coefficients) in performance criteria for serial manipulators, especially in those related to geometry. As an example, it is desirable to be able to assess the ability of a serial chain mechanism to transmit force or velocity to the EEF. The Measure of Transmissibility criterion (MOT) is described as:

$$MOT = \sqrt{det([G^e_\phi][G^e_\phi]^T)} \tag{5.13}$$

The MOT criterion provides an indication of the proximity of the mechanism to a singularity. A singularity is a configuration of a serial chain mechanism in which one of the degrees of freedom is mathematically unavailable. In this case, the coefficients associated with a desired output direction approach or become zero and the system looses the ability to influence the EEF in the specified direction. Mathematically, a singularity occurs when the determinant of the Jacobian of the system is zero. Because the Jacobian of the system relates joint velocities to the EEF output velocities:

$$\dot{u} = [G^e_\phi]\dot{\phi} \tag{5.14}$$

the inverse of the Jacobian may be utilized to determine joint velocities from the EEF output velocities:

$$\dot{\phi} = [G^e_\phi]^{-1}\dot{u} \tag{5.15}$$

The above formulation becomes invalid if taking the inverse of the Jacobian is not possible (zero determinant).

Tisius [84] presents a graphical representation of the MOT criterion in Figure 5.3 for a simplistic, 2R (two rotational joints) planar robot. This figure

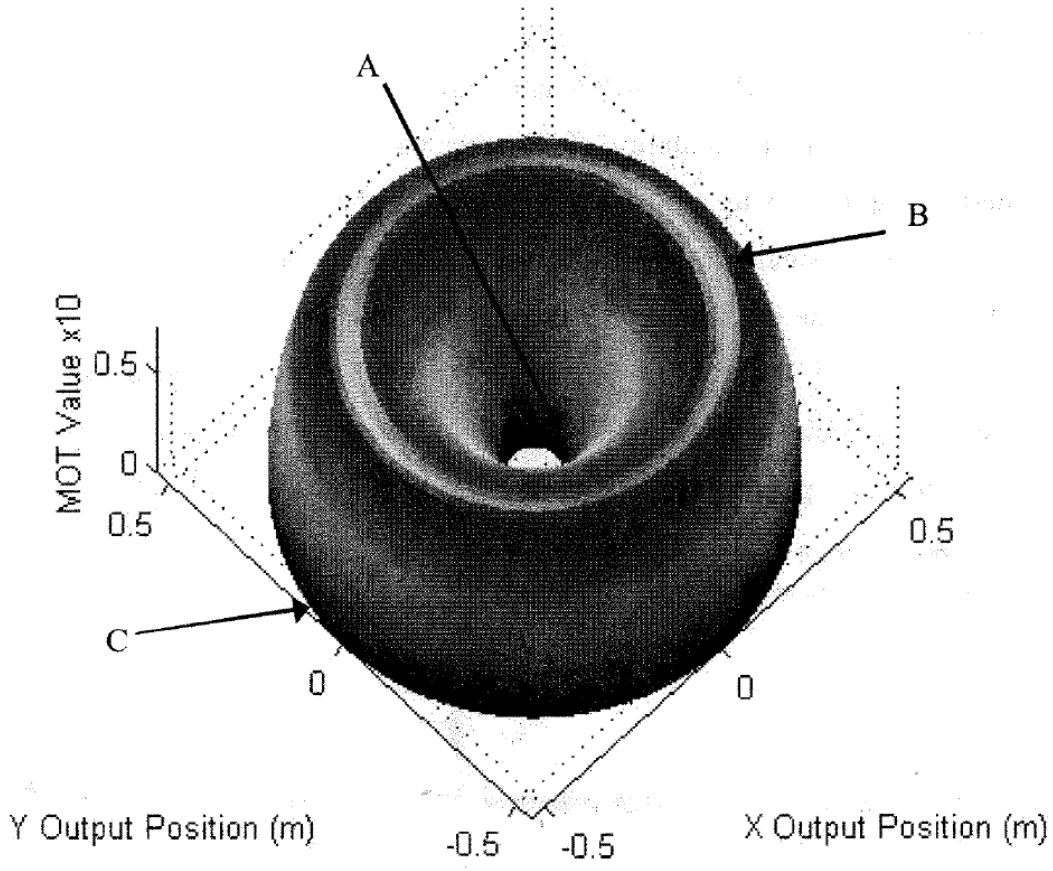

Figure 5.3: Measure of Transmissibility, 2R Planar Mechanism [84]

shows the variation of the MOT criterion as the manipulator moves through the workspace, varying from zero at the edge of the workspace (location C) to a

manipulator dependent maximum (location B) and back to zero when the EEF is near the base of the mechanism (location A). Locations A and C represent a loss of the effectiveness of the inputs on the outputs for the 2R mechanism. The orientations of the manipulator at the corresponding locations (A, B, C) are shown in Figure 5.4.

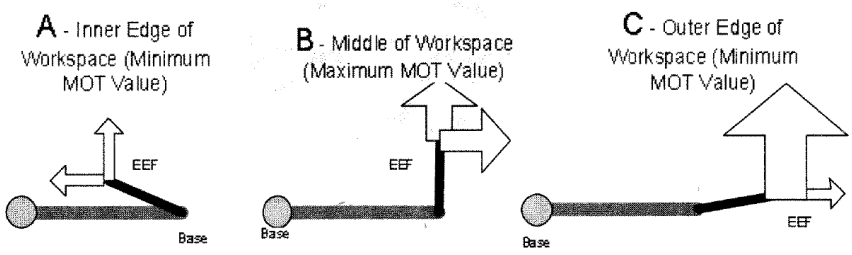

Figure 5.4: MOT, 2R Orientations [84]

While both location A and location C indicate a low MOT value (near zero), it should be noted that the input/output behavior of the mechanism is not the same in both configurations. As shown in Figure 5.4, the mechanism looses the ability to move the EEF in the x direction (along the axis aligned with the first, longer link as indicated in the figure) in the A and C configurations. However, at the inner edge of the workspace (A), large system inputs (joint velocities) result in small velocities of the EFF whereas small inputs will result in large EEF velocities if the system is in configuration C. It is important to note that the MOT approaches zero when *any* degree of freedom is ineffective as the criterion considers the entire Jacobian.

Criteria have been developed in order to assess the directional transmissibility of a serial chain mechanism. For example, Bevill and Tesar [15]

present a directional velocity transmission criteria:

$$\eta_{vx} = \{\sum_{i=1}^{M}[\frac{1}{\sigma_i}(\dot{u}^e)^T h_i]^2\}^{-\frac{1}{2}} \tag{5.16}$$

M - number of degrees of freedom of the end effector

σ_i - the i-th singular value of the Jacobian

$\dot{u}^e$ - desired end effector motion

h_i - the i-th end effector space singular vector

In this case the velocity transmission criterion presented above is for a desired motion in the x direction. Similar criteria have also been developed for the evaluation of torque transmissibility [27]:

$$\eta_{\tau x} = \{\sum_{i=1}^{M}[\sigma_i(L^e)^T h_i]^2\}^{-\frac{1}{2}} \tag{5.17}$$

where L^e is the direction of the force at the end effector. Again, the above criteria is associated with the x direction. Tisius presents an alternate formulation of the Velocity/Power Transmissibility Criterion (VTR):

$$VTR = (\dot{u}^T([G^e_\phi][G^e_\phi]^T)^{-1}\dot{u})^{\frac{1}{2}} \tag{5.18}$$

The $\dot{u}$ term in the above formulation represents the unit velocity vector of the EEF. A plot of the VTR criterion for the simple 2R mechanism previously discussed, and the corresponding manipulator orientations are shown in Figures 5.5 and 5.6, respectively.

The effects of this weighted Jacobian formulation of the mechanism transmissibility are clearly shown in Figure 5.5. As the criterion approaches

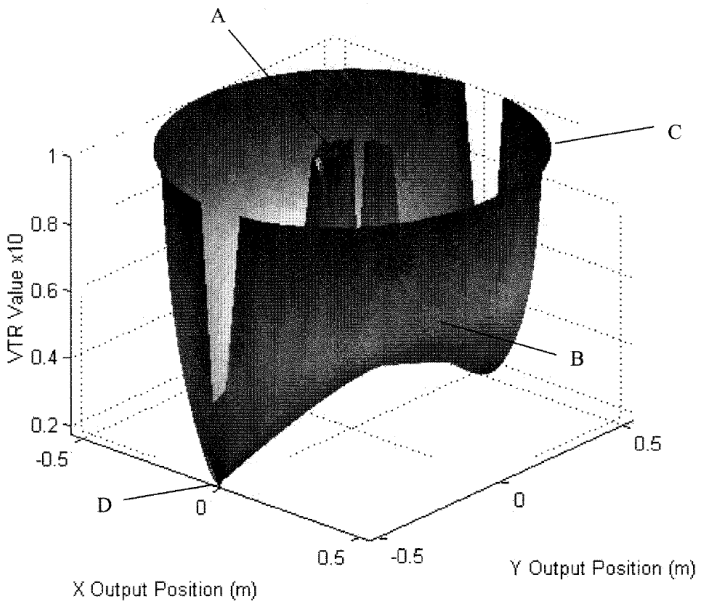

Figure 5.5: Velocity Transmissibility, 2R Planar Mechanism [84]

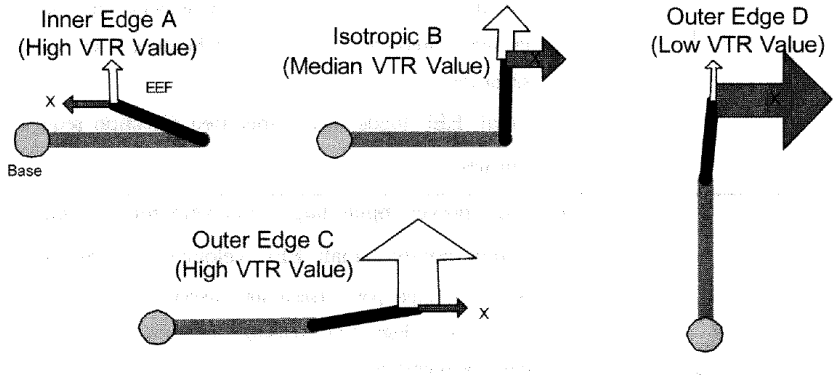

Figure 5.6: VTR, 2R Orientations [84]

zero, the mechanism is well configured for transferring velocity to the EEF (location D). The minimum values of VTR occur when the x direction of motion is ineffective, indicated at locations A and C. It should be noted that as the MOT criterion is dominated by the critical direction/joint as it approaches zero, transmissibility information about other directions is not available. The VTR criterion is a more accurate description of the capabilities of the manipulator due to the directionality of the formulation.

5.1.2.2 The Application of Geometric Criteria to the ICV

These are a number of developed geometric criteria for serial chain mechanisms and it is certainly possible to apply the concepts of geometrically based performance criteria to the suspension kinematics of ground vehicles. In the the case of the ICV, each corner represents a four (suspension, steering, camber drive) DOF serial chain system where the tire contact patch is the output and the reference is the undisturbed planar motion of the vehicle. However, there are several issues in applying these criteria that should be noted.

The first is that the development of a kinematic and dynamic suspension model is required in order to fully appreciate the application of geometric criteria. For example, a model is required in order to understand (physically) the implications of singularity avoidance or system dexterity in terms of specific camber, steering, or suspension linkage configurations. However, unlike serial chain mechanisms, posing a generalized kinematic model of a suspension

system is a complex process, one complicated even further by the prevalence of non-independent suspension types in military vehicles (e.g. beam axle/leaf spring suspensions).

The second issue is that ground vehicle suspension systems are not nearly as dexterous as serial chain mechanisms. Though the actuators utilized in the ICV architecture may individually have a significant range of motion, the EEF in this case (the contact patch) does not experience significant translations or rotations when compared to the chassis reference frame. However, the location of the individual wheel control actuators of the Intelligent Corner will affect the variation of G and H matrices over the workspace (total range of suspension movement), and the variation of criteria derived from influence coefficients will vary depending upon the actuator configuration. As it is not the goal of this report to specify a desired actuator placement (design), the discussion of the application of previously studied serial manipulator criteria in this report will focus mainly on geometric constraint based criteria and those criteria associated with energy content.

5.1.2.3 Corner Actuator Range and Limit Criteria

Joint range criteria, though geometric, are not based on Kinematic Influence Coefficients and are critical for any dexterous system utilizing intelligent actuation. Though the angular position of each individual actuator is not constrained (each is capable of continuous rotation), the kinematics of the suspension and chassis geometry will impose actuator range limitations. The

Joint Range Availability Criteria assesses the ratio of actuator position to a pre-determined limit of each individual actuator. The range availability may be expressed as a sum for the system actuators:

$$JRA = \frac{1}{n}\sum_{i=1}^{n-1}(\frac{|\theta_i - \theta_{i,mid}|}{\theta_{i,max}})^p \tag{5.19}$$

or for a critical joint:

$$JRA = MAX_{i=1}^{n-1}(\frac{|\theta_i - \theta_{i,mid}|}{\theta_{i,max}})^p \tag{5.20}$$

The exponent, p, can be used to make the criteria more critical as it approaches its operating limits. Using a higher exponent value will lower the sensitivity of the criterion near the center of its operating range.

A JRA value of zero indicates that the actuators are all in the mid-range of their travel. A value of one indicates that one of the actuators is reaching the pre-determined position threshold. A JRA value greater than one indicates that at least one of the actuators has exceeded the threshold.

There are a few issues of note when applying this criteria to the ICV. The first is that this criteria should be applied to each individual corner of the ICV, meaning that a vehicle with m corners, each utilizing n actuators (generally $n = 4$) will have m different evaluations of this criteria as each corner may be experiencing a unique position due to the terrain profile. It is important to recognize that the JRA is not applicable to a multi-speed drive wheel (MDW) as this actuator experiences continuous rotation. Therefore, the JRA value of i for each corner will range from 1 to 3. The second issue is that

the threshold for each individual actuator will likely be determined to be some value less than the absolute physical limitation of the vehicle corner, and that the range limitations may not be symmetric about the "mid-range" operating point. For example, the joint range limit for the suspension actuator may be specified such that the suspension JRA value is one when the wheel is within a certain distance of the roof of the wheel well (frame or bodywork) when the suspension is in bump, or the suspension is within a certain distance of the maximum droop capability of the suspension link members, as determined by the link lengths and attachment locations. In other words, the suspension actuator may have different range limitations in bump and in droop, which may not be captured in the JRA formulation above. The distinction between bump and droop is shown in Figure 5.7. It should be noted that Figure 5.7 is not intended to be representative of the ICV architecture and the figure is simply presented in order to differentiate suspension bump and droop.

Ground vehicles are typically designed with a specified "ride height" in mind, which is defined as the suspension position (deflection) when the vehicle is static and under no driving load. Because suspension bump and droop are measured from ride height, this steady-state suspension position should be considered to be the "mid-range" of the suspension movement. Because it is desirable for a JRA to have a value of zero when the actuator is in the ideal,

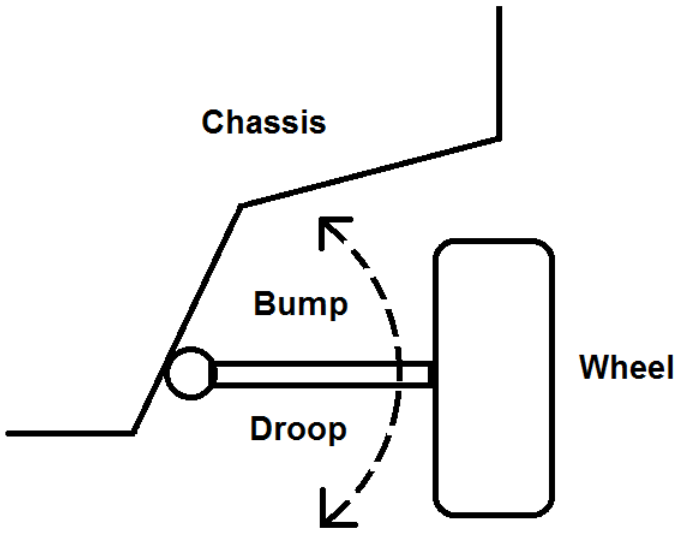

Figure 5.7: Suspension Bump and Droop

"mid-range" position, a new formulation of the JRA criteria is proposed:

$$\begin{aligned} JRA_{sp} &= \left(\frac{|\theta_i - \theta_{i,mid}|}{max(sgn(\alpha)|\theta_B|, sgn(\beta)|\theta_D|)} \right)^p \\ \alpha &= \frac{\theta_i - \theta_i, mid}{\theta_B - \theta_D} \\ \beta &= \frac{\theta_i - \theta_i, mid}{\theta_D - \theta_B} \end{aligned} \tag{5.21}$$

The above formulation of the Joint Range Availability criterion will have a value of zero if the suspension is at ride height and will approach a value of one if the suspension nears either the bump or droop limits, regardless of how the coordinate system is determined. In Equation (5.21), α and β change sign when the reference ride height angle is crossed. When the suspension is in bump, α is positive and β is negative. In droop, α is negative while β is

positive. As a result, the *max* function will select the appropriate (positive) joint range limitation for normalization, θ_B in bump and θ_D in droop. This criteria may also be used to evaluate the actuator position of the other corner actuators should their respective range limitations be asymmetrical.

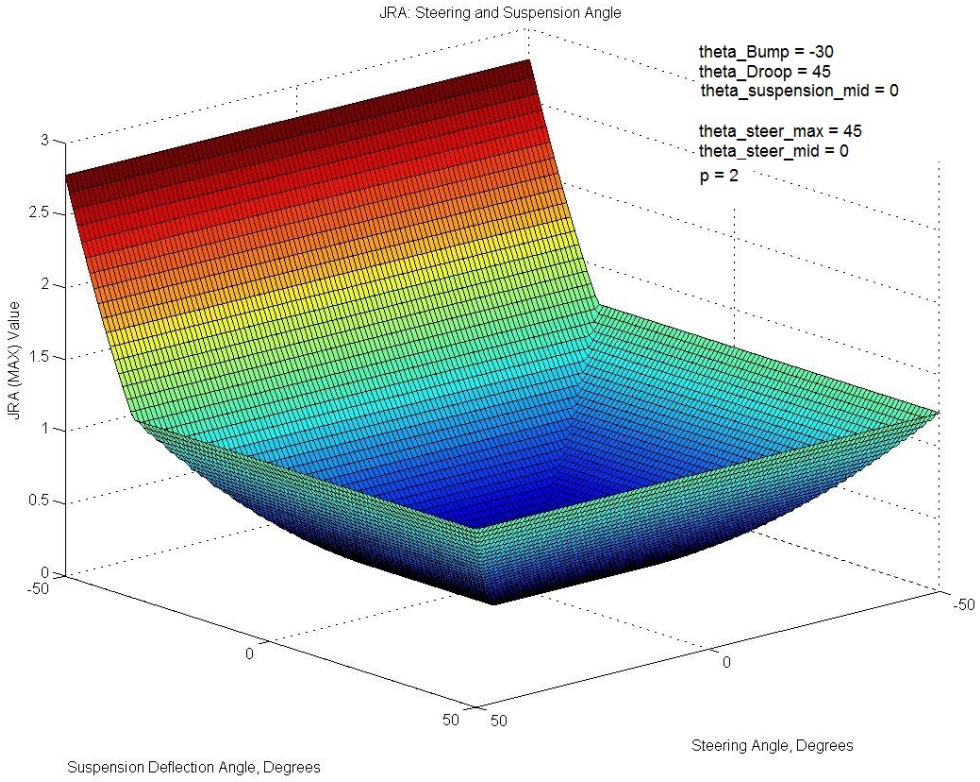

Figure 5.8: Simple Steering and Suspension Angle JRA Evaluation

A simplistic plot of a JRA (MAX) evaluation is shown in Figure 5.8. This plot shows the JRA value for two actuator inputs - steering and suspension. The ranges of both actuators vary from $-50°$ to $50°$. The limit of the steering actuator is $\pm 45°$ and the midpoint is zero. The suspension bump limit

is set to -30° and the droop limit to 45°. The asymmetry of the graph is a result of the asymmetrical evaluation of the suspension JRA formulation of Equation (5.21). It should be noted that the plot shown is scaled ($p = 2$).

The velocities and accelerations of each actuator may be evaluated in a manner similar to that of position. The Velocity Limit Avoidance (VLA) criterion is defined as:

$$VLA = MAX_{i=1}^{n} \left(\frac{|v_i|}{v_{i,max}} \right)^p \tag{5.22}$$

Again, each criteria will need to be evaluated for each corner. If the value of the VLA criterion is zero, the corner is static (no actuator motion). If the VLA value approaches one, at least one actuator is approaching the velocity limit. A VLA value greater than one indicates that at least one actuator has exceeded the limit. If the drive wheel is not included in the VLA formulation for a corner of interest, a value of zero may indicate a steady state maneuver, for example, highway driving at a constant speed, convoy operations, or steady state cornering. If the drive wheel is included, the VLA value will only approach zero when the vehicle is at rest. As such, it may be necessary to formulate a separate VLA criterion for the drive actuator (formulated in an identical manner) so that steady state maneuvers may be evaluated effectively.

The Acceleration Limit Avoidance (ALA) criterion is defined as:

$$ALA = MAX_{i=1}^{n} \left(\frac{|\alpha_i|}{\alpha_{i,max}} \right)^p \tag{5.23}$$

If the ALA criterion has a value of zero, the actuators at the corner of interest are operating at a constant velocity (no acceleration). If the ALA value ap-

proaches one, than at least one actuator is approaching the acceleration limit. An ALA value greater than one indicates that at least one actuator has exceeded the limit. It is important to note that unlike VLA, the ALA criterion is not sensitive to the inclusion of the drive actuator. In addition, both the proposed VLA and ALA criteria consider only the critical joint, rather than taking an average as previously discussed with the JLA criterion.

Just as with position, the actuator limits for velocity and acceleration are likely to be set at a value less than the mechanical limitations of each actuator. Unlike the case of position where limits are defined by the suspension kinematics and chassis geometry, the mechanical limits of velocity and acceleration are determined by the actuator design and dynamics. The set limits may be chosen for a certain operational life cycle or for factor-of-safety concerns. If the actuator limits are equivalent to the mechanical limitations, actuator performance may saturate as the JRA, VLA, or ALA values approach a value of one. In this case, system (corner) performance may be less than what is desired by the operator. If the actuator limits are set below the mechanical limits, a JRA, VLA, or ALA value greater than one indicates that an actuator has exceeded the pre-determined limit but has not yet reached the mechanical limitation of the device, thereby entering the actuator reserve as shown in Figure 5.9.

Entering the actuator reserve may be appropriate for emergency maneuvers (at the cost of actuator life span) or if no other option is available.

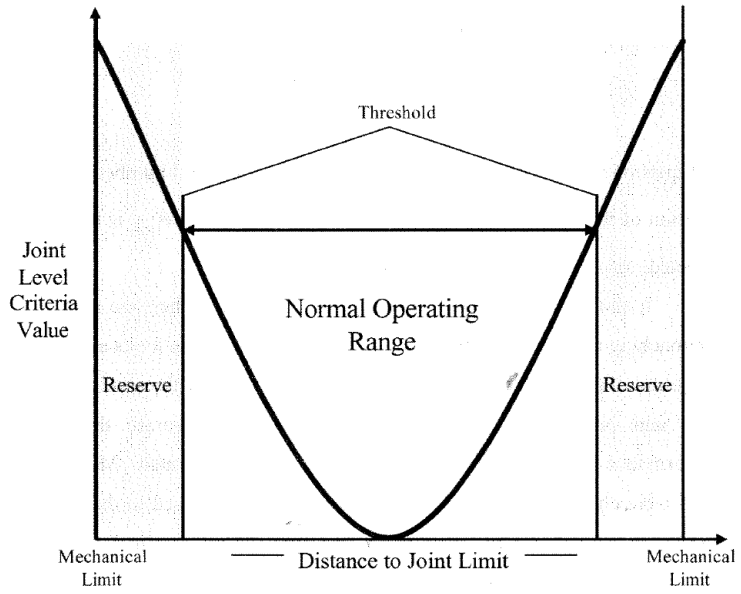

Figure 5.9: Joint Level Constraints [84]

5.1.2.4 Actuator Torque Limit Criteria

Continuing with constraint based criteria, it is important to evaluate the relationship of the torque output of the corner actuators to the torque limits. The Torque Limit Avoidance criterion is defined as:

$$TLA = MAX_{i=1}^{n} \left(\frac{|\tau_i|}{\tau_{i,max}} \right)^p \tag{5.24}$$

Similar to the previously defined constraint criteria, a TLA value of zero indicates zero actuator torque output, while a value approaching one indicates that at least one actuator is approaching the torque limit. A value greater than one indicates that at least one actuator has exceeded the torque limit and has entered the reserve. This is a critical criterion for a suspension.

5.2 Vehicle Energy Content

Criteria have been developed for serial chain mechanisms that evaluate the effects of an EEF movement on the system kinetic energy. For example, the Effective Kinetic Energy (EKE) of a system may be expressed as [27]:

$$EKE = \frac{1}{2}\dot{u}^T[I^*_{uu}]\dot{u} = \frac{1}{2}\dot{u}^T([G^e_\phi]^{-T}[I^*_{\phi\phi}][G^e_\phi]^{-1})\dot{u} \tag{5.25}$$

$[I^*_{uu}]$ - transferred effective inertia matrix

$[I^*_{\phi\phi}]$ - effective inertia matrix

$\dot{u}$ - velocity vector of the EEF

A small value of this criterion indicates that a movement of the EEF in the specified direction will result in a small change in system kinetic energy. Large values indicate EEF movement will result in high gains in kinetic energy. While this criterion is not immediately applicable to wheeled ground vehicles due to the requirement of a model for the suspension kinematics, kinetic energy and the distribution of kinetic energy (energy partition) of the vehicle *chassis* (sprung vs. unsprung kinetic energy) are of great interest to the operator.

5.2.1 Kinetic Energy Content

Vehicle kinetic energy may be broken down into two subsets, planar kinetic energy and non-planar kinetic energy. Planar kinetic energy addresses the desired vehicle motion within a two dimensional plane defined by the road surface - the longitudinal, lateral, and yaw (about the vertical axis) velocities. Non-planar kinetic energy (usually undesired) addresses vehicle motions

outside of this plane - chassis heave/bounce, roll, and pitch. Criteria in the planar category describe vehicle motion associated with the given motion plan as determined by the operator. Criteria in the non-planar category describe chassis motions associated with ground disturbances, aerodynamic effects, and vehicle equipment motion/operation.

The kinetic energy values for a vehicle are the prime descriptors of the changes in vehicle chassis motion due to inputs from the intelligent corner actuators. Kinetic energy values are an indication of both steady state and transient vehicle weight transfer from corner to corner (redistribution of normal loads). Weight transfer can not be eliminated by active suspension actuators but may be controlled to some extent. With a few special case exceptions, any non-zero, out of plane kinetic energy value represents dynamic vehicle weight transfer. As previously discussed, weight transfer generally indicates a decrease in overall vehicle traction capability due to the non-linear relationship between corner weight (vertical force on an individual tire) and maximum force capability. As an initial evaluation of the kinetic energy vehicle operational criteria, it is important to understand the physical meaning of zero, steady state, and non-steady state values of each kinetic energy parameter. [1]

Each of these energy expressions may be plotted in order to evaluate the impact of design variables (chassis mass, etc.) and state variables (vehicle yaw rates, etc.) in order to evaluate vehicle behavior. These performance

[1]The following discussion assumes a body-fixed reference frame as defined by SAE.

maps, previously discussed for tires in Section 3.3.1, are an important tool for the operator - performance maps may be used to generate decision surfaces that may then be evaluated in an effort to determine desirable vehicle operation. Vehicle behavior is highly nonlinear, and performance maps in this case allow these nonlinearities to be characterized and exploited to optimize vehicle performance.

5.2.2 Planar Motion

Planar kinetic energy may be broken down into two components: linear energy resulting from the lateral and longitudinal velocities and rotational energy resulting from the yaw velocity.

$$KE_{pl} = KE_l + KE_\theta \tag{5.26}$$

where:

$$KE_l = \frac{1}{2} m_v \sqrt{V_x^2 + V_y^2} \tag{5.27}$$

$$KE_\theta = \frac{1}{2} I \omega_{zz}^2 \tag{5.28}$$

Linear kinetic energy is a direct indicator of the linear velocity of the vehicle. A KE_l value of zero occurs when the CG of the vehicle body is stationary. It is possible to have a zero KE_l value while the vehicle is not at rest if the chassis is experiencing a purely rotational motion about the CG, either in pitch, roll, or yaw. The reference threshold value of KE_l depends on the maximum allowable vehicle speeds for the given terrain and operating conditions. Since the linear kinetic energy of the vehicle is a function of both the longitudinal and lateral

velocities, observing the relationship between the two may be of benefit to the operator. The two component kinetic energies are defined:

$$KE_{l,x} = \frac{1}{2} m_v V_x^2 \tag{5.29}$$

$$KE_{l,y} = \frac{1}{2} m_v V_y^2 \tag{5.30}$$

Yaw kinetic energy, KE_θ is an indication of the cornering (yaw) rate of the vehicle. The independent operation and dexterity of the corner actuators of the ICV will enable the operator to control the yaw center (instant center of rotation) of the vehicle. This capability has the potential to affect the maximum yaw rate appropriate for the occupants and equipment/cargo. Altering the location of the instant center of rotation of a vehicle, especially during small radius turns, may lessen the amount of centripetal force experienced by the vehicle occupants thereby increasing the maximum possible value of KE_θ.

5.2.3 Non-planar Motion

Non-planar chassis motion describes the remaining three degrees of freedom of the chassis: roll, pitch, and bounce.

5.2.3.1 Roll Kinetic Energy

Vehicle roll is a chassis rotation about the vehicle fore-aft (x, SAE definition) axis.

$$KE_r = \frac{1}{2} I \omega_{xx}^2 \tag{5.31}$$

A zero value for KE_r indicates zero roll motion. This may indicate that the vehicle is in a steady state condition or it may indicate that the chassis is experiencing linear motion only. Assuming a homogeneous, flat terrain, a zero KE_r value corresponding with a non-zero yaw (KE_θ) or non-zero lateral velocity ($KE_{l,y}$) condition indicates steady state lateral weight transfer as a result of the centripetal acceleration. A non-zero value of KE_r indicates a transient motion - the vehicle is experiencing a roll motion due to changes in the lateral tire forces.

5.2.3.2 Pitch Kinetic Energy

Vehicle pitch is a chassis rotation about the vehicle lateral (y) axis.

$$KE_p = \frac{1}{2} I \omega_{yy}^2 \tag{5.32}$$

Pitch kinetic energy is similar to roll kinetic energy. Pitch occurs during transient and steady state longitudinal vehicle motion. A zero value of KE_p indicates zero pitch velocity, meaning the vehicle is either at rest or is undergoing a steady state motion. Similar to roll kinetic energy, a zero value of KE_p coupled with a non-zero value of KE_l, x indicates steady state longitudinal weight transfer. A non-zero value of KE_p indicates a transient motion - the vehicle is experiencing a pitching motion due to changes in the longitudinal tire forces.

5.2.3.3 Bounce Kinetic Energy

Vehicle bounce/heave is a vertical chassis movement along the z axis.

$$KE_b = \frac{1}{2} m_v V_z^2 \tag{5.33}$$

A zero value of KE_b indicates zero vertical motion of the chassis CG, either due to a steady state maneuver or zero vehicle motion. Unless the vehicle is only experiencing a change in vehicle ride height (as directed by the vehicle operator), a roll or pitch maneuver due to a chassis acceleration will likely be accompanied by a non-zero value of KE_b.

5.2.4 Partial Energy Values

The following section describes the kinetic energy distribution of the chassis motion and the subsequent implications for vehicle behavior. Note - some of the following criteria will be undefined if the vehicle is at rest.

5.2.4.1 Partial Energy, System

The ratio of planar kinetic energy to the system kinetic energy is defined as:

$$PV_{pl/s} = \frac{KE_{pl}}{KE_s} \tag{5.34}$$

A $PV_{pl/s}$ value of one indicates completely planar motion. It is important to note that a value of one does not indicate a level chassis (orientation with respect to a grounded reference frame) as kinetic energy only describes vehicle velocities and does not provide information about chassis position/orientation.

Maintaining a $PV_{pl/s}$ value of one is advantageous as it results in minimized transitory states of the vehicle, indicating the rapid establishment of steady state wheel loads. A $PV_{pl/s}$ value of zero indicates purely non-planar chassis motion. This condition will occur only if the vehicle is experiencing a pure bounce, roll, or pitch motion (as commanded by the operator) while the wheel angular velocities are zero. If the vehicle is completely at rest, $PV_{pl/s}$ is undefined.

The ratio of non-planar to planar kinetic energy is defined as:

$$PV_{np/pl} = \frac{KE_{np}}{KE_{pl}} \tag{5.35}$$

$PV_{np/pl}$ is the ratio of non-planar kinetic energy to planar kinetic energy. Ideally this value should be low (close to zero) as non-planar energy should be minimized. A value of zero indicates steady state planar vehicle motion. This ratio will be undefined if the vehicle is rolling, pitching, or experiencing bounce while the wheels are static. This situation may occur if the operator is commanding a change in vehicle ride height while the wheels are at rest. This maneuver may be the result of the operator positioning a piece of on-board equipment such as a camera, sensor, or weapon system.

5.2.4.2 Partial Energy, Planar

The partial energy content of the longitudinal and lateral velocities are defined as:

$$PV_{x/l} = \frac{KE_{l,x}}{KE_{l}} \tag{5.36}$$

$$PV_{y/l} = \frac{KE_{l,y}}{KE_l} \tag{5.37}$$

Defining the components of the linear velocity give the operator the ability to observe the individual linear velocity contributions to the total linear energy content. This ability may be important in the application of vehicle equipment that is directionally sensitive. An ICV with sufficient corner dexterity may be able to move so that the partial energy content $PV_{y/l}$ achieves a value of one and the KE_θ is zero (pure lateral movement). For example, an operator of an armored vehicle may be able to specify a motion path by observing the partial energy content such that the vehicle always presents the front of the vehicle, which is generally the most heavily armored, to an perceived threat.

Simplistic representations of lateral and longitudinal partial kinetic energies (with respect to linear kinetic energy) are show in Figures 5.10 and 5.11. The formulation of these partial energy values are simple enough that representations may be generated without defining complex vehicle motions. Each plot shows the value of the partial energy with respect to the total linear energy as each velocity, lateral and longitudinal, is varied from zero to 10 m/s. Presenting maps such as these provide the operator with the ability to visually observe the current linear energy distribution.

The ratios of linear and yaw kinetic energy to planar energy are expressed as:

$$PV_{l/pl} = \frac{KE_l}{KE_{pl}} \tag{5.38}$$

$$PV_{\theta/pl} = \frac{KE_\theta}{KE_{pl}} \tag{5.39}$$

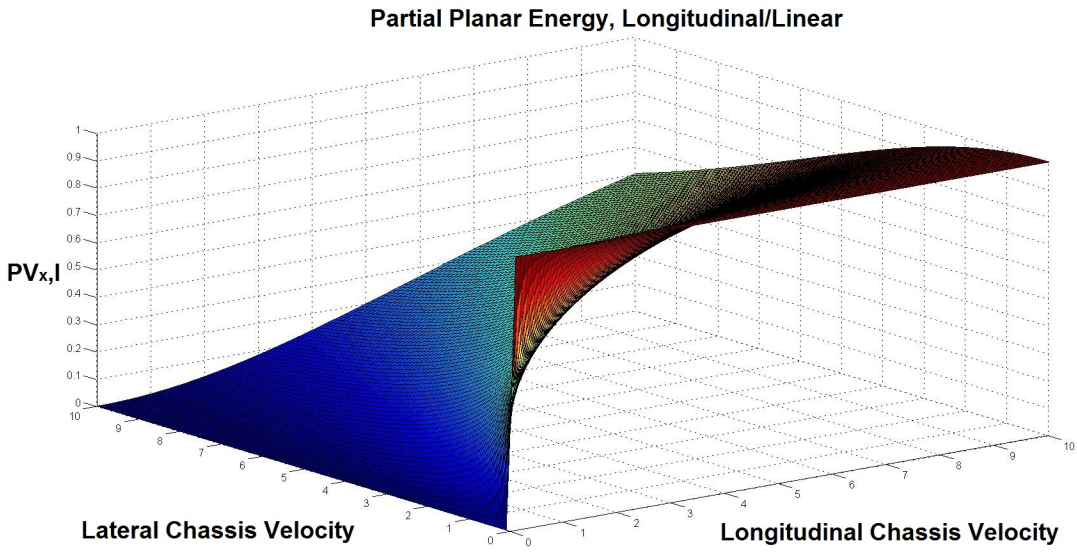

Figure 5.10: Ratio of Longitudinal Kinetic Energy to Vehicle Linear Kinetic Energy

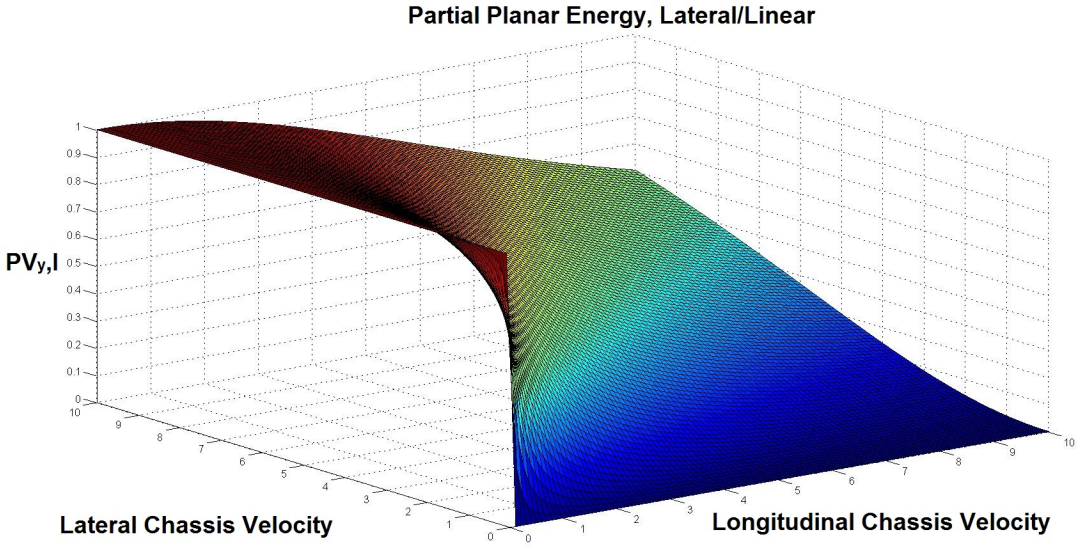

Figure 5.11: Ratio of Lateral Kinetic Energy to Vehicle Linear Kinetic Energy

These two values are an indication of the turning radius of the vehicle. A $PV_{\theta/pl}$ value of 1 ($PV_{l/pl}$ is 0) indicates a pure yaw about the vehicle CG (turn diameter is the length of the vehicle) and a $PV_{l/pl}$ of 1 ($PV_{\theta/pl}$ is zero) indicates completely longitudinal motion. The optimal value of $PV_{l/pl}$ and $PV_{\theta/pl}$ are specific to the situation. The operator will determine the ideal (or intended) turn radius depending on the vehicle planned motion path.

The ratios of pitch and roll energy to non-planar energy are:

$$PV_{p/np} = \frac{KE_p}{KE_{np}} \tag{5.40}$$

$$PV_{r/np} = \frac{KE_r}{KE_{np}} \tag{5.41}$$

The values of $PV_{p/np}$ and $PV_{r/np}$ are most significant when evaluated with respect to one another. A combination of chassis pitch and roll occurs during transient cornering maneuvers and is accompanied by lateral and longitudinal load transfer. For example, a vehicle approaching a corner will generally experience a pitch motion as braking occurs, followed by a combined pitch and roll motion as the vehicle enters the corner, and finally a combined reverse pitch and roll motion as the vehicle accelerates longitudinally out of the corner. Diagonal load transfer during transient cornering maneuvers affects the understeer coefficient (discussed in Chapter 6) of the vehicle and is largely unavoidable. However, minimizing pitch and roll will improve the chassis response of the vehicle.

The ratio of bounce kinetic energy to the non-planar kinetic energy is

expressed as:

$$PV_{b/np} = \frac{KE_b}{KE_{np}} \tag{5.42}$$

A $PV_{b/np}$ value of one indicates a change in the vehicle ride height without associated pitch or roll movements. This may or may not occur while the vehicle is in motion. A non-zero value of $PV_{b/np}$ is not an indicator of poor vehicle performance; changing the vehicle ride height (corner heights) is often necessary and may be required by the operator for vehicle visibility reasons.

The ratios of pitch energy and roll energy to the system energy are expressed as:

$$PV_{p/s} = \frac{KE_p}{KE_s} \tag{5.43}$$

$$PV_{r/s} = \frac{KE_r}{KE_s} \tag{5.44}$$

A $PV_{p/s}$ or $PV_{r/s}$ value of one indicates a special case vehicle operating condition - the vehicle is experiencing a pure roll or pure pitch movement. These conditions may be specified by the operator if a particular vehicle body attitude is required, for example, in aiming a piece of on board equipment.

The ratio of bounce to system energy is:

$$PV_{b/s} = \frac{KE_b}{KE_s} \tag{5.45}$$

The $PV_{b/s}$ value is another indication of a special case of vehicle motion. A $PV_{b/s}$ value of one indicates a change in ride height while the vehicle is (otherwise) not in motion. This situation may occur due to vehicle loading (adding of cargo) or due to preparation for obstacle avoidance. If the value of $PV_{b/s}$

is less than one but greater than zero, the vehicle is experiencing a vertical displacement of the chassis CG while the vehicle is in motion. Unless the vehicle suspension actuators are capable of completely isolating the chassis from road disturbances (100% active suspension), the chassis will experience continual vertical displacements, most likely coupled with bounce and roll motions. The values of $PV_{b/s}$ and $PV_{b/np}$ may be used to assess the vehicle chassis accelerations for which the operator may specify limits associated with driver comfort.

5.3 Criteria Summary

Table 5.1 lists the various criteria described in this chapter, the definitions (symbol and expression), and the associated physical meanings.

Table 5.1: Summary of Criteria Based on Serial Chain Robotic Systems

Criteria	**Symbol**	**Definition**	**Meaning**
Joint Range Availability	JRA	$MAX_{i=1}^{n-1}(\frac{\lvert\theta_i-\theta_{i,mid}\rvert}{\theta_{i,max}})^p$	A value of zero indicates the actuators are in the middle of their range of position. A value of one indicates that at least one actuator is at its range threshold and a value greater than one indicates that at least one actuator has entered its reserve.
Joint Range Availability, Suspension	JRA_{sp}	$\left(\frac{\lvert\theta_i-\theta_{i,mid}\rvert}{max(sgn(\alpha)\lvert\theta_B\rvert,sgn(\beta)\lvert\theta_D\rvert)}\right)^p$	This JRA formulation is for suspension actuators with asymmetric range limits. The meaning of the values are the same as those of JRA.
Velocity Limit Avoidance	VLA	$MAX_{i=1}^{n}\left(\frac{\lvert v_i\rvert}{v_{i,max}}\right)^p$	A value of zero indicates that the corner of interest is at rest (static). A value of one indicates that at least one actuator is approaching its velocity limit. A value greater than one indicates that at least one actuator has entered its reserve.

Table 5.1: Summary of Criteria Based on Serial Chain Robotic Systems, Continued

Criteria	**Symbol**	**Definition**	**Meaning**
Acceleration Limit Avoidance	ALA	$MAX_{i=1}^{n}\left(\frac{\lvert\alpha_i\rvert}{\alpha_{i,max}}\right)^p$	A value of zero indicates that the actuators at the corner of interest are operating at a constant velocity or at rest. A value of one indicates that at least one actuator is reaching its acceleration threshold. A value greater than one indicates that at least one actuator has entered its threshold.
Torque Limit Avoidance	TLA	$MAX_{i=1}^{n}\left(\frac{\lvert\tau_i\rvert}{\tau_{i,max}}\right)^p$	A value of zero indicates zero actuator torque output for the corner of interest. A value of one indicates that at least one actuator has reached the torque limit. A value greater than one indicates that at least one actuator has entered its reserve.
System Kinetic Energy	KE_s	$KE_{pl} + KE_{np}$	System kinetic energy is the summation of chassis planar (pl) and chassis non-planar (np) kinetic energy.
Planar Kinetic Energy	KE_{pl}	$KE_l + KE_\theta$	Planar kinetic energy is the summation of the chassis linear and yaw kinetic energy values.

Table 5.1: Summary of Criteria Based on Serial Chain Robotic Systems, Continued

Criteria	**Symbol**	**Definition**	**Meaning**
Linear Kinetic Energy	KE_l	$\frac{1}{2}m_v\sqrt{V_x^2+V_y^2}$	Linear kinetic energy is linear energy associated with the lateral and longitudinal velocity vector summation. The value is zero when the center of gravity (CG) of the vehicle is stationary with respect to the plane of motion.
Linear Kinetic Energy, X	$KE_{l,x}$	$\frac{1}{2}m_v V_x^2$	Longitudinal component of the linear chassis kinetic energy.
Linear Kinetic Energy, Y	$KE_{l,y}$	$\frac{1}{2}m_v V_y^2$	Lateral component of the linear chassis kinetic energy.
Yaw Kinetic Energy	KE_θ	$\frac{1}{2}I\omega_{zz}^2$	Yaw kinetic energy is the rotational energy of the chassis about the z axis. A value of zero indicates no yaw motion of the vehicle.
Non-Planar Kinetic Energy	KE_{np}	$KE_r + KE_p + KE_b$	The non-planar chassis energy is the summation of the roll, pitch, and bounce kinetic energies.
Roll Kinetic Energy	KE_r	$\frac{1}{2}I\omega_{xx}^2$	Roll kinetic energy is describes vehicle rotation about the x axis. Non-zero values occur during transient vehicle motions.

Table 5.1: Summary of Criteria Based on Serial Chain Robotic Systems, Continued

Criteria	**Symbol**	**Definition**	**Meaning**
Pitch Kinetic Energy	KE_p	$\frac{1}{2}I\omega_{yy}^2$	Pitch kinetic energy is similar to roll energy and describes vehicle rotation about the y axis.
Bounce Kinetic Energy	KE_b	$\frac{1}{2}m_v V_z^2$	Bounce kinetic energy indicates a translation of the vehicle chassis along the z axis (with respect to the ground plane). A zero value indicates zero vertical CG motion as a result of a static vehicle or a steady state maneuver.
Partial, Planar/System	$PV_{pl/s}$	$\frac{KE_{pl}}{KE_s}$	A value of one indicates purely planar motion and a value of zero indicates purely non-planar motion. Maintaining a value of one is beneficial as it minimizes vehicle transient motion.
Partial, Non-Planar/Planar	$PV_{np/pl}$	$\frac{KE_{np}}{KE_{pl}}$	A value of zero (not undefined) also indicates purely planar chassis motion. Maintaining a value close to zero will minimize vehicle transient states.
Partial, Longitudinal/Linear	$PV_{x/l}$	$\frac{KE_{l,x}}{KE_l}$	A value of one indicates purely longitudinal motion.

Table 5.1: Summary of Criteria Based on Serial Chain Robotic Systems, Continued

Criteria	**Symbol**	**Definition**	**Meaning**
Partial, Lateral/Linear	$PV_{y/l}$	$\frac{KE_{l,y}}{KE_l}$	A value of one indicates purely lateral motion. This is only possible if the ICV is of sufficient (corner) dexterity or the vehicle is experiencing pure lateral sliding.
Partial, Linear/Planar	$PV_{l/pl}$	$\frac{KE_l}{KE_{pl}}$	A value of one indicates purely linear planar motion, possibly coupled with out of plane chassis motion.
Partial, Yaw/Planar	$PV_{\theta/pl}$	$\frac{KE_\theta}{KE_{pl}}$	A value of one indicates purely yaw motion about the CG of the vehicle.
Partial, Pitch/Non-Planar	$PV_{p/np}$	$\frac{KE_p}{KE_{np}}$	A value of one indicates only pitch non-planar chassis energy, possibly coupled with planar chassis motion.
Partial, Roll/Non-Planar	$PV_{r/np}$	$\frac{KE_r}{KE_{np}}$	A value of one indicates only roll non-planar chassis energy, possibly coupled with planar chassis motion.
Partial, Bounce/Non-Planar	$PV_{b/np}$	$\frac{KE_b}{KE_{np}}$	A value of one indicates only bounce non-planar chassis energy, possibly coupled with planar chassis motion.
Partial, Pitch/System	$PV_{p/s}$	$\frac{KE_p}{KE_s}$	A value of one indicates a pure pitch chassis motion about the CG.
Partial, Roll/System	$PV_{r/s}$	$\frac{KE_r}{KE_s}$	A value of one indicates a pure roll chassis motion about the CG.

Table 5.1: Summary of Criteria Based on Serial Chain Robotic Systems, Continued

Criteria	**Symbol**	**Definition**	**Meaning**
Partial, Bounce/System	$PV_{b/s}$	$\frac{KE_b}{KE_s}$	A value of one indicates a purely vertical (along z axis) motion - a change of vehicle ride height.

5.4 Chapter Summary

This chapter reviews performance criteria developed by the Robotics Research Group (RRG) for evaluating the motion of serial chain mechanisms, their application to the Intelligent Corner Vehicle (ICV) concept, and the subsequent physical meanings of each criteria. Each criteria presented, along with the associated symbol, definition, and physical meaning, is listed in table 5.1. Table 5.2 presents the key findings, conclusions, and recommendations of the chapter.

Table 5.2: Chapter 5 Key Findings, Conclusions, and Recommendations

Result	**Conclusion**	**Recommendation**
The various inverse kinematic solutions for serial chain robotic systems may be **evaluated with** a variety of **motion criteria** developed by the Robotics Research Group (RRG).	Motion criteria that are task independent are applicable to any dynamic system of sufficient geometric complexity.	Motion criteria derived from Kinematic Influence Coefficients (Summarized in Table 5.1) may be applied to automotive suspension systems both as a method of evaluation (motion) and as a comparison between the capabilities of various suspension layouts.
Criteria developed by the RRG may be classified as constraint based or non-constraint based criteria. Constraint based criteria **focus on physical limitations and safety** while non-constraint based criteria focus more on quality of motion.	Constraint based criteria are more readily applicable to the ICV architecture as the reliable, safe operation of the intelligent actuator components is of greater concern to the operator than kinematic precision and quality.	The initial application of serial chain derived motion criteria should prioritize constraint based criteria.
The **application of geometric criteria** to the suspension kinematics of ground vehicles requires the development of suspension models (Section 5.1.2.2).	Unlike serial chain mechanisms, developing a generalized kinematic/dynamic model is a difficult process, one that is made more complex by the prevalence of non-independent suspension types on military vehicles.	Fully evaluating geometrically based criteria will require the development of a variety of representative suspension models (a library) that include both independent and dependent suspension types.

Table 5.2: Key Findings, Conclusions, and Recommendations (Continued)

Result	**Conclusion**	**Recommendation**
Vehicle suspension systems are not as dexterous as serial chain robotic systems and criteria formulated with Kinematic Influence Coefficients may not vary significantly over any individual workspace.	While the variation of geometric criteria may be small for a specific suspension type, the range of variation will change both with suspension type and the location (mounting) of actuators in the Intelligent Corner.	Range of geometric criteria variation may be used as a method for evaluating the effectiveness of various suspension types and actuator mounting locations.
Actuator range and limit criteria (Summarized in Table 5.1) are important for any dexterous system utilizing intelligent actuation and may be applied to the Intelligent Corner Vehicle (ICV, Section 4.4).	Actuator limits and "mid-range" points will be determined by chassis geometry in addition to actuator limitations, and this class of criteria will need to be evaluated for each individual Intelligent Corner.	The range/limit criteria evaluations of different corners should be evaluated with full vehicle models as the relationships between values may yield additional insight into the quality of vehicle motion.
Criteria that describe the **energy content and distribution** of a serial chain mechanisms are the prime descriptors of both steady state motion and component accelerations and may be applied to the ICV (Section 5.2).	The critical values (thresholds) and range of these criteria, listed in Table 5.1, are heavily dependent upon vehicle type and maximum allowable vehicle speeds for a given terrain/operating conditions.	The critical values and ranges should be evaluated with full vehicle models (representing a variety of suspension types) for a range of operating conditions.

Chapter 6

Concepts of Vehicle Dynamics as Applied to the Intelligent Corner Vehicle Architecture

This chapter presents an overview of classic vehicle dynamics and the associated concepts that are applicable to the ICV architecture. This chapter begins with a discussion of the impact of tire behavior and the subsequent implications for vehicle control.

6.1 Tire Criteria

Chapter 3 presented a brief overview of the behavior of pneumatic tires. The following section discusses the performance criteria that may be derived from tire behavior and the associated physical meanings of each.

6.1.1 Longitudinal and Lateral Force Generation

6.1.1.1 Peak Slip Values

As mentioned in Chapter 3, the generation of tire forces is a function of lateral and longitudinal slip (slip ratio and slip angle). The peak tractive force, laterally and longitudinally, occurs at some value of slip and this critical value is a function of the tire properties and operating condition (e.g. normal force on the tire, road surface condition, etc.). If the slip value required for maximum

lateral or longitudinal force is known for a given set of operating conditions, the behavior of the tire may be characterized by slip ratios. For longitudinal force generation, the Normalized Slip Ratio Margin for each corner, n is defined as:

$$\begin{aligned} NSRM_t &= \frac{i_{n,peak} - i_n}{i_{n,peak}} \\ NSRM_b &= \frac{i_{s,n,peak} - i_{s,n}}{i_{s,n,peak}} \end{aligned} \tag{6.1}$$

$i_{n,peak}$ - slip ratio at which maximum longitudinal force is achieved, wheel n

$i_{s,n,peak}$ - skid-slip ratio at which maximum braking force is achieved, wheel n

i_n - slip ratio, wheel n

$i_{s,n}$ - skid-slip ratio, wheel n

There are two definitions for the NRSM criterion, one for tractive effort ($NSRM_t$), which is a function of the wheel slip ratio, i, and one for braking effort ($NSRM_b$), which is a function of the skid-slip, i_s. For the NSRM criterion, a value of one indicates that the vehicle is generating zero longitudinal force, the wheel slip is zero, and the thrust margin is 100% in traction or in braking. The tire approaches peak traction capability as the value approaches zero, and a value less than zero indicates that the tire has exceeded the peak longitudinal force region of the slip/force curve and is operating below its peak capability. It is also important to note that slip ratio values less than zero for the $NSRM_t$ criterion result in unstable tire behavior as the frictional resistive force decreases as wheel speed increases as seen in Figure 3.3 in Chapter 3. As a result, slip percentage values must be monitored (closed loop) in order to avoid unstable behavior.

For lateral force generation, the Normalized Slip Angle Margin is defined as:

$$\begin{aligned} NSAM_{(+)} &= \frac{\alpha_{n,peak,(+)} - \alpha_n}{\alpha_{n,peak,(+)}} \\ NSAM_{(-)} &= \frac{\alpha_{n,peak,(-)} - \alpha_n}{\alpha_{n,peak,(-)}} \end{aligned} \tag{6.2}$$

where $\alpha_{n,peak,\pm}$ is the slip angle at which maximum longitudinal or lateral force is achieved, wheel n, for either positive (+) or negative (-) slip angle values, and α_i is the slip angle of wheel n. A distinction here is necessary between positive and negative slip angle values because the lateral tractive capability of a tire is asymmetrical. For example, positive or negative wheel camber will cause slight differences in the $\pm y$ lateral force generation capability and as such, the values of $\alpha_{n,peak}$ will be slightly different. A value of NSAM of one indicates that the tire is generating zero lateral force and 100% of the lateral force margin is available. A value of zero for either criteria indicates that the lateral performance of the tire is saturated and any further increase in α will result in a negative criterion value and diminished tire performance.

Because the peak longitudinal and lateral forces are coupled (recall the traction circle, Figure 3.16) and are functions of the tire normal load, the peak i and α values will fluctuate as the slip conditions change and the corner loads change during transient maneuvers. Values of $\alpha_{n,peak,\pm}$, $i_{n,peak}$, and $i_{s,n,peak}$ are specific to the road condition, tire load, tire type, slip state, etc. For example, the slip ratio at which peak longitudinal force occurs will decrease as the steering angle, and subsequently the slip angle (α), increases. Determining

these peak valves and predicting force generation capability will depend on the tire model utilized for predicting the performance of the ICV.

6.1.1.2 Peak Torque Values

It is possible to evaluate peak force generation as a function of tractive effort (thrust) rather than as a function of slip. As previously discussed, for any given terrain type there exists a peak thrust force that the tire/terrain will tolerate. If the maximum possible tractive effort is represented as $f_{t,i}$, then the associated wheel torque is expressed as:

$$T_{i,peak} = r_{e,n} * f_{t,n} \tag{6.3}$$

where $r_{e,n}$ represents the effective radius of the wheel. For a given wheel torque, T_n, the normalized wheel torque margin is then:

$$\tau_n = \frac{T_{n,peak} - T_n}{T_{n,peak}} \tag{6.4}$$

A value of one indicates no wheel torque. A value of zero indicates torque saturation and a further increase in torque (negative τ value) will result in decreased performance and an unstable tire loading condition, assuming a forward tractive effort.

Similar to the peak slip ratio, the value of $T_{i,peak}$ will fluctuate with the road surface and operating condition of the tire. It should be noted that the NSRM and τ_i criteria are *not* independent as the maximum possible thrust is a function of wheel slip. Dependent criteria for slip and wheel torque are

provided here in order to facilitate different control schemes that may attempt to control either wheel speed or torque.

When evaluating wheel torque margins, the torque distribution must also be taken into account. In the case of non-homogeneous terrain or non-static operating conditions, the normalized torque margins may all be equal despite a difference in wheel torques, but this may not be advantageous for maximizing vehicle capability. For any given operating environment, it may be possible to establish an average torque margin, $\bar{\tau}$. The ratio of normalized torque margin to the average may be then expressed:

$$\tau_{n,i} = \frac{\tau_i}{\bar{\tau}} \tag{6.5}$$

A value of one indicates that the specific tire is operating at the desired average torque margin. The value of $\bar{\tau}$, as chosen by the operator or control software, will depend on the desired level of safety for the operating environment. Maintaining a constant value of $\tau_{n,i}$ allows each wheel to respond to wheel disturbances and changes in the terrain while retaining a specified torque safety margin for executing sudden vehicle maneuvers.

6.1.2 Lateral/Longitudinal Force Ratio

Similar to side-slip as discussed in Chapter 5, the ratios of lateral and longitudinal forces to the total force of a given tire are of interest to the operator. The ratio of lateral tire force to total tire force generation (lateral

and longitudinal) is expressed as:

$$LatFR = \frac{F_{y,n}}{F_{y,n} + F_{x,n}} \tag{6.6}$$

The ratio of lateral tire force to total tire force is an indication of the cornering condition of the tire. A value of zero indicates no lateral force generation, and a value of one indicates purely lateral force generation. A value of one is desirable for steady state cornering maneuvers, but, in practice, a value of exactly one is highly unlikely due to tire resistances and may be an indication that the wheel or vehicle is experiencing purely lateral sliding. Purely lateral sliding is likely an indication of vehicle instability or a poorly configured wheel and is undesirable.

The ratio of longitudinal force to total tire force generation is expressed as:

$$LongFR = \frac{F_{x,n}}{F_{y,n} + F_{x,n}} \tag{6.7}$$

Similar to the lateral force ratio, a value of one indicates purely longitudinal force generation. This condition is desirable for straight-line vehicle motion such as convoy maneuvers and emergency braking. Due to aerodynamic effects and road irregularities, a value of one is highly unlikely. A value of zero indicates a lack of longitudinal tire force generation. This may be an indication of lateral sliding (undesirable) or the vehicle may be static.

It should be noted that the lateral and longitudinal tire force ratios are independent of the chassis lateral and longitudinal kinetic energy ratios as, 1) the independent steering of the intelligent corners allows the wheels to assume

arbitrary steering angles with respect to one another, and 2) the independent tires only generate forces when they are in contact with the ground. A tire not in contact with the road surface will not generate force regardless of the chassis motion.

6.1.3 Camber Force Generation

Similar to lateral and longitudinal force, camber force (or camber thrust) peaks at a certain value of camber. Camber thrust adds or detracts from the lateral tire force. As previously discussed, this angle may be small (5°) for radial ply tires and large (50°) for bias ply tires. The nonlinear behavior of tire camber is shown in Figure 3.8. Camber force is beneficial during cornering maneuvers and optimizing camber force is critical if peak performance is desired by the operator.

$$NCTM = \frac{\gamma_{n,peak} - \gamma_n}{\gamma_{n,peak}} \tag{6.8}$$

The Normalized Camber Thrust Margin (NCTM) for the specified tire, n, is interpreted the same way as NSRM and NSAM - a value of one indicates zero camber thrust (usually corresponding to zero camber angle, depending on the terrain), a value of zero indicates camber thrust saturation, and a value less than zero indicates diminished camber performance. It is important to note that values exceeding the maximum camber thrust angle result in potentially detrimental heat build up in the corner (near the sidewall) of the tire. This effect is most significant in radial ply tires, which feature a flatter tread design as opposed to bias ply motorcycle tire which features a rounded tread pattern.

In this scenario, the sidewall of the tire is experiencing significant deformation as it enters and leaves the contact patch. As a result, heat generation (due to hysteresis, etc.) increases which has detrimental effects on both the tractive capabilities of the tire and the lifespan of the tire.

6.2 Predicting on road capability

The following section discusses the prediction of vehicle performance on prepared, non-deformable terrains (on-road).

6.2.1 Acceleration Prediction

The longitudinal performance of an on road, four wheeled, traditional vehicle may be predicted by the following model [87]:

$$m\frac{d^2x}{d^2t} = \frac{W}{g}a = F_f + F_r - R_a - R_rf - R_rr - R_d - R_g \tag{6.9}$$

m - mass of the vehicle

W - vehicle weight

g - gravitational acceleration constant

F_f - thrust of vehicle front axle

F_r - thrust of vehicle rear axle

R_a - aerodynamic resistance

R_rf - rolling resistance of the front tire

R_rr - rolling resistance of the rear tire

R_d - drawbar load

R_g - grade resistance

The above equation assumes the vehicle is symmetric. The forces described in Equation 6.9 are shown in Figure 6.1.

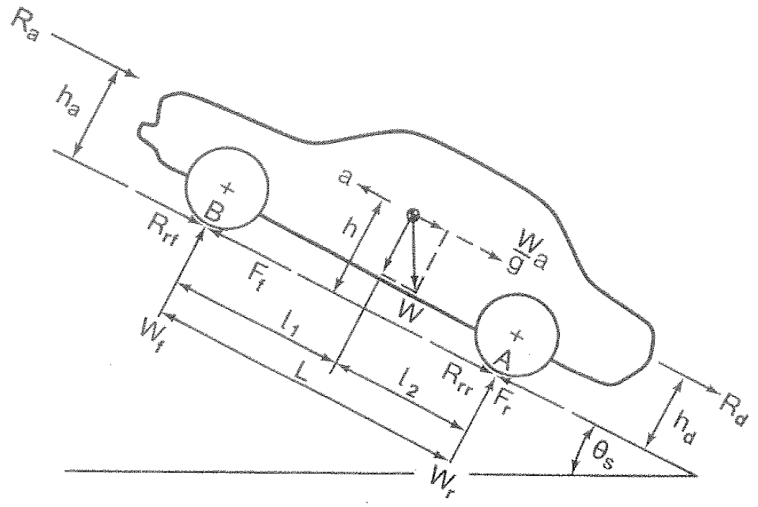

Figure 6.1: Forces Acting on a Symmetrical, Two-Axle Vehicle [87]

If the front and rear thrust terms are combined, Equation 6.9 may be rewritten as:

$$F = R_a + R_r + R_d + R_g + \frac{aW}{g} \tag{6.10}$$

For any given value of thrust (front and rear), maximizing the vehicle acceleration, $\frac{aW}{g}$, requires minimizing the aerodynamic, rolling, drawbar, and grade resistances. It is important to note that the maximum vehicle thrust is a function of both the traction capabilities at each wheel (axle) and the torque characteristics of the prime mover, in this case, the MDW. As previously

discussed, the total traction capability of a vehicle is affected by dynamic weight transfer resulting from chassis accelerations. The nonlinear relationship of the normal force/peak normalized traction curve results in a net traction loss when dynamic weight transfer occurs. As a result, the maximum possible longitudinal thrust is a function of vehicle acceleration. The individual axle loads may be determined by taking a summation of moments about points A and B in Figure 6.1 [87]:

$$W_f = \frac{W l_2 \cos\theta_s - R_a h_a - \frac{haW}{g} - R_d h_d \mp W h \sin\theta_s}{L} \tag{6.11}$$

$$W_r = \frac{W l_1 \cos\theta_s + R_a h_a + \frac{haW}{g} + R_d h_d \pm W h \sin\theta_s}{L} \tag{6.12}$$

l_1 - distance from the center of gravity to the front axle

l_2 - distance from the center of gravity to the rear axle

h_a - height of the point of application of aerodynamic resistance

h - height of the center of gravity

h_d - height of the drawbar hitch

L - vehicle wheelbase

θ_s - slope angle

The $\pm$ is determined by the uphill or downhill nature of the gradient. The minus sign is used for an uphill gradient in Equation 6.11. If small angles are assumed ($\cos(\theta_s) \approx 1$) and the aerodynamic and drawbar resistances are applied at the height of the center of gravity, Equations 6.11 and 6.12 may be simplified and combined with Equation 6.10 to obtain:

$$W_f = \frac{l_2}{L}W - \frac{h}{L}(F - R_r) \tag{6.13}$$

$$W_r = \frac{l_1}{L}W - \frac{h}{L}(F - R_r) \tag{6.14}$$

Note - the first term on the right hand side of the above equations represents the static axle load (no acceleration) and the second term represents the dynamic weight transfer as a function of total thrust, F. Because the normal loads on the front and rear wheels (axles) are functions of the longitudinal tire forces and related through the vehicle geometry, maximizing longitudinal acceleration requires maximizing the NSRM criteria for each wheel. Any criteria presented here in relation to maximizing longitudinal vehicle performance will not be independent of the slip ratio criteria.

6.2.1.1 Rolling Resistance

As discussed in Chapter 3, the rolling resistance of a tire is a function of tire construction, vehicle speed, inflation pressure, and the road surface. Of the factors that determine the rolling resistance and coefficient of rolling resistance, the vehicle and/or operator can not influence the tire type, road condition, or (generally speaking) normal load, but may have control over the inflation pressure of the tire. Increasing or decreasing the inflation pressure, as seen in Figures (3.9), will affect the rolling resistance experienced by the vehicle. Military vehicles utilize real-time control over tire pressures through the use of CTIS as described in Chapter 4. However, adjusting the inflation

pressure may have a negative impact on other aspects of vehicle performance, such as cornering stiffness, etc.

6.2.1.2 Aerodynamic Effects

Aerodynamic resistance is generally expressed in the following way [87]:

$$R_d = \frac{\rho}{2} C_D A_f V_r^2 \tag{6.15}$$

ρ - mass density of air

C_D - coefficient of aerodynamic resistance

A_f - characteristic area of the vehicle

V_r - speed of the vehicle relative to the wind

Without presenting a complete analysis of road vehicle aerodynamics, two items of note should be discussed. The first is that the aerodynamic resistance of a vehicle is a function of the characteristic vehicle frontal area, A_f, and minimizing this area will decrease the aerodynamic resistance. Lowering the vehicle ground clearance, which is the same as lowering the vehicle ride height, will reduce the vehicle frontal area, thereby minimizing the aerodynamic resistance. Lowering the aerodynamic resistance reduces the resistances acting on the vehicle, thereby improving vehicle fuel efficiency as shown in Figure 6.2 (P - engine power, F - vehicle frontal area, W - vehicle weight).

In addition to reducing drag, lowering the vehicle ride height will reduce the height of the application of aerodynamic resistive force, as represented by

h_a in Equations 6.11 and 6.12. A reduction in this moment arm will reduce the contributions of the aerodynamic force to the longitudinal dynamic weight transfer.

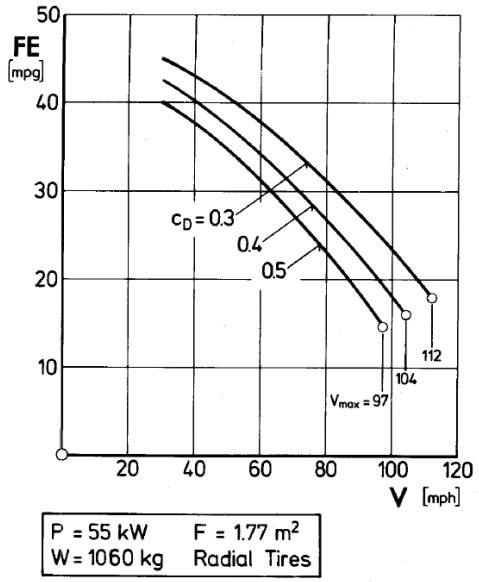

Figure 6.2: Effect of Reduction of Aerodynamic Resistance on Vehicle Fuel Economy [41]

The ability of any vehicle to lower its ride height is a function of both the irregularities and variations in the height of the road surface and restrictions of the suspension kinematics. For example, the M1 Abrams tank has a standard ground clearance of approximately 1.5 ft which may be reduced significantly depending on the motion range of the suspension linkages, but vehicles such as the FMTV fleet, which utilize beam axle type suspensions will benefit little from a reduction in chassis height due to the interference of the beam axle structures. However, it is possible that reducing the ride height of a military

vehicle may make the vehicle chassis more vulnerable to IED threats.

The second item of note is that the coefficient of aerodynamic resistance (in addition to the characteristic area) is a function of vehicle configuration for those vehicles with movable on-board equipment. This includes vehicles with articulated weapon systems such as turrets, as featured on the M1 Abrams and M2 Bradley, as well as tactical vehicles with installed overhead gunner kits, such as the HMMWV. As a result, there will be an ideal configuration for each vehicle that will minimize the aerodynamic resistances. Because the aerodynamic resistance is a function of the square of speed, minimizing C_D and A_f may only be significant at highway speeds (convoy maneuvers, etc.).

The JRA criterion from Chapter 5 may be adapted for assessing the configuration for minimizing aerodynamic resistance. If it is assumed that every n articulated elements on the chassis have a position (translational or rotational) for which the total aerodynamic drag is at a minimum, then the following criterion, Articulated Equipment Drag, may be posed:

$$AED = \frac{1}{n}\sum_{i=1}^{n}(|\theta_i - \theta_{i,C_{D,min}}|)^p \tag{6.16}$$

$\theta_{i,C_{D,min}}$ - Angle or orientation at which drag is minimized for the i^{th} element

The angular value, θ_i, of the above criterion may represent either a rotation or longitudinal displacement. The value of AED will range from zero, indicating that all articulated elements are positioned in a way to minimize drag, to a platform/equipment dependent maximum.

6.2.2 Braking Performance

The total braking force of a vehicle may be expressed much the same way as the total acceleration force [87]:

$$F_{res} = F_b + f_r W \cos\theta_s + R_a \pm W \sin\theta_s + R_t \tag{6.17}$$

where the terms are the same as Equation 6.9, F_b is the braking force, and R_t is the transmission, or drivetrain, resistance. These forces are shown in Figure 6.3.

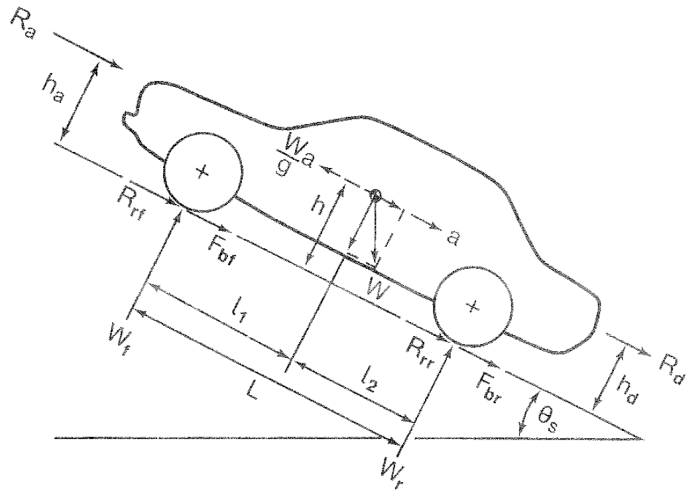

Figure 6.3: Braking Forces Acting on a Symmetrical, Two-Axle Vehicle [87]

Equation 6.17 assumes the drawbar load is zero and that the aerodynamic resistance is applied at the height of the center of gravity. The positive sign term for $Wsin(\theta_s)$ should be used when the vehicle is going uphill. Longitudinal weight transfer also occurs during braking, and the individual axle

loads may be expressed as:

$$W_f = \frac{1}{L}[Wl_2 + h(\frac{W}{g}a - R_a \pm W\sin\theta_s)] \tag{6.18}$$

$$W_r = \frac{1}{L}[Wl_2 - h(\frac{W}{g}a - R_a \pm W\sin\theta_s)] \tag{6.19}$$

In this case, the negative sign term for $W\sin\theta_s$ should be used when the vehicle is traveling uphill. If the force equilibrium in the horizontal direction is considered:

$$F_b + f_r W = F_{bf} + F_{br} + F_r W = \frac{W}{g}A - R_a \pm W\sin\theta_s \tag{6.20}$$

and substituted into Equations 6.18 and 6.19, the normal loads on the axles may be expressed as:

$$W_f = \frac{1}{L}[Wl_2 + h(F_b + f_r W)] \tag{6.21}$$

$$W_r = \frac{1}{L}[Wl_1 - h(F_b + f_r W)] \tag{6.22}$$

For a given normal load on a tire, there exists a maximum braking force that may be exerted by the tire before the onset of sliding. If the maximum longitudinal force that may be generated is expressed as the product of a coefficient of road adhesion and the normal force, the front and rear tire forces may be expressed as:

$$F_{bf,max} = \mu W_f = \frac{\mu W[l_2 + h(\mu + f_r)]}{L} \tag{6.23}$$

$$F_{br,max} = \mu W_r = \frac{\mu W[l_1 - h(\mu + f_r)]}{L} \tag{6.24}$$

Wong [87] notes that the above equations indicate that total braking force is maximized when the distribution of braking forces (between the front and rear axles) is the same as the distribution of normal load:

$$\frac{K_{bf}}{K_{br}} = \frac{F_{bf,max}}{F_{br,max}} = \frac{l_2 + h(\mu + f_r)}{l_1 - h(\mu + f_r)} \tag{6.25}$$

where K_{bf} is the proportion of total braking force, front, and K_{br} is the proportion of total braking force, rear. It should be noted that this model assumes identical tires operating on a homogeneous road surface.

If the braking force on either axle exceeds the traction capability of the tire, gross sliding occurs (as discussed in Chapter 3) and the wheels effectively "lock up". If the distribution of braking force is not equal to the distribution of normal load, either the front tires or rear tires will lock up first as the total braking force increases. The behavior of the vehicle varies significantly depending on which axle locks up first as braking force is applied. If gross sliding is taking place in the contact patch of a tire, the ability of that tire to resist lateral forces (as well as longitudinal) is severely diminished. In addition, if the wheel is steered, directional control is lost. If the rear tires lock up first, the resulting system is unstable [87]. Any lateral perturbation of the system (wind, etc.) results in an inertial yawing moment is produced about the yaw center of the front axle. The moment arm of the inertial force increases with the yaw angle, increasing the yaw rate, until the vehicle has rotated 180° as shown in Figure 6.4.

A loss of traction in the front wheels results in a loss of directional

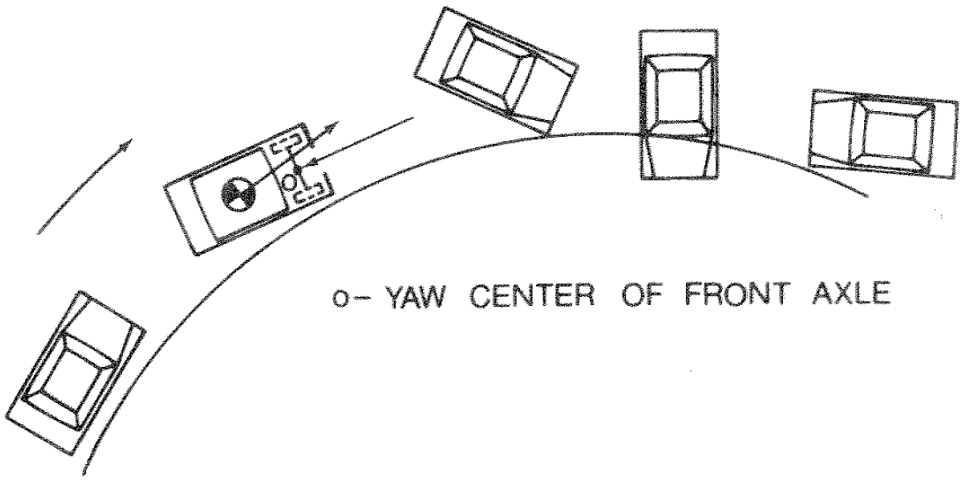

Figure 6.4: Loss of Directional Stability Due to Rear Tire Lock-Up [87]

control due to the inability of the steered wheels to effectively transmit lateral forces to the road surface. However, the resulting vehicle system is stable. In this case, the inertial yawing moment produced as the result of a perturbation will generate is self correcting and will drive the vehicle back to a steady state, straight line orientation [87].

If the only vehicle resistance considered is rolling resistance, Wong presents two equations describing the rate of acceleration for which the front and rear wheels will lock up:

$$\left(\frac{a}{g}\right)_f = \frac{\mu l_2/L + K_{bf} f_r}{K_{bf} - \mu h/L} \tag{6.26}$$

$$\left(\frac{a}{g}\right)_r = \frac{\mu l_2 1/L + (1 - K_{bf}) f_r}{1 - K_{bf} + \mu h/L} \tag{6.27}$$

such that the front tires will lock up first if the associated front acceleration

is less than that of the rear:

$$\left(\frac{a}{g}\right)_f < \left(\frac{a}{g}\right)_r \tag{6.28}$$

and the rear tires will lock up first if the opposite is true:

$$\left(\frac{a}{g}\right)_r < \left(\frac{a}{g}\right)_f \tag{6.29}$$

It is important to note that if the braking distribution is constant, optimal braking (both front and rear tires lock at the same time) will only occur for a specific value of μ. In other words, because equations (6.26) and (6.27) both contain a specific μ term, a vehicle will only experience optimal braking on a specific road surface for a specific braking force distribution. If the coefficient of braking distribution is variable, the operator or control software may vary the braking distribution in order to maintain optimal braking. Again, this model assumes identical tires operating on a homogeneous terrain.

The braking behavior of a vehicle may also be characterized by the braking efficiency, defined as:

$$\eta_b = \frac{a/g}{\mu} \tag{6.30}$$

The value of μ in this case is road surface specific. The important concept is that the distribution of braking forces must be a function of the road surface type and normal wheel loads in order to maximize braking performance and avoid a condition of instability. Just as with tractive performance, optimizing braking requires optimizing the NSRM values for the skid-slip condition.

6.2.3 Vehicle Cornering Performance

The following section presents a basic evaluation of vehicle cornering performance and one of the most important concepts in vehicle corning behavior - vehicle understeer/oversteer. Understeer and oversteer are a measure of the sensitivity of the steering of a vehicle with respect to forward velocity during a steady state cornering scenario. In discussing the steady state cornering behavior of a wheeled vehicle, Milliken and Milliken [57] present a simple, two dimensional, bicycle model, shown in Figure 6.5.

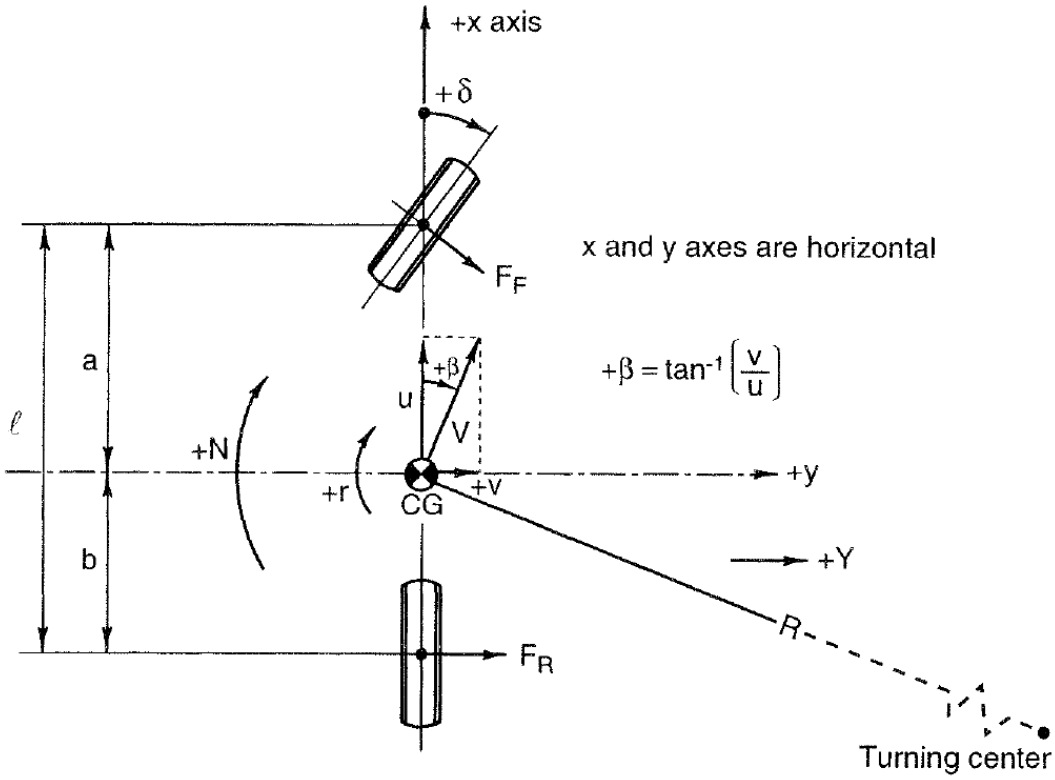

Figure 6.5: Simple Bicycle Model [57]

This model necessarily makes a series assumptions about the constrained behavior of the vehicle. The first is that there is no lateral or longitudinal load transfer. Each wheel of the bicycle model is intended to represent an axle (front or rear) and the normal axle loads are equivalent to the static vehicle weight distribution. All motion is planar, i.e., there are no rolling or pitching motions of the chassis. The tires operate in the linear range, meaning the lateral force generation of each tire may be represented as a linear function of tire slip angle as discussed in Chapter 3. The velocity of the vehicle is constant and aerodynamic effects are not included. The model does not take into account suspension or chassis compliance effects. Small wheel and operating angles are assumed.

6.2.3.1 Neutral Steer

Milliken and Millken use the bicycle model representation to evaluate three different scenarios involving three different locations of the chassis CG along the x (SAE) axis. In the first example, the CG is located in the middle of the chassis, equidistant from both axles ($a = b = l/2$), as shown in Figure 6.6. The front and rear tire cornering stiffnesses, C_F and C_R, are equivalent.

Because the behavior of the vehicle in this scenario is steady state, the chassis may be thought of as a beam in lateral force and moment equilibrium:

$$\text{Force Equilibrium } : CF = Y_F + Y_R = C_F\alpha_F + C_R\alpha_R \tag{6.31}$$

$$\text{Moment Equilibrium} : C_F\alpha_F a = C_R\alpha_R b \tag{6.32}$$

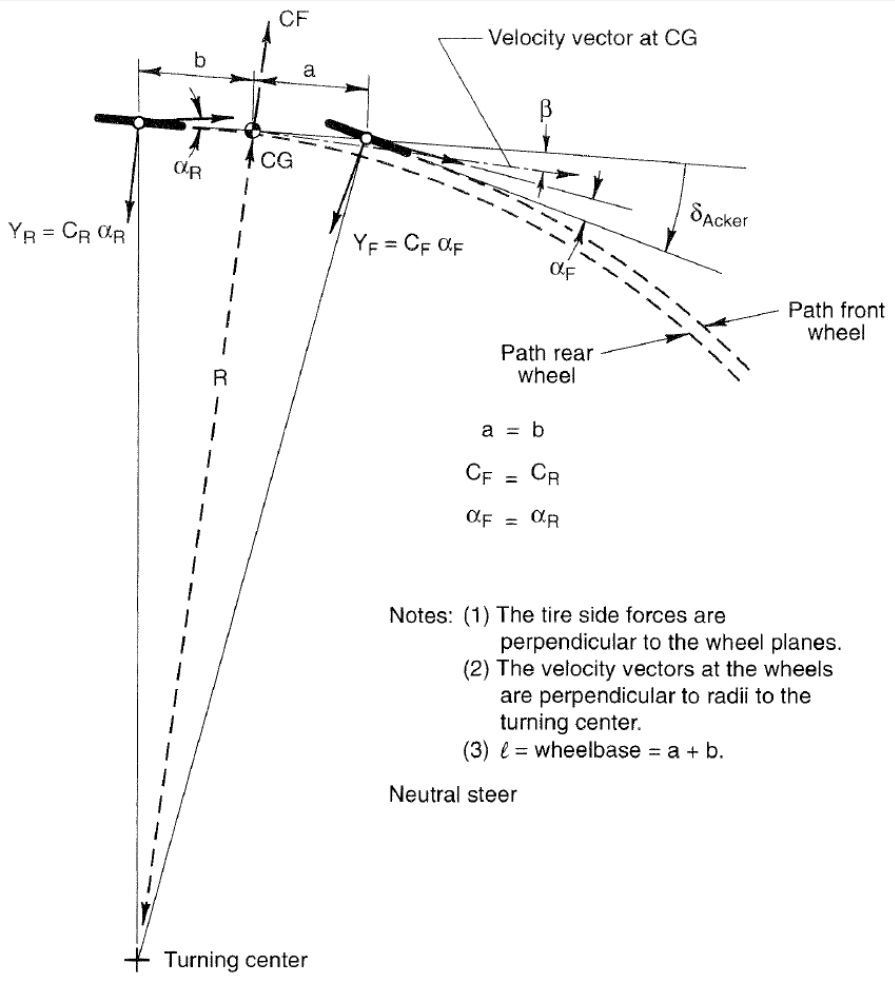

Figure 6.6: Neutral Steer Bicycle Model [57]

In this scenario, the slip angles of the front and rear tires are equivalent ($\alpha_F = \alpha_R$) since $C_F = C_R$ and $a = b$. As a result, the steer angle required to negotiate the curve is not a function of vehicle speed - the steering angle is entirely a function of the radius of curvature, which (due to the small angle approximation) is equivalent to l/R as shown in Figure 6.7. This is referred to as the "Ackermann" steering angle for the bicycle model.

Because the required steering angle is independent of vehicle speed, the vehicle in this case is referred to as neutral steer (NS). More specifically, for a neutral steer vehicle, the change in slip angle with respect to a change in lateral acceleration ($\Delta\alpha/\Delta A_Y$) is equivalent for both the front and rear wheels:

$$\frac{\Delta\alpha_F}{\Delta A_Y} = \frac{\Delta\alpha_R}{\Delta A_Y} \tag{6.33}$$

A driver operating a vehicle along a constant radius turn may increase or decrease the vehicle speed and maintain the radius of curvature of the turn without altering the neutral steering angle.

6.2.3.2 Understeer

The second scenario considers the same vehicle with the CG located closer to the front axle - at 1/3 the wheelbase ($b = 2a$) as shown in Figure 6.8. From the force balance equations (the system is in steady state equilibrium), the front wheel must provide 2/3 of the total cornering force and the rear 1/3 of the total cornering force. Because the cornering stiffnesses are identical, the front tire must assume a slip angle that is twice that of the rear - $\alpha_F/\alpha_R = 2$.

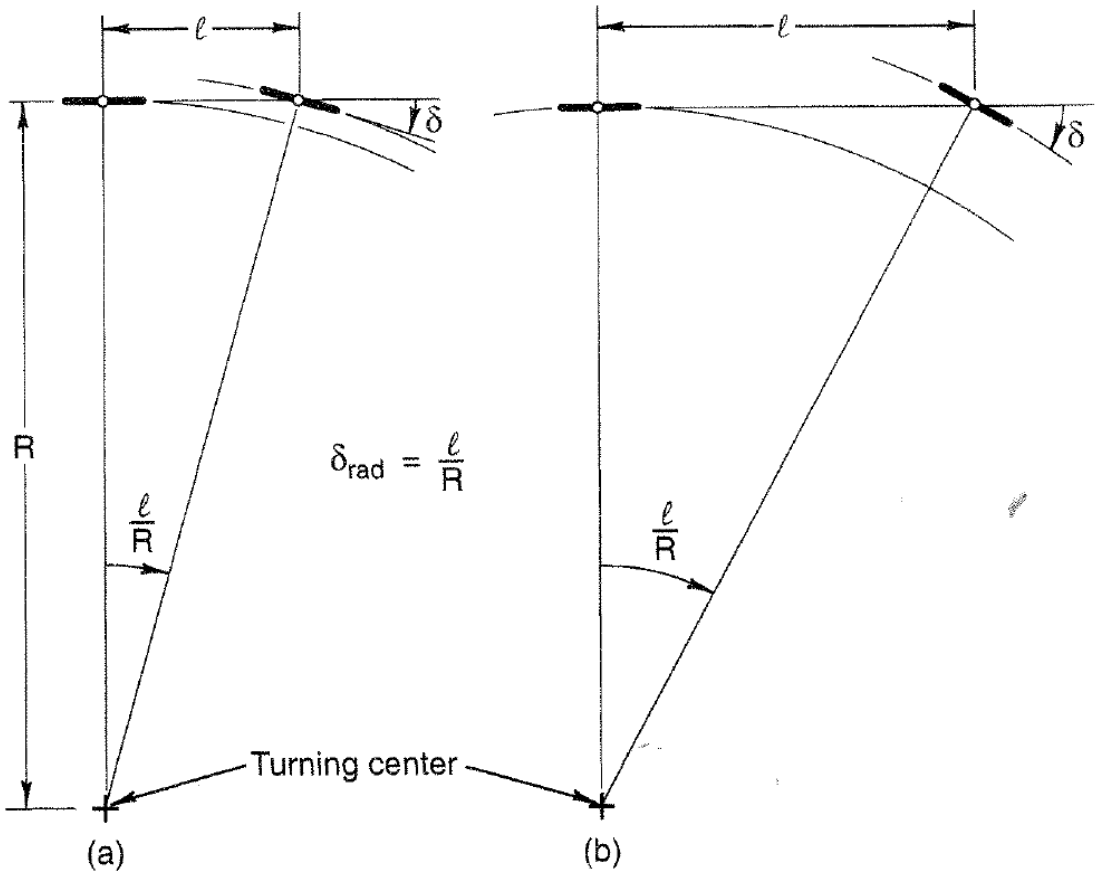

Figure 6.7: Ackermann Steering Angle, Bicycle Model [57]

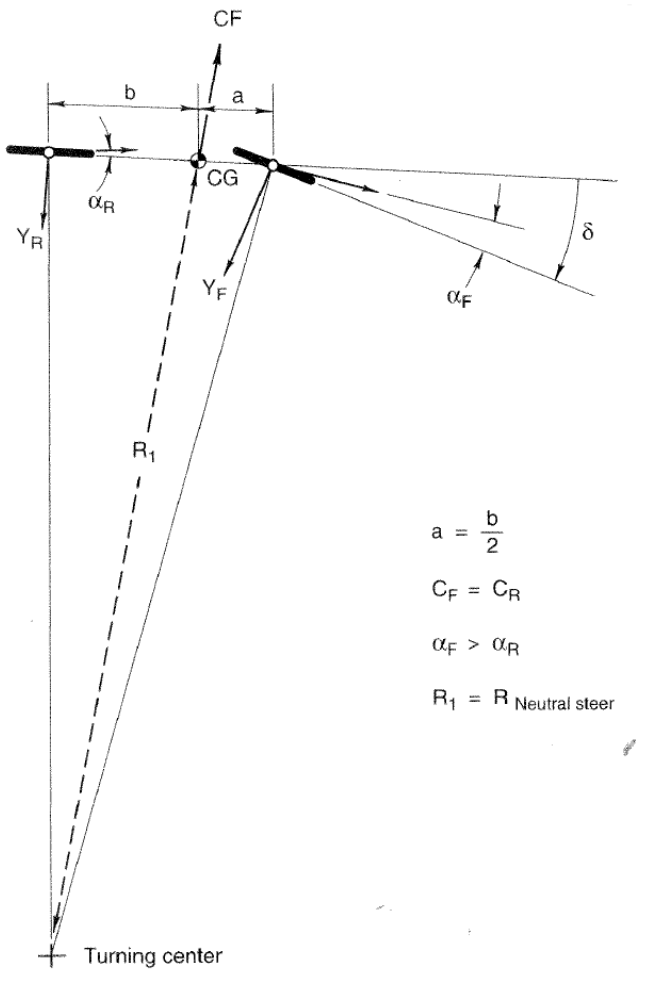

Figure 6.8: Understeer Bicycle Model [57]

For the neutral steer vehicle the lateral force, WA_Y, is equivalent to $2C\alpha_1$ because the front and rear slip angles and cornering stiffnesses are identical. In this case, α_1 refers to the neutral steering angle (Ackermann). However, for this configuration of the vehicle:

$$WA_Y = C(\alpha_F + \alpha_R) = C(2\alpha_R + \alpha_R) = 3C\alpha_R \tag{6.34}$$

Because the lateral accelerations are the same between cases:

$$3C\alpha_R = 2C\alpha_1 \tag{6.35}$$

or:

$$\alpha_R = \frac{2}{3}\alpha_1 \tag{6.36}$$

In addition:

$$WA_Y = \frac{3}{2}C\alpha_F = 2C\alpha_1 \tag{6.37}$$

or:

$$\alpha_F = \frac{4}{3}\alpha_1 \tag{6.38}$$

In other words, the front and the rear tires must assume slip angles that are 4/3 and 2/3 of the neutral steer slip angle (α_1) in order to maintain the same lateral acceleration. For this simple bicycle model, steering angle relationship is defined as:

$$\delta = \delta_{\text{Ackermann}} + (-\alpha_F + \alpha_R) \tag{6.39}$$

$$\delta = \frac{l}{R} + (-\alpha_F + \alpha_R) \tag{6.40}$$

It follows that for the forward CG configuration, the steering relationship is (substituting Equation (6.38) into (6.39)):

$$\delta = \frac{l}{R} + (-\frac{2}{3}\alpha_1) \tag{6.41}$$

What this means is that for a given turning radius and lateral acceleration ($\frac{a_y}{g}$), the CG forward vehicle must assume a larger steering input than the neutral steer vehicle. If the CG forward vehicle were to assume the neutral steer (Ackermann) steering angle, the turning radius of the vehicle would be larger due to the smaller steering input. In this case, the chassis attempts to "understeer" the neutral steer radius, and as such, the CG forward vehicle behavior is referred to as understeer (US). The behavior of the understeer vehicle is shown in Figure 6.9.

Because the steering angle required for the understeer vehicle is a function of the slip angle required for the neutral steer vehicle (Equation 6.41), the rates of change of the front/rear slip angles with respect to the lateral acceleration of the vehicle are not identical. As the lateral acceleration of the NS vehicle increases, the required steering angle increases (α_1), and the steering angle required of the US vehicle (for the same turning radius) increases. In order to maintain a constant radius turn, the operator of a conventional vehicle must increase steering angle as the forward velocity (lateral acceleration) is increased - also shown in Figure 6.9.

A similar but opposite behavior is observed if the CG of the vehicle is moved rearward as shown in Figure 6.10. In this case however, the rear tire

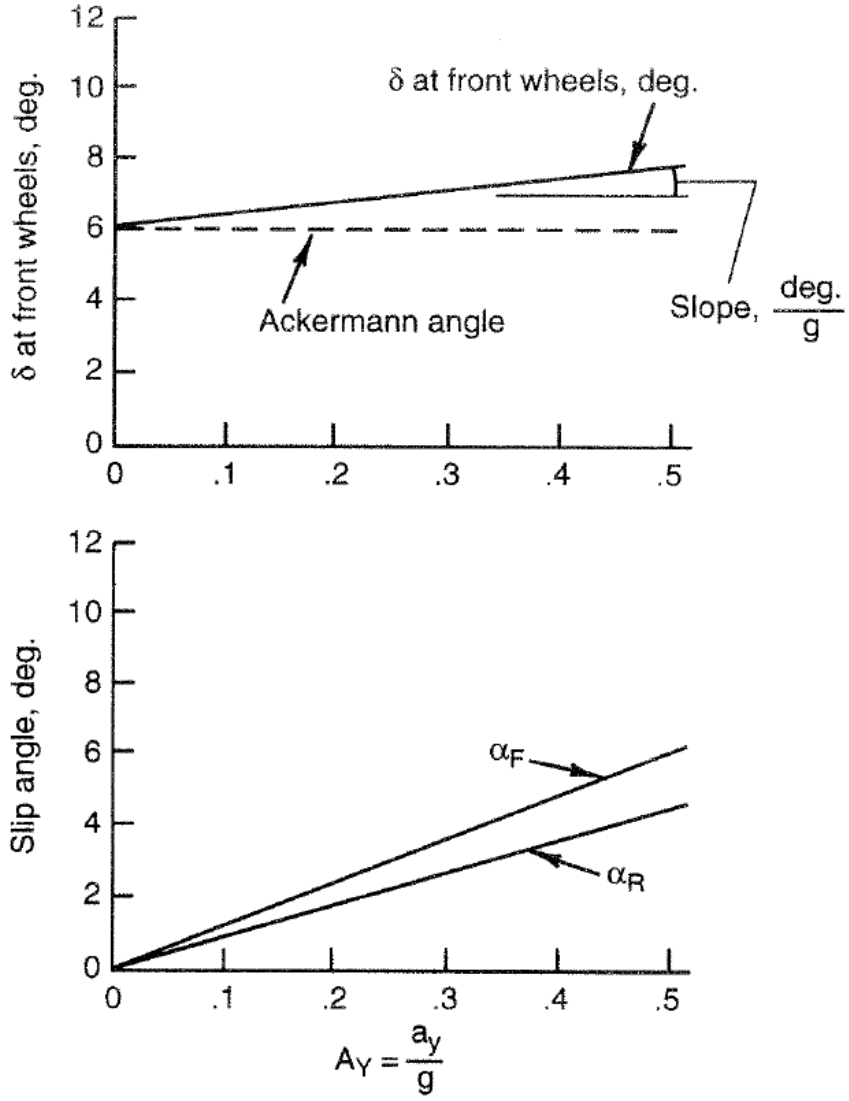

Figure 6.9: Steering Angle and Front/Rear Slip Angle vs. Lateral Acceleration ($\frac{a_y}{g}$), Understeer, Constant Radius [57]

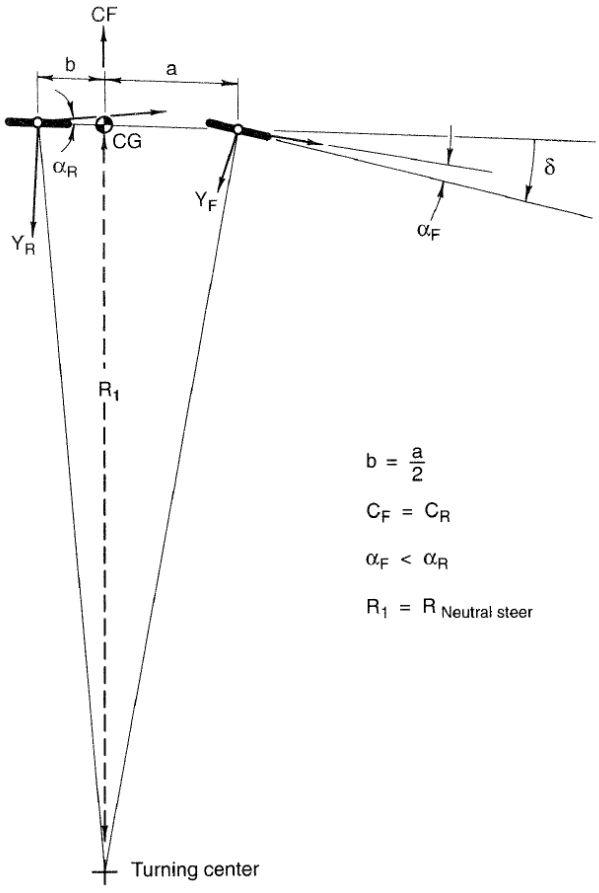

Figure 6.10: Oversteer Bicycle Model [57]

must assume a greater slip angle than the front:

$$\alpha_F = \frac{2}{3}\alpha_1 \tag{6.42}$$

$$\alpha_R = \frac{4}{3}\alpha_1 \tag{6.43}$$

where α_1 is the required steering angle for the neutral steer vehicle. For this vehicle condition, maneuvering along a steady state radius turn requires less steering angle than that of the neutral steer vehicle:

$$\delta = \frac{l}{R} + (-\alpha_F + \alpha_R) = \frac{l}{R} + \left(\frac{2}{3}\right)\alpha_1 \tag{6.44}$$

Similar to the US case, for a given turning radius and lateral acceleration ($\frac{a_y}{g}$), the rearward CG vehicle must assume a smaller steering input than the neutral steer vehicle in order to satisfy the smaller required slip angle - Equation 6.42. If the rearward CG vehicle were to assume the same steering input as the NS vehicle, the resulting turning radius would decrease as a result of the larger steering input. In this case, the chassis will attempt to "oversteer" the neutral steer radius, and as such, the rearward CG vehicle behavior is referred to as oversteer (OS). Again, because the required steering angle for the OS vehicle is a function of the NS slip angle required for a give lateral acceleration (Equation 6.44), the steering input for an OS vehicle is a function of vehicle speed. As an OS vehicle increases speed during a constant radius cornering maneuver, the steering input (for a conventional vehicle) must decrease in order to maintain the corner radius.

It is important to note that the understeer/oversteer behavior affects vehicle performance under any lateral acceleration. For example, a vehicle

operating on a banked road (lateral incline) experiences a lateral acceleration as a result of the inclination. Assuming a steering angle of zero, the CG of a neutrally steered vehicle will moved down the incline but the attitude of the vehicle will remain constant as the front and rear tires build slip angle (and therefore lateral force) at the same rate. Understeer and oversteer vehicles do not exhibit the same motion - the disparity in the rate of generation of lateral cornering force will result in a vehicle yaw motion (curvature of the vehicle path), again, assuming zero steering angle. This behavior is shown in Figure 6.11.

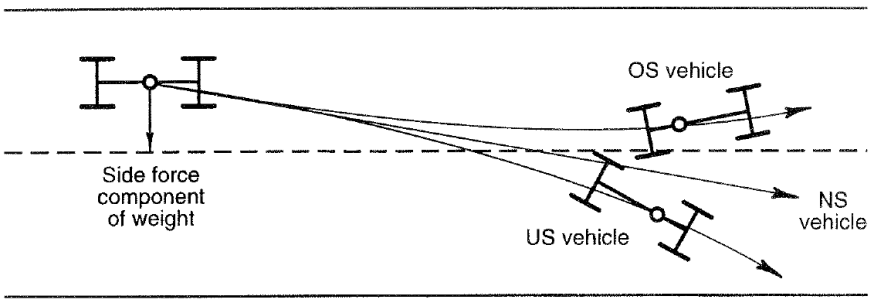

Figure 6.11: Behavior of Neutral Steer (NS), Understeer (US), and Oversteer (OS) Vehicles Experiencing a Lateral Force Input [57]

The US vehicle is dominated by the front slip angle, and as such, the vehicle will turn down the slope. Conversely, the OS vehicle will turn up the slope.

The following equations, presented by Wong in [87], pose the issue of understeer slightly differently. Returning to the force balance of the vehicle (W_f is the weight on the front tire, and W_r is the weight on the rear tire), if

the lateral acceleration of the vehicle is expressed as V^2/R, the front and rear tire forces may be expressed:

$$F_{yf} = W_f \frac{V^2}{gR} \tag{6.45}$$

$$F_{yr} = W_r \frac{V^2}{gR} \tag{6.46}$$

and the front and rear slip angles may be represented as (again, assuming linear cornering stiffnesses):

$$\alpha_f = \frac{F_{yf}}{C_{\alpha f}} = \frac{W_f}{C_{\alpha f}} \frac{V^2}{gR} \tag{6.47}$$

$$\alpha_r = \frac{F_{yr}}{C_{\alpha r}} = \frac{W_r}{C_{\alpha r}} \frac{V^2}{gR} \tag{6.48}$$

Combining these equations with Equation (6.40) yields:

$$\begin{aligned} \delta_f &= \frac{L}{R} + \left(\frac{W_f}{C_{\alpha r}} - \frac{W_r}{C_{\alpha r}} \right) \frac{V^2}{gR} \\ &= \frac{L}{R} + K_{us} \frac{V^2}{gR} \\ &= \frac{L}{R} + K_{us} \frac{a_y}{g} \end{aligned} \tag{6.49}$$

Where K_{us} represents the understeer coefficient. The value of K_{us} is an indication of the understeer/oversteer behavior of the vehicle. Positive values of K_{us} indicate understeer behavior, and negative values indicate oversteer behavior, illustrated in Figure 6.12.

As previously discussed, oversteer vehicles assume smaller steering angles than the neutral steer for equal radius/lateral acceleration cornering. As the operator of the vehicle increases the vehicle speed (lateral acceleration),

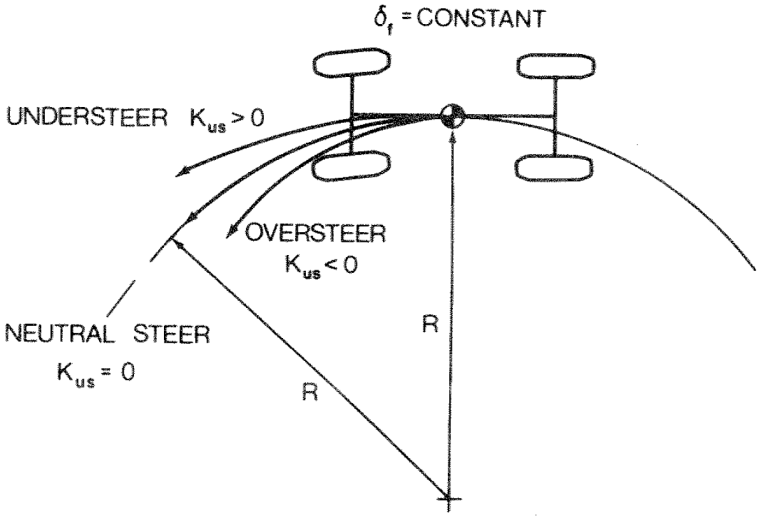

Figure 6.12: Effect of K_{us} on Curvature Response [87]

the operator must reduce the steering angle in order to maintain a constant radius. If the operator continues to increase the lateral acceleration, the required steering angle will eventually become zero. At this point the vehicle becomes unstable and is subject to rapid yaw and a loss of control (spinning out) [87]. The speed at which this occurs may be determined from Equation (6.49) by setting the steering angle value to zero:

$$V_{crit} = \sqrt{\frac{gL}{-K_{us}}} \tag{6.50}$$

The required steering angle as a function of vehicle speed for a representative vehicle is shown in Figure 6.13.

As a result of the potential for yaw instability, oversteer can be undesirable, depending on the extent of oversteer experienced [57]. Most passenger vehicles exhibit some degree of understeer for this reason. In addition, slight

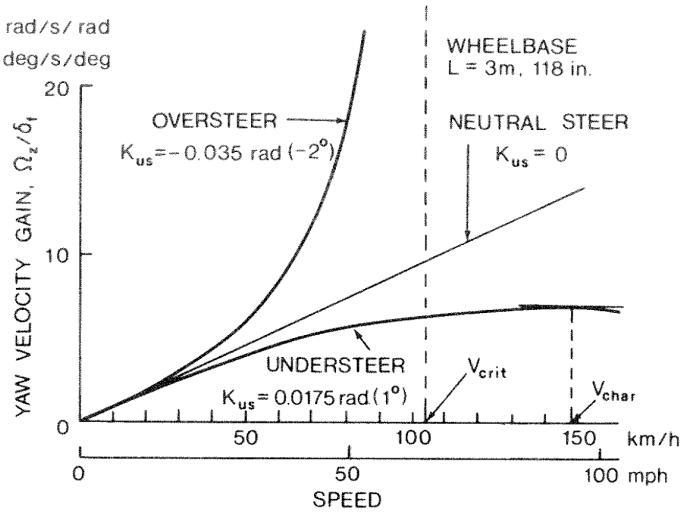

Figure 6.13: Vehicle Yaw Behavior as a Function of Vehicle Speed for NS, OS, and US Behavior [87]

understeer is beneficial as opposed to neutral steer as the understeer behavior provides a degree of driver feedback (absent in the neutral steer case).

6.2.4 ICV Cornering Behavior

Due to its dexterity and independent wheel control, the ICV can not be appropriately characterized by a simplified bicycle model. As such, it is difficult to pose a single, specific criterion based on a generalized vehicle geometry to address this behavior. Until a detailed model of the ICV is established, it will be sufficient to pose the following condition:

$$K_{ICV} = \frac{d\sigma_{ICV}}{da_{y_{cg}}} \tag{6.51}$$

where σ_{ICV} represents a generalize operator input for vehicle yaw, and $a_{y_{cg}}$ represents the lateral acceleration of the vehicle CG. The independent wheel

actuation of the ICV will allow the vehicle to adjust each slip angle individually to meet the demands of the operator. This will allow the ICV to balance the slip angles of the individual wheels to compensate for understeer or oversteer influences on the cornering behavior of the vehicle. In addition, the individual MDW actuators will be able to alter the torque distribution between the wheels, thereby affecting the yaw motion of the vehicle. This torque distribution, commonly referred to as torque-vectoring, has been demonstrated on passenger vehicles as a method of maintaining cornering stability [62].

An ideal value of this criterion will likely be a small, positive number, but the exact value will depend on the ability of the corner actuators to maintain this condition in addition to the required driver feedback. The control scheme or level of operator training may allow the vehicle to manage the individual wheel slip angles so as to maintain a neutral steer vehicle.

6.3 Predicting Off-Road Capability

The off road performance of wheeled ground vehicles is difficult to quantify due to the deformable nature of the terrain. The following section describes the basic behavior of wheeled vehicles in deformable terrains.

6.3.1 Vehicle Cone Index

The study of the off-road vehicle performance of military vehicles began in earnest during the Second World War. The Waterways and Experiments Station (WES) branch of the U.S. Army was tasked with developing a basic

method to establish "go/no go" capability for military vehicles [86]. The concept was to operate groups of representative vehicles over various terrains in an effort to establish relationships between soil type and vehicle capability. WES developed an empirical method that uses vehicle total contact patch area in conjunction with soil property measurements made with a cone penetrometer to determine vehicle capability. A cone penetrometer is a device that used to quantify soil resistance to deformation by measuring the force is required to push the penetrometer into various soils. An empirical correlation is then established between penetrometer data and vehicle capability.

This correlation utilizes the vehicle ground pressure (a function of estimated running gear contact area and weight) and a series of empirically derived factors to determine a "mobility index" for the specified vehicle. The mobility index is then utilized to calculate the "vehicle cone index (VCI)," an indication of the required soil strength, as determined by the cone penetrometer, for the vehicle to pass over the terrain in question a specified number of times. The process of determining the VCI for a wheeled vehicle is shown below [86]:

$$\mathrm{MI} = (\frac{\mathrm{CPF} * \mathrm{WF}}{\mathrm{TF} * \mathrm{GF}} + \mathrm{WLF} - \mathrm{CF}) * \mathrm{EF} * \mathrm{TrF} \tag{6.52}$$

MI - Mobility Index

CPF - Contact Pressure Factor

WF - Weight Factor

TF - Tire Factor

GF - Grouser Factor

WLF - Wheel Load Factor

EF - Engine Factor

TrF - Transmission Factor

Each factor is calculated from the vehicle attributes and a number of empirically derived constants. For example, the "Contact Pressure Factor" is calculated in the following way:

$$\text{Contact Pressure Factor} = \frac{\text{Gw}}{\text{Tw} * \text{Tr} * \text{Nt}} \tag{6.53}$$

Gw - Gross weight of the vehcile, lbs.

Tw - Tire width (nominal), in.

Tr - Radius of tire, outside, in.

Nt - Number of tires

The Vehicle Cone Index (VCI) is then calculated from the Mobility Index and additional empirically derived constants. The VCI is typically calculated for one theoretical pass over a section of terrain or fifty passes (in the case of a convoy, etc.) and represents the minimum soil strength in order for the vehicle to operate over the specified terrain. For example, the VCI for a powered (non-towed) vehicle for one pass over a specified terrain is defined as:

$$VCI_1 = 11.48 + 0.2MI - \frac{39.2}{MI + 3.74} \tag{6.54}$$

Military vehicle architectures (engine, transmission, drive shafts, beam axles) haven't changed significantly since this method was developed. As a result, the VCI method, which is applicable to tracked vehicles as well, is still used to evaluate basic off-road capability. Though VCI is not suitable for extrapolation to new vehicle architectures as a result of the empirical nature of the method, it is presented here in order to illustrate the complexity of vehicle performance prediction over unprepared/deformable terrains.

6.3.2 Vehicle Performance Characteristics

For most off-road vehicles, the ability of the vehicle to apply a force or drawbar load (pull) is of significant importance as it is an indication of the ability of the vehicle to perform work. This is especially prevalent for military engineering vehicles operating off-road. Physically, the drawbar may be considered to be a solid coupling between a vehicle and towed load. The drawbar pull force, F_d, is equivalent to the difference between the force applied by the running gear (tractive effort F) and the resistive forces:

$$F_d = F - \sum R \tag{6.55}$$

The losses considered include running gear losses such as tire hysteresis, losses due to the tire/terrain interaction, and aerodynamic losses.

The ability of the vehicle to apply generated power to the drawbar (to do work) can be expressed as the drawbar (or tractive) efficiency:

$$\eta_d = \frac{P_d}{P} = \frac{F_d V}{P} = \frac{(F - (\sum R) V_t (1 - i)}{P} \tag{6.56}$$

P_d - drawbar power

P - prime mover power

$\sum R$ - sum of vehicle resistances

V_t - theoretical speed

i - slip

This equation represents the general case of a vehicle operating in deformable terrain. The individual wheel slip values are not considered. According to the drawbar efficiency expression, all of the tractive effort at the contact patch is available to perform work only if all of the vehicle resistances, including those of the powertrain/prime mover, are zero, the vehicle is experiencing a non-zero velocity, and the (overall) vehicle slip is zero. However, this condition is unlikely and the influence of the vehicle losses and slip must be considered.

The prime mover power may be expressed as a function of the drivetrain (transmission) efficiency and power available at the driven wheel:

$$P = \frac{FV_t}{\eta_t} \tag{6.57}$$

P - delivered engine power

η_t - drivetrain efficiency

Combining the above equations yields:

$$\eta_d = \frac{(F - \sum R)}{F}(1 - i)\eta_t = \frac{F_d}{F}(1 - i)\eta_t = \eta_m \eta_s \eta_t \tag{6.58}$$

where η_m is the efficiency of motion, and η_s is the efficiency of slip. In this case, the efficiency of motion, η_m, is equivalent to F_d/F and represents the

losses associated with transforming the tractive effort (force at the wheels) to the drawbar pull force. The efficiency of slip, η_s is $(1 - i)$ and represents the losses and reduction in vehicle speed associated with running gear slip. The relationship between the drawbar force and the motion, slip, and drivetrain efficiencies is shown in Figure 6.14.

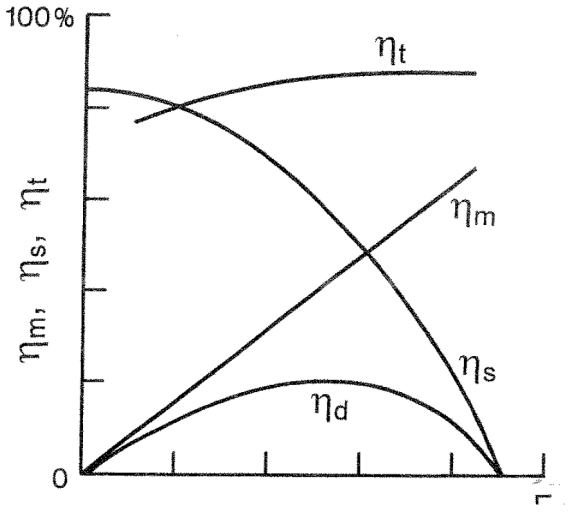

Figure 6.14: Variation of Drawbar (Tractive) (η_d), Motion (η_m), Slip (η_s), and Transmission (η_d) efficiencies with Drawbar Pull [87]

For vehicles with multiple drive axles, such as the ICV, it is important to note the slip and slip efficiencies of all driven wheels. For example, in [88], Wong proposes the following expression for the efficiency of slip for a four wheel drive (two drive axle) vehicle:

$$\eta_{s4} = 1 - \frac{i_f M_f \omega_f + i_r M_r \omega_r}{M_f \omega_f + M_r \omega_r} = 1 - \frac{i_f V_{tf} F_f + i_r V_{tr} F_r}{V_{tf} F_f + V_{tr} F_r} \tag{6.59}$$

$M_{f/r}$ - drive torque at the front/rear wheels

$\omega_{f/r}$ - angular speed of front/rear wheels

Table 6.1: Drawbar, Motion, Slip, and Transmission Efficiencies

Efficiency	**Symbol**	**Meaning**
Drawbar Efficiency	η_d	The drawbar (tractive) efficiency represents the ability of the vehicle to apply generated power to the vehicle drawbar
Motion Efficiency	η_m	The motion efficiency represents the losses associated with vehicle resistances (rolling, terrain, aerodynamic, etc.)
Slip Efficiency	η_s	The slip efficiency represents the reduction in vehicle speed/losses associated with wheel slip
Transmission Efficiency	η_t	The transmission efficiency represents losses associated with the vehicle drivetrain

$V_{tf/r}$ - theoretical speed of the front/rear wheels (equal to $\omega *$ wheel radius)

$i_{f/r}$ - slip of front/rear wheels

This expression assumes a laterally symmetric vehicle in weight distribution and wheel behavior operating on a homogeneous terrain type.

From the relationship between front and rear wheel translatory speeds:

$$V_{tf}(1 - i_f) = V_{tr}(1 - i_r) = V \tag{6.60}$$

where V is the longitudinal speed of the vehicle, the following may be expressed:

$$K_v = \frac{V_{tf}}{V_{tr}} = \frac{\omega_f r_f}{\omega_r r_r} = \frac{(1 - i_r)}{(1 - i_f)} \tag{6.61}$$

In this equation, K_v is the theoretical speed ratio and $r_{f/r}$ is the free rolling radius of the front/rear tire.

The slip efficiency of a four-wheel-drive vehicle may then be expressed:

$$\eta_{s4} = 1 - \frac{[(1-i_r)/(1-i_f)]i_f V_{tr} F_f + i_r V_{tr} Fr}{[(1-i_r)/(1-i_f)]V_{tr} F_f + V_{tr} Fr} = 1 - \frac{i_f(i-i_r) - (i_f - i_r)K_d}{(i-i_r) - (i_f - i_r)K_d} \tag{6.62}$$

where K_d is the coefficient of thrust distribution between the front and rear axles. The coefficient of thrust distribution is equal to $F_r/(F_f + F_r)$. The above equation indicates that for any given operating condition, there exists a distribution of thrust that will maximize the efficiency of slip. The partial derivative of Equation 6.62 with respect to K_d is:

$$\frac{\partial \eta_{s4}}{\partial K_d} = \frac{(1-i_f)(1-i_r)(i_f - i_r)}{[(1-i_r) - (i_f - i_r)K_d]^2} \tag{6.63}$$

This expression is only equal to zero when either the front or rear slip values are 100% (indicating no vehicle motion) or the front or rear slip values are equivalent. The condition of equivalent front and rear wheel slip values maximizes the vehicle slip efficiency in this case (four wheel drive). Wong also states that by substituting the theoretical speed ratio for $(1-i_r)/(1-i_f)$ in Equation 6.62 and taking the partial derivative with respect to K_d and setting the result to zero results in a similar conclusion - the theoretical speed ratio must be equal to 1 in order to maximize slip efficiency.

While Equation 6.63 indicates that K_d does not affect the slip efficiency when it is maximized, K_d does affect the tractive efficiency. The effects of the thrust distribution on tractive efficiency depend on the type of torque

coupling and the ratio of theoretical speeds (front to rear). However, the ICV architecture does not utilize a mechanical torque coupling between any of the drive wheels. In general, the torque distribution should be managed such that the differences in theoretical speeds of the individual wheels does not result in slip-skid braking (wheel drag). This distribution will be dependent on the terrain type and operating conditions.

The motion efficiency for the ICV architecture may be expressed as:

$$\eta_{m,ICV} = \frac{F_d}{\sum_{i=1}^{n} F_i} \tag{6.64}$$

where n is the number of vehicle corners and F_i is the tractive effort for wheel i.

The drivetrain efficiency, taking into account the losses of electrical power source, for the ICV may be expresses as:

$$\eta_{t,ICV} = \frac{\sum_{i=1}^{n} F_i V_{t,i}}{P} \tag{6.65}$$

In this case, P refers to the power dissipated or distributed from the electrical energy storage element of the ICV. The slip efficiency of the ICV is:

$$\eta_{s,ICV} = 1 - \frac{\sum_{i=1}^{n} i_i M_i \omega_i}{\sum_{i=1}^{n} M_i \omega_i} \tag{6.66}$$

And the tractive efficiency is then:

$$\eta_{d,ICV} = \frac{\sum_{i=1}^{n} F_i V_{t,i}(1 - i_i)}{\sum_{i=1}^{n} P_{\text{sup,MDW},i} \eta_{\text{MDW},i}} \tag{6.67}$$

While all of these efficiencies of the ICV should be maximized for ideal off road operation, they are constantly in conflict (as shown in Figure 6.14).

Maximizing the ability of the ICV to apply the running gear (wheels) to a deformable terrain surface and to apply a drawbar force will require optimizing the efficiencies for the operating conditions. The ideal values for each will likely be a function of the vehicle state and terrain conditions, and as such, a model of the ICV will be required in order to evaluate optimal efficiency values.

6.4 Criteria Summary

Table 6.2 lists the various criteria described in this chapter, the definitions (symbol and expression), and the associated physical meanings.

Table 6.2: Summary of Criteria Based on Classic Vehicle Dynamics

Criteria	**Symbol**	**Definition**	**Meaning**
Normalized Slip Ratio Margin, Traction	$NSRM_t$	$\frac{i_{n,peak}-i_n}{i_{n,peak}}$	This ratio is a description of the slip ratio (traction) of a wheel with respect to the slip value required for maximum longitudinal traction. Traction is maximized as this value approaches zero.
Normalized Slip Ratio Margin, Braking	$NSRM_b$	$\frac{i_{s,n,peak}-i_{s,n}}{i_{s,n,peak}}$	This ratio is a description of the slip ratio (braking) of a wheel with respect to the slip value required for maximum braking force. Braking is maximized as this value approaches zero.
Normalized Slip Angle Margin	$NSAM_{(\pm)}$	$\frac{\alpha_{n,peak,(\pm)}-\alpha_n}{\alpha_{n,peak,(\pm)}}$	This ratio describes the slip angle of a wheel with respect to the value required for maximum lateral acceleration. Lateral force is maximized when this value approaches zero.
Normalized Wheel Torque Margin	τ_n	$\frac{T_{n,peak}-T_n}{T_{n,peak}}$	This ratio indicates the current drive torque of a wheel with respect to the torque value associated with peak traction. A value of zero indicates the peak traction torque. A negative value is an indication of traction instability.

Table 6.2: Summary of Criteria Based on Classic Vehicle Dynamics, Continued

Criteria	**Symbol**	**Definition**	**Meaning**
Normalized Average Wheel Torque Margin	$\mathcal{T}_{n,i}$	$\frac{\tau_i}{\bar{\tau}}$	The torque margin with respect to an established average is an indication of the desired torque distribution. This value should approach one for desirable operation.
Lateral Force Ratio	$LatFR$	$\frac{F_{y,n}}{F_{y,n}+F_{x,n}}$	The lateral force ratio is an indication of the cornering condition of the tire. Desired values are specific to the desired motion.
Longitudinal Force Ratio	$LongFR$	$\frac{F_{x,n}}{F_{y,n}+F_{x,n}}$	The longitudinal force ratio is an indication of the longitudinal traction condition of the tire. Desired values are specific to the desired motion.
Normalized Camber Thrust Margin	$NCTM$	$\frac{\gamma_{n,peak}-\gamma_n}{\gamma_{n,peak}}$	The camber thrust margin is a description of the current camber angle with respect to the camber value for maximum camber thrust. A value of zero indicates peak camber generation.
Articulated Equipment Drag	AED	$\frac{1}{n}\sum_{i=1}^{n}(\lvert\theta_i - \theta_{i,C_{D,min}}\rvert)^p$	Articulated equipment drag should be minimized for reducing vehicle drag and maximizing longitudinal vehicle performance.

Table 6.2: Summary of Criteria Based on Classic Vehicle Dynamics, Continued

Criteria	**Symbol**	**Definition**	**Meaning**
Braking Efficiency	η_b	$\frac{a/g}{\mu}$	Braking efficiency is an indication of the braking capability of the vehicle. This criterion is a function of the road surface type and requires evaluating the slip ratio margins (braking) for maximum vehicle braking performance.
Coefficient of Understeer, ICV	K_{ICV}	$\frac{d\sigma_{ICV}}{da_{ycg}}$	The understeer coefficient is an indication of the cornering behavior of the vehicle. Optimal values will be specific to the operator and vehicle control system.
Efficiency of Motion, ICV	$\eta_{m,ICV}$	$\frac{F_d}{\sum_{i=1}^{n} F_i}$	The efficiency of motion is an indication of the losses associated with transforming tractive effort to drawbar force.
Drivetrain Efficiency, ICV	$\eta_{t,ICV}$	$\frac{\sum_{i=1}^{n} F_i V_{t,i}}{P}$	The drivetrain efficiency is an indication of the losses associated with distributing power from the vehicle energy source.
Efficiency of Slip, ICV	$\eta_{s,ICV}$	$1 - \frac{\sum_{i=1}^{n} i_i M_i \omega_i}{\sum_{i=1}^{n} M_i \omega_i}$	The efficiency of slip represents losses associated with running gear slip.

Table 6.2: Summary of Criteria Based on Classic Vehicle Dynamics, Continued

Criteria	**Symbol**	**Definition**	**Meaning**
Tractive Efficiency, ICV	$\eta_{d,ICV}$	$\frac{\sum_{i=1}^{n} F_i V_{t,i}(1-i_i)}{\sum_{i=1}^{n} P_{\text{sup,MDW},i}\eta_{\text{MDW},i}}$	The tractive efficiency is an indication of the ability of the vehicle to apply generated power to the vehicle drawbar.

6.5 Chapter Summary

This chapter reviews performance criteria derived from classic vehicle dynamics principles, their application to the Intelligent Corner Vehicle (ICV) concept, and the subsequent physical meanings of each criteria. Each criteria presented, along with the associated symbol, definition, and physical meaning, is listed in table 6.2. Table 6.3 presents the key findings, conclusions, and recommendations of the chapter.

Table 6.3: Chapter 6 Key Findings, Conclusions, and Recommendations

Result	**Conclusion**	**Recommendation**
The **maximum** lateral and longitudinal **force capability of the tires**, measurable as slip ratios (Table 6.2), will fluctuate during transient maneuvers due to operating conditions and terrain characteristics.	Slip percentage ratios, if utilized to maximize force generation, must be monitored and controlled (closed loop) in order to avoid unstable tire behavior.	The ability of the MDW to control slip ratios should be evaluated with a full vehicle model.
The **torque limit** and torque **ratios** (Table 6.2) will also fluctuate due to operating conditions and terrain characteristics.	Torque distribution must be taken into account when evaluating wheel torque margins as the normalized values may be equal despite a difference in wheel torques (non-homogeneous terrain, etc.). This may not be advantageous for maximizing vehicle capability.	The development of further criteria to evaluate torque distributions as functions of terrain conditions will require full vehicle and terrain models.
Vehicle resistances, which include tire rolling resistances and aerodynamic drag, need to be minimized in order to maximize vehicle performance.	There exists a vehicle configuration (tire pressures, positions of articulated chassis elements/equipment) that minimizes resistance values, but will be specific to each vehicle and operating condition.	The ideal values of tire pressure and orientations of articulated chassis elements should be evaluated with a vehicle model.

Table 6.3: Key Findings, Conclusions, and Recommendations (Continued)

Result	**Conclusion**	**Recommendation**
There exists a **distribution of braking effort/force** that will maximize vehicle deceleration without resulting in wheel lock-up that is dependent upon the terrain surface.	Any distribution of braking effort must be a function of the terrain type as well as the operating condition of the vehicle in order to avoid vehicle instability due to a loss of traction. Similar to tractive performance, optimal braking requires optimizing the slip ratio values (Table 6.2) for the skid-slip condition.	The ability of the MDW to control ski-slip ratios should be evaluated with a full vehicle model.
Posing a criterion that effectively captures the **oversteer/understeer behavior** of the Intelligent Corner Vehicle (ICV) is difficult due to independent wheel actuation and control.	The proposed generalized criterion (Table 6.2) may allow the ICV to balance slip angles to compensate for oversteer/understeer influences on vehicle cornering behavior.	The ideal value of the generalized criterion will need to be evaluated with a full vehicle model.
Torque distribution between axles/wheels may be optimized for tractive effort on deformable terrains.	As the ICV architecture does not utilize mechanical torque couplings, torque should be managed such that differences in theoretical wheel speeds do not result in slip-skid braking (wheel drag).	This distribution will be affected by the vehicle operating conditions and terrain type and should be evaluated with a full vehicle model.

Table 6.3: Key Findings, Conclusions, and Recommendations (Continued)

Result	**Conclusion**	**Recommendation**
Vehicle motion on **deformable terrains** may be characterized by a series of vehicle efficiencies (Table 6.1).	Optimizing vehicle performance requires optimizing these efficiencies for the given operating conditions and terrains.	The ideal values will likely be functions of the terrain and vehicle state, and a full vehicle model will be required to determine these optimal values.

Chapter 7

Conclusion and Future Work

The following chapter provides a summary of the work previously presented, broken down by chapter. The first section discusses the important concepts from the literature and lists the key references. The second section discusses the results from discussing the key concepts and how they apply to military vehicles and the Intelligent Corner Vehicle concepts. The third section presents the conclusions drawn from the results, and the final section lists issues for consideration in future work.

7.1 Key Concepts From the Literature

The following section lists and describes the key concepts from the literature, presented by chapter.

7.1.1 Military Vehicles

Key references: [3, 47, 48, 67, 72]

1. Many current military vehicle platforms were structured to address the traditional battlefield roles defined by past conflicts.

2. Military vehicles developed for these traditional roles performed well

during large scale military operations, but were not effective in conflicts involving asymmetric warfare and non-state actors.

3. The U.S. Military developed vehicle armor upgrades in an attempt to meet rapidly changing protection requirements.

4. These upgrades significantly reduced vehicle. mobility, performance, and capability.

5. MRAP vehicles were rapidly developed as a new platform (based on traditional drive/suspension components) designed to directly address threat requirements.

6. MRAP vehicles sacrificed mobility for protection and divested the U.S. Department of Defense from their overall ground vehicle strategy and doctrine.

7. The Army's Future Combat Systems program, designed to completely modernize military vehicle fleets, produced few results and no procurable vehicles.

8. The Iron Triangle compromise (power, protection, payload) is permanent.

9. The U.S. Military is currently developing new vehicle platforms (JLTV, etc.).

7.1.2 Tire Behavior

Key references: [10, 57, 87]

1. Tire force generation is characterized by slip ratio and slip angle and the force/slip relationships are nonlinear.

2. The relationship between tire load and maximum possible lateral/longitudinal force is also nonlinear.

3. Tire camber affects lateral force generation.

4. Tire construction affects tire force generation properties.

5. Combined loading affects both lateral and longitudinal force generation.

6. Combined loading conditions may be plotted on a traction circle.

7. The tire contact patch will vary with the properties of a deformable terrain.

8. The behavior of any complex system may be characterized by performance maps that may be combined into visual decision making surfaces.

7.1.3 Vehicle Architectures

Key references: [13, 18, 19, 26, 28, 36, 45, 52, 62, 63, 71, 75, 82]

1. Most modern steering systems are linkage systems.

2. Active steering systems have been developed that provide variable steering ratios.

3. Wheel camber is traditionally determined by the suspension kinematics.

4. Active camber systems have been developed for high-performance vehicles.

5. Most modern vehicles are powered by an internal combustion engine in conjunction with a transmission and transfer cases/differentials.

6. Managed differential systems provide real-time influence over torque distribution to co-axial wheels.

7. Traditional vehicle suspensions utilize passive elements.

8. A variety of active suspension systems have been developed.

9. Several types of electric vehicle, an alternative to the traditional IC engine architecture, are in development.

10. Several varieties of hybrid powertrain systems are in production on passenger vehicles.

11. NASA unmanned rover systems utilize electrical, in-wheel drive motors and non-traditional suspension types.

12. NASA manned rover prototypes have been developed that utilize active suspension components in conjunction with in-wheel drive motors.

13. The U.S. Military has developed active suspension prototypes for wheeled vehicles.

14. The U.S. Military has also evaluated hybrid powertrain systems for a range of ground vehicle weight classes.

15. An alternative vehicle architecture, the Intelligent Corner Vehicle (ICV), has been proposed to take advantage of open architecture, modular, intelligent actuator technology.

7.1.4 Serial Chain Robotics Criteria

Key references: [14, 20, 27, 40, 83, 84]

1. The Robotics Research Group (RRG) has developed a large number of performance criteria for the evaluation of serial chain robotic systems.

2. Criteria may be constraint based or non-constraint based.

3. Many of these criteria are derived from Kinematic Influence Coefficients.

4. The inverse kinematics of serial chain mechanisms may be determined through a direct search method utilizing multiple performance criteria.

7.1.5 Vehicle Dynamics

Key references: [57, 86, 87]

1. Wong [87] describes models for longitudinal acceleration and braking that are functions of both tractive effort and vehicle resistances.

2. From the longitudinal equations, Wong derives the axle loads as functions of vehicle acceleration (weight transfer).

3. Wong presents he maximum possible braking force and subsequent distribution of braking effort.

4. Milliken and Milliken [57] describe a simple vehicle model (bicycle model) that is then used to describe neutral steer, oversteer, and understeer cornering behavior.

5. Wong [86] presents a series of vehicle efficiencies that characterize vehicle tractive effort over deformable terrains.

7.2 Results

The following section lists the important results, presented by chapter.

7.2.1 Military Vehicles

1. Military vehicle platforms developed during the Cold War era were not adequate for the mission requirements experienced during the conflicts in Iraq and Afghanistan (Section 2.3).

2. Military vehicles in development (intended to replace current platforms) have not yet been deployed (Section 2.6).

7.2.2 Tire Behavior (Parametric Representation)

1. The nonlinear nature of tire force generation needs to be completely characterized (Section 3.1.2.1).

2. The influences of normal load, tire camber, tire construction, and combined loading on force/slip relationships also need to be characterized (Sections 3.1.2.4, 3.1.2.5, 3.1.3).

3. The friction circle is a useful visual representation of the force generation capabilities of the tire that relays real-physical meaning to the operator (Section 3.1.5.1).

4. The force generation capability of the tire is affected by terrain type and the effects should be characterized (Section 3.2.1).

5. Performance maps are able to provide a representation of the behavior of a complex system to an operator in real-time (Section 3.3.1).

7.2.3 Vehicle Architectures

1. Variable steering ratios (as functions of speed) improve vehicle performance but the systems retain traditional linkages (Section 4.1.1.1).

2. Active camber systems have shown improvements in vehicle performance (Section 4.1.1.2).

3. Traditional IC engine/transmission systems only provide options to the operator in the form of gear selection (Section 4.1.1.3).

4. Managed differential systems improve vehicle performance but retain traditional drivetrain elements (Section 4.1.1.3).

5. Passive suspension elements must be selected to address a wide range of potential operating conditions - a compromise (Section 4.1.1.4).

6. Active suspension systems have shown improvements in vehicle performance (Section 4.1.1.4).

7. Electric drivetrains provide some advantages over traditional drivetrains (Section 4.2.1).

8. Hybrid vehicle architectures offer significant flexibility in drivetrain component layout (Section 4.2.2).

9. The in-wheel motors of NASA rovers provide significant flexibility in torque application (Section 4.2.3.1).

10. The drive/suspension components of the NASA Chariot provide significant operational flexibility (Section 4.2.3.2).

11. U.S. Military active suspension systems have not been adopted by fielded platforms (Section 4.3.3).

12. Hybrid systems developed by the military have also not been adopted by fielded platforms (Section 4.3.4).

13. The ICV concept is intended to provide maximum operational flexibility to the operator in order to address the wide range of military vehicle requirements (Section 4.4).

7.2.4 Serial Chain Robotics Criteria

1. Performance criteria developed by the RRG may be applied to the ICV architecture (Section 5.1.2).

2. Constraint based criteria focus on physical limitations and safety while non-constraint based criteria focus on quality of motion (Section 5.1.2).

3. Kinematic Influence Coefficients may be applied to models of vehicle suspensions (Section 5.1.2.2).

4. Criteria based on Kinematic Influence Coefficients may not vary significantly over the workspace of a suspension model (Section 5.1.2.2).

5. Criteria describing energy content and distribution are prime descriptors of both steady state and transient motions (Section 5.2).

7.2.5 Vehicle Dynamics

1. The maximum lateral and longitudinal force capability of a tire are measurable as slip ratios and will fluctuate (Section 6.1.1.1).

2. The subsequent torque limits and ratios will also fluctuate (Section 6.1.1.2).

3. Vehicle resistances need to be minimized for maximum vehicle performance (Section 6.2.1).

4. There exists an optimal braking force distribution that will maximize braking capability, depending upon the terrain surface (Section 6.2.2).

5. The traditional representations of oversteer/understeer are not directly applicable to the ICV due to the individual wheel actuation (Section 6.2.4).

6. Torque distribution between axles/wheels may be optimized for maximum tractive effort on deformable terrains (Section 6.3.2).

7. The vehicle efficiencies for deformable terrains are applicable to the ICV architecture (Section 6.3.2).

7.3 Conclusions

The following section lists the conclusions drawn from the results/literature, presented by chapter.

7.3.1 Military Vehicles

1. Expanding/updating existing military vehicles to meet modern, rapidly changing battlefield requirements is not an adequate solution.

2. Updating and improving military ground vehicles will require the adoption of open architectures and intelligent actuator technology.

3. Conclusions may not be drawn about the performance of military vehicle platforms in development due to the lack of data and results.

7.3.2 Tire Behavior

1. Characterizing tire behavior can be done through the generation of numerous tire performance maps that may then be combined into visual decision making surfaces.

2. Tire performance maps will need to address a range of camber values, normal loads, combined loading conditions, and tire construction types.

3. A friction circle is dependent upon the tire properties and operating condition and the represented values will vary during operation.

4. Military vehicles are regularly expected to operate over unprepared terrains and the relevant tire behavior should be characterized with performance maps.

5. The complexities of tire force generation make tire behavior an ideal candidate for the application of performance maps and this method of decision making.

7.3.3 Vehicle Architectures

1. The retention of traditional steering linkages does not allow wheel slip angles to be independently optimized.

2. The active camber systems described may not scale appropriately for vehicles with large suspension movements and tires of significantly lower stiffness values.

3. Actively controlled, independent steering and camber are required for optimizing tire force generation.

4. The coupled nature of the power generation/utilization elements of traditional drivetrains limit the ability of the system to respond to the commands of the operator.

5. Vehicles that retain traditional drivetrain elements are still subject to the associated design restrictions.

6. Torque generation and torque utilization components must be decoupled to provide maximum vehicle responsiveness.

7. Passive suspension elements do not respond effectively for vehicles with a significant range of operating requirements (military vehicles).

8. The adoption of developed active suspension systems involves increases in cost, vehicle mass, and presents significant component packing challenges.

9. Electrical energy storage elements increase vehicle weight and the typical single-motor designs result in the retention of traditional drivetrain elements.

10. Electric prime mover components should independently apply torque to each wheel directly.

11. Typical hybrid systems retain traditional drivetrain elements and are subject to the same design restrictions.

12. the ICV concept should utilize a series hybrid layout in conjunction with independent in-wheel drive motors.

13. The rover architecture prioritizes low complexity/weight and may not be scaled effectively.

14. The Chariot architecture is intended for low-speed, off-road operation only.

15. The military has indicated a need for active chassis elements, but the failure of the FCS program has hindered progress.

16. Vehicles must meet basic performance requirements in order to be useful to the military, regardless of potential fuel economy improvements.

17. The core ICV concept, the Intelligent Corner, has the potential to provide significant capability and responsiveness to the operator.

18. The ICV architecture requires the utilization of performance criteria in order to effectively assess vehicle motion.

7.3.4 Serial Chain Robotics Criteria

1. Motion criteria derived from Kinematic Influence Coefficients may be used as a method of evaluation as well as a method of comparison of various suspension types.

2. Constraint based criteria are more readily applicable to the ICV architecture.

3. Evaluating the application of criteria to suspension systems can not be done with a generalized model.

4. The range of criteria variation over a suspension workspace may be used to evaluate actuator mounting locations.

5. Range and limit criteria boundaries will be determined by chassis geometry and should be evaluated for every corner independently.

6. Criteria limits (threshold values) are heavily dependent upon vehicle type.

7.3.5 Vehicle Dynamics

1. Slip percentage ratios must be monitored and controlled real time in order to prevent unstable operation.

2. Torque distribution must be taken into account when evaluating wheel torque margins.

3. The vehicle configuration that minimizes resistances will be specific to each individual vehicle type/configuration.

4. Distribution of braking effort must take the terrain characteristics into account in order to avoid instability/loss of traction.

5. The ICV architecture may be able to balance individual wheel slip values in order to compensate for oversteer/understeer influences.

6. The ICV architecture may be able to manage distributed torque in order to avoid slip-skid braking.

7. Optimizing vehicle performance on deformable terrain will require individual motion efficiencies to be optimized.

7.4 Future Work

The following section presents concepts for further work, listed by chapter.

7.4.1 Military Vehicles

1. The progress and capabilities of military vehicles in development should continue to be observed.

7.4.2 Tire Behavior

1. Producing tire performance maps will require significant tire testing.

2. Tire testing should cover an appropriate range of operating conditions and construction types, and these ranges will need to be determined.

3. Capturing the effects of combined loading will require a detailed, standardized testing procedure for generating the necessary performance maps.

7.4.3 Vehicle Architectures

1. Effectively assessing and comparing vehicle architectures requires a significant modeling effort.

2. Full vehicle models are required for both traditional architectures as well as the ICV.

3. This modeling effort will allow the benefits of the application of intelligent actuation to each of the four degrees of freedom of each wheel to be shown.

4. Developed models must be sufficiently complex in order to fully demonstrate the benefits of the ICV architecture.

5. The continued assessment of the ICV architecture requires a continual effort to develop and demonstrate performance criteria.

7.4.4 Serial Chain Robotics Criteria

1. A model library of both dependent and independent suspension types should be generated in order to evaluate various motion criteria.

2. The application of criteria to the ICV should begin with constraint based criteria.

3. Variation of geometric criteria over a suspension workspace should be the foundation for the design of actuator mounting locations and the determination of actuator sizes/torque capability.

4. The relationships between the range/limit criteria values between ICV corners should be evaluated with a full vehicle model.

5. The critical range values of various criteria will need to be evaluated with vehicle models of varying type over a variety of operating conditions.

7.4.5 Vehicle Dynamics

1. Evaluating the ability of the ICV to optimize slip ratios (including slip-skid) should be evaluated with a vehicle/terrain model.

2. The development of further criteria to evaluate torque distribution should be done with a full vehicle model.

3. Any ideal configuration of a vehicle to minimize resistances should be individually determined with a model.

4. Ideal values of the generalized understeer/oversteer criterion should be determined through simulation.

5. Ideal values of vehicle efficiencies over deformable terrain should also be determined through simulation.

Bibliography

[1] Bmw technology guide: Dynamic drive. http://www.bmw.com/com/en/insights/technology/technology_guide/articles/dynamic_drive.html.

[2] Sae j670e vehicle dynamics terminology, July 1976.

[3] The army tactical wheeled vehicle (twv) strategy. Department of the Army, 2010. Office of the Vice Chief of Staff.

[4] Quadrennial defense review report. United States Department of Defense, February 2010.

[5] 2014 army equipment modernization plan. United States Army, May 13 2013.

[6] M1078 lmtv, April 2014. http://www.military-today.com/trucks/m1078_lmtv.htm.

[7] National Aeronautics and Space Administration. Space exploration vehicle concept: Nasa facts, March 2014. http://www.nasa.gov/pdf/464826main_SEV_FactSheet_508.pdf.

[8] Oleg Alexandrov. Tesla motors model s base. Creative Commons, CC-BY, April 2014. http://en.wikipedia.org/wiki/File:Tesla_Motors_Model_S_base.JPG.

[9] DoD photo by: Cpl. Michael Curvin American Special Ops. A m-atv (right) pictured next to a hmmwv, April 2014. http://www.americanspecialops.com/vehicles/m-atv/.

[10] Pradeepkumar Ashok and Delbert Tesar. The need for a performance map based decision process, December 2013.

[11] Rick Atkinson. *Crusade: The Untold Story of the Persian Gulf War*. Houghton Mifflin, 1993.

[12] Rimac Automobili. Introduction, April 2014. http://www.rimac-automobili.com/concept_one/introduction-20.

[13] Pinhas Barak. Passive versus active and semi-active suspension from theory to application in north american industry, September 1992.

[14] C.E. Benedict and D. Tesar. Model formulation of complex mechanisms. *Journal of Mechanical Design*, 100:747–761, 1978.

[15] P. J. Bevill and D. Tesar. Criteria normalization to support decision making in intelligent machines. The University of Texas Report to the U.S. Department of Energy, Austin, Texas, May 1990.

[16] Martin Blumenson. Kasserine pass, 30 january - 22 february 1943. In Major Steven Barry and Major Jonathan Due, editors, *History of the Military Art Since 1914*. Pearson Custom Publishing, 2008.

[17] Jr. Brigadier General (Ret.) Robert H. Scales. Forging a new army. In Major Steven Barry and Major Jonathan Due, editors, *History of the Military Art Since 1914*. Pearson Custom Publishing, 2008.

[18] Gregory D. Buckner, Karl T. Schuetze, and Joe H. Beno. Active vehicle suspension control using intelligent feedback linearization, June 2000.

[19] Paul W. Claar and Jeraid M. Vogel. A review of active suspension control for on and off-highway vehicles, November 1989.

[20] K. Cleary and D. Tesar. Incorporating multiple criteria in the operation of redundant manipulators. In *Proceedings, 1990 IEEE International Conerence on Robotics and Automation*, volume 1, pages 618–623, 1990.

[21] B.L. Collier and J.T. Warchol. The effect of inflation pressure on bias, bias-belted, and radial tire performance, 1980.

[22] Peter Collins. Gloom and boom. *The Economist*, April 20th 2013.

[23] Nissan Motor Company. 2014 nissan leaf, April 2014. `http://www.nissanusa.com/electric-cars/leaf/`.

[24] James F. Cuttino, John Stewart Shepherd, and Maruti N. Sinha. Design and development of an optimized, passive camber system for vehicles, December 2008.

[25] Chris Dixon. Big wheels for iraq's mean streets. *New York Times*, page AU1, February 24 2008.

[26] John C. Dixon. *Suspension Geometry and Computation.* John Wiley & Sons, 1rd edition, 2009.

[27] M. J. Van Doren. Criteria development to support decision making software for modular, reconfigurable robotic manipulators. Master's thesis, The University of Texas at Austin, 1992.

[28] Mehrdad Ehsani, Yimin Gao, Sebastien E. Gay, and Ali Emadi. *Modern Electric, Hybrid Electric, and Fuel Cell Vehicles.* CRC Press, 1st edition, 2005.

[29] FavCars.com. Bae fmtv ltas 4x4, April 2014. `http://www.favcars.com/wallpapers-bae-fmtv-ltas-4x4-2008-123406`.

[30] Andrew Feickert. The army's future combat systems (fcs): Background and issues for congress. Congressional Research Service, May 12 2008.

[31] Pearson Scott Foresman. Differential gear. Creative Commons, February 2014. `http://commons.wikimedia.org/wiki/File:Differential_gear_(PSF).png`.

[32] AM General. M1025 5, April 2014. `http://www.amgeneral.com/corporate/media/photos.php?pID=00062`.

[33] Thomas D. Gillespie. *Fundamentals of Vehicle Dynamics.* Society of Automotive Engineers, Inc., 1992.

[34] Mike Hanlon. Audi's new magnetic semi-active suspension system. *Gizmag*, June 17 2006.

[35] Brian D. Harrington and Chris Voorhees. The challenges of designing the rocker-bogie suspension for the mars exploration rover. In *Proceedings of the 37th Aerospace Mechanisms Symposium, Johnson Space Center*, May 19-21 2004.

[36] Dan A. Harrison, Robert Ambrose, Bill Bluethmann, and Lucien Junkin. Next generation rover for lunar exploration. In *IEEE Aerospace Conference*, December 2007.

[37] R. J. Hayes, J. H. Beno, D. A. Weeks, A. M. Guenin, J. R. Mock, M. S. Worthington, E. J. Triche, D. Chojecki, and Drew Lippert. Design and testing of an active suspension system for a 2-1/2 ton military truck, April 2005.

[38] Francis B. Hoogterp, Mikell K. Eiler, and William J. Mackie. Active suspension in the automotive industry and the military, February 1996.

[39] Francis B. Hoogterp, Nancy L. Saxon, and Peter J. Schihl. Semiactive suspension for military vehicles, March 1993.

[40] Richard N. Hooper. *Multicriteria Inverse Kinematics for General Serial Robots*. PhD thesis, The University of Texas at Austin, 1994.

[41] W. H. Hucho, L. J. Janssen, and H. J. Emmelmann. The optimization of body details-a method for reducing the aerodynamic drag of road vehicles, February 1976.

[42] Karl Iagnemma. Mobile robot rough-terrain control (rtc) for planetary exploration. In *Proceedings of the 26th ASME Biennial Mechanisms and Robotics Conference, DETC*, pages 10–13, 2000.

[43] Jeffery J. Jaczkowski. Robotic technology integration for army ground vehicles. In *Digital Avionics Systems 20th Conference*, volume 2, pages 9B1/1 – 9B1/8, October 2001.

[44] Robert W. Kaczmarek. Central tire inflation systems (ctis) - a means to enhance vehicle mobility. In *Proceedings of the International Conference on the Performance of Off-Road Vehilces and Machines (8th)*, volume 3. U.S. Army Tank-Automotive Command, August 5-11 1984.

[45] Takeshi Katayama, Yoshiki Yasuno, Tomoaki Oida, Masayuki Sao, Masayuki Imamura, Nagatoshi Seki, and Yasuharu Satou. Development of 4 wheel active steer, April 2008.

[46] Orr Kelly. *King of the Killing Zone*. W.W. Norton % Company, Inc., 1989.

[47] Terence K. Kelly, John E. Peters, Eric Landree, Luis R. Moore, Randall Steeb, and Aaron Martin. The u.s. combat and tactical wheeled vehicle

fleets: Issues and suggestions for congress. Published 2011 by the RAND Corporation, 2011.

[48] Terrence K. Kelly, John E. Peters, Eric Landree, Louis R. Moore, Randall Steeb, and Aaron Martin. The u.s. combat and tactical wheeled vehicle fleets: Issues and suggestions for congress. Published 2012 by the RAND Corporation, 20011.

[49] Philip Koehn and Michael Eckrich. Active steering - the bmw approach towards modern steering technology, March 2004.

[50] Denise Kramer and Gordon Parker. Current state of military hybrid vehicel development. U.S. Army TARDEC, 2011.

[51] Biorobotics Laboratory. Modular snake robots. Carnegie Mellon University, April 2014. `http://biorobotics.ri.cmu.edu/projects/modsnake/images/hidef/IMG_4778.jpg`.

[52] Randel A. Lindemann, Donald B. Bickler, Brian D. Harrington, Gary M. Ortiz, and Christopher J. Voorhees. Mars exploration rover mobility development: Mehcanical mobility hardware design, development, and testing. *IEEE Robotics & Automation Magazine*, June 2006.

[53] Randel A. Lindemann and Chris J. Voorhees. Mars exploration rover mobility assembly design, test and performance. NASA Jet Propulsion Laboratory, 2005.

[54] Timothy Lupfer. The dynamics of doctrine: The changes in german tactical doctrine during the first world war. In Major Steven Barry and Major Jonathan Due, editors, *History of the Military Art Since 1914*. Pearson Custom Publishing, 2008.

[55] Paul McLeary. Us army chief confirms: Ground combat vehicle is dead (for now). *Defense News*, January 23 2014.

[56] Jens Meiners. Driven: Mercedes-benz magic body control. *Car and Driver*, September 2010.

[57] William F. Milliken and Douglas L. Milliken. *Race Car Vehicle Dynamics*. Society of Automotive Engineers, Inc., 1995.

[58] Michael Moss. Pentagon asks contractor to speed production of armored humvees for use in iraq. *New York Times*, page A6, December 11 2004.

[59] Michael Moss. Safer vehicles for soliders: A tale of delays and glitches. *New York Times*, page 1, June 26 2005.

[60] General Motors. 2014 spark ev, April 2014. `http://www.chevrolet.com/spark-ev-electric-vehicle.html`.

[61] Tesla Motors, April 2014. teslamotors.com.

[62] Satoshi Murata. Vehicle dynamics innovation with in-wheel motor, May 2011.

[63] Harald Naunheimer, Bernd Bertsche, Joachim Ryborz, and Wolfgang Novak. *Automotive Transmissions: Fundamentals, Selection, Design, and Application*. Springer, 2nd edition, 2011.

[64] F.J. Newman and J. Ledwinka. Electrically propelled vehicle, 1901.

[65] Donald L. Nordeen and Anthony D. Cortese. Force and moment characteristics of rolling tires, January 1964.

[66] Department of Defense. Conduct of the persian gulf conflict: An interim report to congress. Washington, D.C.: DoD, July 1991.

[67] Department of Defense. Conduct of the persian gulf conflict: Final report to congress. Washington, D.C.: DoD, April 1992.

[68] Department of the Army. Jpo mrap all terrain vehicle (m-atv), November 2008. Solicitation Number: W56HZV-09-R-0115.

[69] American Special Ops. Marsoc marines engage the taliban from a hmmwv during operations gereshk, afghanistan august 11, 2007, April 2014. `http://www.americanspecialops.com/photos/marsoc/marsoc-hmmwv.php`.

[70] Pantoine. Car steering scheme. Creative Commons, CC-BY, March 2014. `http://commons.wikimedia.org/wiki/File:Direction_cre.jpg`.

[71] John Park, Jeff Dutkiewicz, and Ken Cooper. Simulation and control of dana's active limited-slip differential e-diff, April 2005.

[72] Christopher G. Pernin, Elliot axelband, Jeffery A. Drezner, Brian B. Dille, John Gordon IV, Bruce J. Held, K. Scott McMahon, Walter L. Perry, Christopher Rizzi, Akhil R. Shah, Peter A. Wilson, and Jerry M. Sollinger. Lessons from the army's future combat systems program. Published 2012 by the RAND Corporation, 2012.

[73] Jornsen Reimpell, Helmut Stoll, and Jurgen Betzler. Steering. In David A. Crolla, editor, *Automotive Engineering: Powertrain, Chassis System and Vehicle Body*. Elsevier, Inc., 2009.

[74] Yaskawa: Motoman Robotics. Mh 80, April 2014. `http://www.motoman.com/datasheets/MH80.pdf`.

[75] Isabel Ramirez Ruiz. Active kinematics suspension for a high performance sports car, April 2013.

[76] H. Sakai. The dynamic properties of tires. Bulletin, JSAE No. 3, p.70-71., 1971.

[77] Carroll Smith. *Tune To Win: The art and science of race car development and tuning*. Aero Publishers, Inc., 1978.

[78] Naoyasu Sugimoto, Shuuichi Buma, Shingo Urababa, Akio Nishihara, and Akiya Taneda. Electronic active stabilizer suspension system. `http://www.jsme.or.jp/English/awards/awardn06-05.pdf`.

[79] J.J. Taborek. Mechanics of vehicles, May 30 - Dec. 26 1957.

[80] D. Tesar, P. S. March, A. S. Boddiford, and M.-K. Park. Geometric-based spatial path planning: Part i framework and application.

[81] Del Tesar. Benefits of performance map utilization in intelligent actuators. Whitepaper, 2012.

[82] Del Tesar. Modernization of open architecture battlefield vehicles. Whitepaper, 2012.

[83] M. Thomas and D. Tesar. Dynamic modeling of serial manipulator arms. *Journal of Dynamic Systems, Measurement, and Control*, 104:218–228, 1982.

[84] Mark S. Tisius. An emperical approach to performance criteria and redundancy resolution. Master's thesis, The University of Texas at Austin, 2004.

[85] Fara Warner. Army stepping up its humvee orders for troops in iraq. *New York Times*, page C1, December 25 2003.

[86] J. Y. Wong. *Terramechanics and Off-Road Vehicle Engineering*. Elsevier, Ltd., 2nd edition, 2001.

[87] J. Y. Wong. *Theory of Ground Vehicles*. John Wiley & Sons, 3rd edition, 2001.

[88] Jo-Yung Wong. Optimization of the tractive performance of four-wheel-drive off-road vehicles, February 1970.

[89] Timothy P. Woodard. Multi-speed electric hub drive wheel design. Master's thesis, The University of Texas at Austin, 2013.